

https://dspace.org/

Comparative analysis of ordinary kriging and sequential Gaussian simulation for recoverable reserve estimation at Kayelekera Mine

Gulule, Ellasy Priscilla

2016-09-16
http://hdl.handle.net/10539/21049

Downloaded from a DSpace repository. https://dspace.org/

COMPARATIVE ANALYSIS OF ORDINARY KRIGING AND SEQUENTIAL GAUSSIAN SIMULATION FOR RECOVERABLE RESERVE ESTIMATION AT KAYELEKERA MINE

Ellasy Priscilla Gulule

A research report submitted to the Faculty of Engineering and the Built Environment, University of the Witwatersrand, Johannesburg, in partial fulfilment of the requirements for the degree of Master of Science in Engineering.

Johannesburg, 2016

DECLARATION

I declare that this research report is my own unaided work. It is being submitted for the Degree of Master of Science in Engineering to the University of the Witwatersrand, Johannesburg. It has not been submitted before for any degree or examination to any other University

_____

_____day of _____, _____

ABSTRACT

It is of great importance to minimize misclassification of ore and waste during grade control for a mine operation. This research report compares two recoverable reserve estimation techniques for ore classification for Kayelekera Uranium Mine. The research was performed on two data sets taken from the pit with different grade distributions. The two techniques evaluated were Sequential Gaussian Simulation and Ordinary Kriging. A comparison of the estimates from these techniques was done to investigate which method gives more accurate estimates. Based on the results from profits and loss, grade tonnage curves the difference between the techniques is very low. It was concluded that similarity in the estimates were due to Sequential Gaussian Simulation estimates were from an average of 100 simulation which turned out to be similar to Ordinary Kriging. Additionally, similarities in the estimates were due to the close spaced intervals of the blast hole/sample data used. Whilst OK generally produced acceptable results like SGS, the local variability of grades was not adequately reproduced by the technique. Subsequently, if variability is not much of a concern, like if large blocks were to be mined, then either technique can be used and yield similar results.

FOR MY FAMILY

ACKNOWLEDGMENTS

I thank all that have been helpful during the time of writing this research report. My sincere gratitude should go to Professor Minnitt for his tireless guidance in helping me complete this study. I would also like to acknowledge the financial support from Paladin Energy LTD, who funded my studies. I would also like to acknowledge many friends and colleagues who assisted, advised and supported me throughout the time I was writing the report. Especially I need to express my sincere gratitude to Mr Dave Princep for his mentoring and technical advice. To my family, thank you for the support given to me.

TABLE OF CONTENTS

CONTENTS **Page**

DECLARATION ..... **ii**

ABSTRACT ..... **iii**

ACKNOWLEDGMENTS ..... **v**

LIST OF FIGURES ..... **ix**

LIST OF TABLES ..... **xii**

LIST OF SYMBOLS AND COMMON NOTATION ..... **xiii**

1 INTRODUCTION **1**

1.1 Background **1**

1.2 Study Area **2**

1.3 Geological Setting **2**

1.3.1 Regional Geology 3

1.3.2 Stratigraphy of the Kayelekera deposit 4

1.3.3 Kayelekera mine geology and mineralisation 5

1.3.4 Disequilibrium state of the deposit 6

1.4 Kayelekera Mine Reserves **8**

1.5 Problem Statement **8**

1.6 General Objective **11**

1.7 Thesis Outline **12**

2 LITERATURE REVIEW **13**

2.1 Chapter Overview **13**

2.2 Geostatistics and Recoverable Reserve Estimation **13**

2.3 Kriging **15**

2.3.1 Ordinary Kriging 16

2.4 Conditional Simulation **19**

2.4.1 Sequential Gaussian Simulation 22

2.5 Variogram Analysis **25**

2.6 Comparison of Ordinary Kriging and Conditional Simulation **27**

2.7 Chapter Summary **29**

3 METHODOLOGY 31

3.1 Chapter Overview 31

3.2 Data Collection 31

3.3 Data Validation 40

3.4 Statistical Data Analysis 40

3.4.1 Histograms and Cumulative Frequency Curves 40

3.4.2 Descriptive statistics 42

3.5 Probability Plots 42

3.6 Data Domaining 43

3.7 Declustering 44

3.8 Data Transformation 44

3.9 Variogram Analysis 46

3.9.1 Variogram maps 47

3.9.2 Variogram modelling 49

3.9.3 Variogram modelling for non-transformed data 50

3.9.4 Variogram modelling for transformed data 54

4 ESTIMATION OF RECOVERABLE RESERVES USING ORDINARY KRIGING AND SEQUENTIAL GAUSSIAN SIMULATION 59

4.1 Chapter Overview 59

4.2 Ordinary Kriging Recoverable Estimates 59

4.3 Sequential Gaussian Simulation (SGS) recoverable reserve estimates 60

4.4 Summary 61

5 COMPARISON OF ORDINARY KRIGING AND SEQUENTIAL GAUSSIAN SIMULATION ESTIMATES 63

5.1 Chapter Overview 63

5.2 Visual Examination of Estimates 63

5.2.1 Comparison of maps of estimates with adjacent blast holes 63

5.2.2 Comparison of cumulative frequency plots 70

5.2.3 Comparison of histograms 72

5.2.4 QQ Plots comparison 74

5.3 Quantitative Comparison of Estimates with Actual Values 75
5.3.1 Comparison of descriptive statistics..... 75
5.3.2 Grade tonnage results and curves..... 76
5.3.3 Correlation coefficients and correlation graphs 80
5.3.4 Profit and loss from the estimates 81
5.4 Chapter Summary 85
6 CONCLUSION AND RECOMMENDATIONS 87
REFERENCES 89
APPENDIX A: CONSOLIDATED FILE WITH ALL DATA TYPES..... 92
APPENDIX B: GRADE TONNAGE CURVE CALCULATIONS..... 94
APPENDIX C: PROFIT/LOSS CALCULATED FOR ALL CUT-OFFS 96

LIST OF FIGURES

Figure **Page**

Figure 1.1: Location of the Kayelekera Mine in Northern Malawi 2
Figure 1.2: Regional Geology of Northern Malawi (Shaw, 1990) 3
Figure 1.3: Stratigraphy of alternating arkose and mudstone forming the Kayelekera Mine Deposit (Paladin Internal Report, 2007) 4
Figure 1.4: West-East Section of Geology and Mineralization for KM Deposit (Paladin Internal Report, 2007) 6
Figure 1.5: Kayelekera Ore Deposit Model (Paladin Internal Report, 2007) ... 7
Figure 1.6: Individual simulated realizations of grade distribution at Kayelekera mine and a comparison of OK and an average of 100 simulated realizations (last two panels) 10
Figure 2.1: The basic steps in SGS algorithm (Deustch and Journel, 1992 and Asghari et al, 2009) 25
Figure 2.2: Types of variogram models 27
Figure 3.1: Location of Study Areas A and B within the open pit mining operations 32
Figure 3.2: Gamma vs. XRF Scatter Plots for Area A and Area B 33
Figure 3.3: Geology sectional view of drill holes samples for Area A 34
Figure 3.4: Geology sectional view of drill holes samples for Area B 35
Figure 3.5: Drill hole with geology, XRF and Gamma logged for each depth 35
Figure 3.6: Area A drill hole data locations colour coded by U_3O_8 grades 37
Figure 3.7: Area A drill hole data East – West view(Cross-sectional View) . 38
Figure 3.8: Area B drill hole data locations colour coded by U_3O_8 grades 39
Figure 3.9: Area B drill hole data East – West view (Cross-sectional View) 39
Figure 3.10: Histograms for U_3O_8 for Area A (Left) and Area B (Right) 41
Figure 3.11: Cumulative Histogram of U_3O_8 for Study Area A and Area B .. 41
Figure 3.12: Probability plot for Area A..... 43
Figure 3.13: Probability Plot for Area B..... 43
Figure 3.14: Map showing domained zones for Area A 44

Figure 3.15: Cumulative Curves for Untransformed (Left) and Transformed (Right) U_3O_8 for Area A 45
Figure 3.16: Cumulative Curves for Untransformed (Left) and Transformed (Right) U_3O_8 for Area B 45
Figure 3.17: Area A non-transformed and transformed U_3O_8 distribution 46
Figure 3.18: Area B non-transformed and transformed U_3O_8 distribution 46
Figure 3.19: Plan View U_3O_8 Variogram Map for Area A 47
Figure 3.20: Plan View U_3O_8_normal score transformed Variogram Map for Area A 48
Figure 3.21: Plan View U_3O_8 Variogram Map for Area B 48
Figure 3.22: Plan View U_3O_8_normal score transformed Variogram Map for Area B 49
Figure 3.23 : Area A Vertical Variogram model using Non-transformed Data (max of 6m downhole data) 51
Figure 3.24: Area A East-West Variogram model using Non-transformed Data 51
Figure 3.25: Area A North-South Variogram model using Non-transformed Data 52
Figure 3.26: Area A NNW-SSE (AZM 120º) Variogram model using Non-transformed Data 52
Figure 3.27 : Area B Vertical Variogram model using Non-transformed Data (max of 6m downhole data) 53
Figure 3.28: Area B East-West Variogram model using Non-transformed data 53
Figure 3.29: Area B North-South Variogram model using Non-transformed Data 54
Figure 3.30: Area A East-West Variogram model using transformed data 55
Figure 3.31: Area A North-South Variogram model using transformed data. 55
Figure 3.32: Area A Vertical Variogram model using transformed data (max of 6m downhole data) 56
Figure 3.33: Area A NNW-SSE (AZM 120º) Variogram model using transformed data 56

Figure 3.34: Area B Vertical Variogram model using transformed Data (max of 6m downhole data) 57
Figure 3.35: Area B East-West Variogram model using transformed data 57
Figure 3.36: Area B North-South Variogram model using transformed Data 58
Figure 4.1: OK block estimates for Area A (Left) and Area B (Right) 59
Figure 4.2: SGS block estimates for Area A (Left) and Area B (Right) 61
Figure 5.1: Area A comparison of blast hole data with OK model, bench 1 .. 64
Figure 5.2: Area A comparison of blast hole data with SGS model, bench1 1 64
Figure 5.3: Area A comparison of blast hole data with OK model, bench 2 .. 65
Figure 5.4: Area A comparison of blast hole data with SGS model, bench 2 65
Figure 5.5: Area A comparison of blast hole data with OK model, bench 3 .. 66
Figure 5.6: Area A comparison of blast hole data with SGS model, bench 3 66
Figure 5.7: Area B comparison of blast hole data with OK model, bench 1 .. 67

LIST OF TABLES

Table **Page**

Table 1.1: KM total reserves as of June, 2013 (Paladin Financial Report, 2013) .. 8
Table 2.1: Advantages and Disadvantages of SGS and OK 30
Table 3.1: Lithology of Samples from Area A and B 34
Table 3.2: Sample of Consolidated file 36
Table 3.3: Descriptive statistics for U3O8 for Area A and B 42
Table 3.4: Area A directional variogram parameters 49
Table 3.5: Area B directional variogram parameters 50
Table 4.1: Ordinary Kriging Estimates at 400ppm cut-off grade 60
Table 4.2: SGS Estimates at 400ppm cut-off grade 61
Table 4.3: Grade, tonnage and metal estimates from OK and SGS 62
Table 5.1: Comparison of statistics for actual data, OK and SGS estimates 76
Table 5.2: Grade, tonnes and contained U3O8 (metal) above cut-off grades by actual data, OK and SGS estimates for Area A 77
Table 5.3: Grade, tonnes and contained U3O8 (metal) above cut-off grades by actual data, OK and SGS estimates for Area B 78
Table 5.4: Correlation coefficients of blast hole data, OK and SGS estimates 81
Table 5.5: Economic parameters for calculating profits/loss 82
Table 5.6: Profits and losses from Actual, OK and SGS estimates for Area A 82
Table 5.7: Profits and losses from Actual, OK and SGS estimates for Area B 83
Table A1: Sample of file with all data collected……..……..92
Table B1: Comparison of Tonnage and Grades at different Grade Cut Offs for Blast hole Data, OK and SGS estimates for Area ……..……..….94
Table: B2: Comparison of Tonnage and Grades at different Grade Cut Offs for Blast hole Data, OK and CS estimates for Area B……..……..95
Table C1: Calculated profits/losses at all cut offs for Area A and B ……..…....96

LIST OF SYMBOLS AND COMMON NOTATION

CPS	Counts per Second
CS	Conditional Simulation
KM	Kayelekera Mine
MIK	Multiple Indicator Kriging
Mt	Million Tonnes
OK	Ordinary Kriging
PPM	Parts per Million
SGS	Sequential Gaussian Simulation

1 INTRODUCTION

1.1 Background

Mining, which involves extracting valuable material from the earth, is one of the most profitable but financially risky ventures. Mining involves a number of processes and one of the most important processes is estimating recoverable reserves for grade control during mining production. Ravenscroft (1992) defines recoverable reserves as the tonnage and grade that can be recovered above a given cut-off grade in a selective mining operation. From the recoverable reserves an area can be separated into ore and waste for grade control purposes, also grade and tonnage above cut-off grade. The decision on whether or not to send material for extraction depends on the estimated recoverable reserves (Vizi, 2008). Therefore, accurate estimation of local reserves is essential for a successful mining operation, and the accuracy of the selection process of ore and waste from the recoverable reserves has an impact on the economic valuation of the whole mining project. Improper classification of ore and waste during mining has a negative financial consequence for the mining company, as it puts the company at financial risk (Lipton et al, 1998). Minimal ore and waste misclassification during grade control will directly increase the mine operation's revenues. On the other hand, reliable, local reserve estimates boost confidence in the mining activities as well as in the wider resource model that is used in mine planning (Ravenscroft, 1992). As a consequence a stable mill feed can be guaranteed on a continuous basis due to the reliable estimates. The process of estimating recoverable reserves is simplified when an appropriate estimation method for the existing deposit type is identified. The recoverable reserve estimation for grade control as well as mine planning is widely done using geostatistics. A number of authors (Deutsch, 2002; Sinclair and Blackwell, 2002 and Clarke, 1979), have defined geostatistics as the study of phenomena that vary in space and/or time. Geostatistics helps to determine the reliability of the estimates obtained. There are several types of geostatistical techniques which are used, and the choice of the technique will depend on the grade continuity, geology and structure of the deposit as well as the technology of extraction. Understanding grade continuity, the style of

mineralisation, and the spatial distribution of the data are important factors in grade estimation as they relate to the different parameters that must be taken into account, for example search radii for the applied variogram (Coombes, 1997).

1.2 Study Area

The Kayelekera Uranium Mine located in Northern Malawi, is the focus of this study. The location of Kayelekera mine in the extreme northern tip of Malawi is shown in Figure 1.1, in the Karonga District about 35 km from Karonga's main township and 650km north of Lilongwe, the capital city of Malawi.

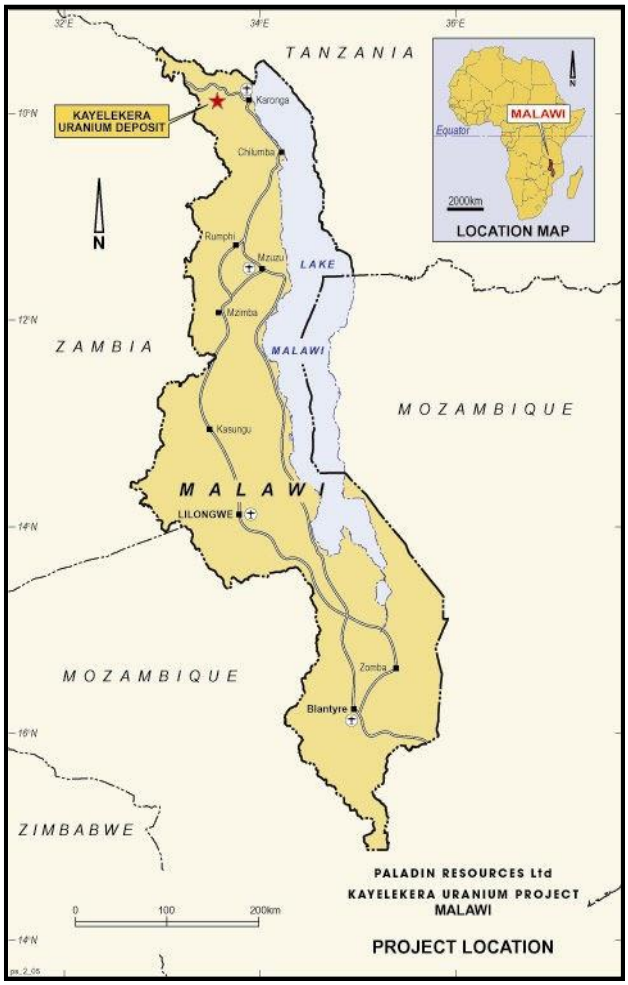


Figure 1.1: Location of the Kayelekera Mine in Northern Malawi

1.3 Geological Setting

The Kayelekera uranium deposit is a Karoo age sandstone hosted uranium deposit and is underlain Pre-Karoo basement rocks.

1.3.1 Regional Geology

The regional geology of northern Malawi, taken from the Geology of Kayelekera Deposit, Shaw (1990), is shown in Figure 1.2. Karonga district is mainly underlain by metamorphic and igneous rocks of the Pre-Karoo basement complex (Shaw, 1990), with small basins of Karoo sediments overlying the basement complex. Near Lake Malawi the Basement Complex is overlain by Cretaceous to recent lacustrine sediments. Early rift faulting in the Upper Jurassic established a basin of deposition in the area which represents northern Lake Malawi. Faulting and subsidence which ended with the initiation of the Gondwana cycle accompanied the deposition of Karoo sediments. The Karoo sedimentation leading to the formation of local basins like Kayelekera is part of the north Rukuru Basin, which in turn is part of the larger, regional Luangwa Karoo Basin.

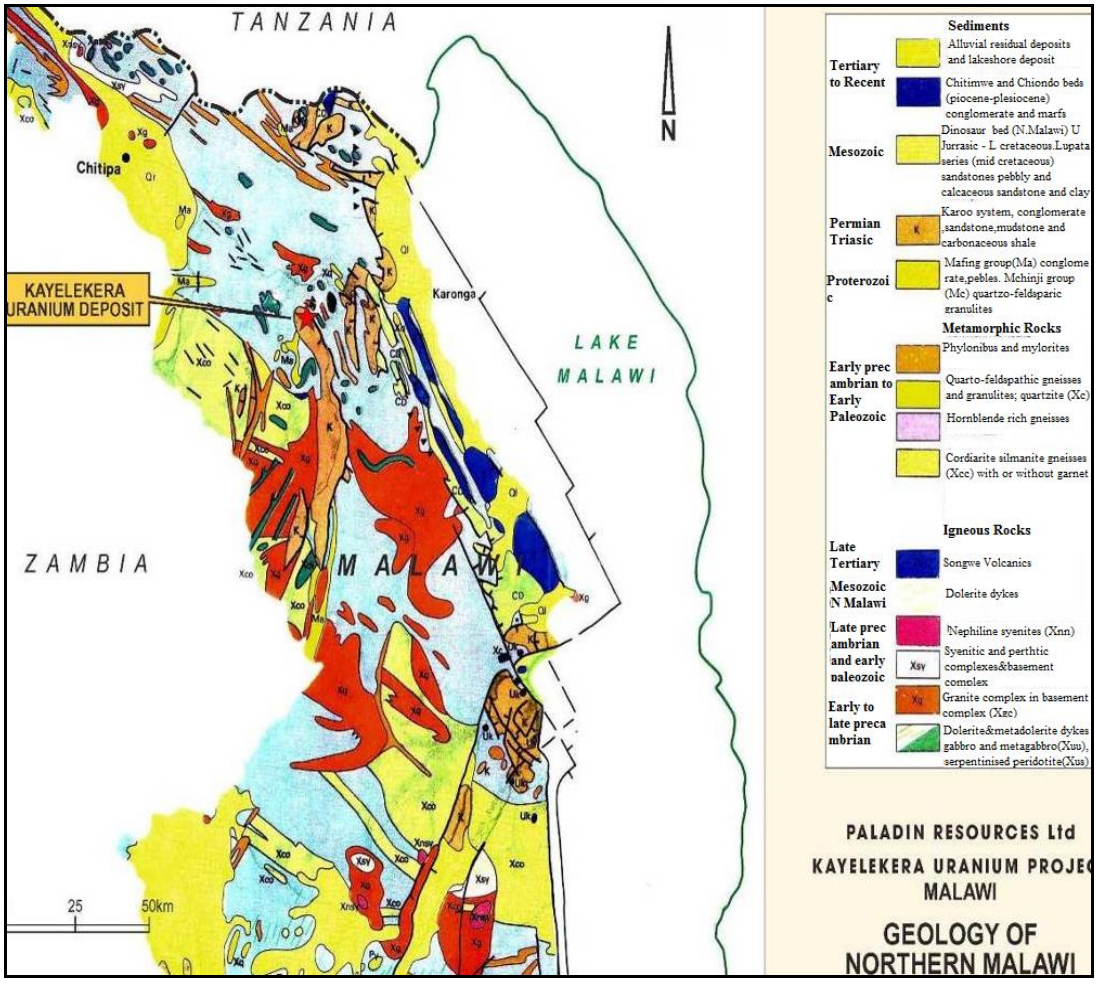


Figure 1.2: Regional Geology of Northern Malawi (Shaw, 1990)

1.3.2 Stratigraphy of the Kayelekera deposit

During drilling and surface geological mapping, eight lenses of arkose with interbedded mudstone to silty mudstone layers were identified, the arkose and mudstone being in an approximate ratio of 1:1. The stratigraphic sequence for the Kayelekera deposit, taken from the Paladin internal report (2007), is shown in Figure 1.3. For identification, these arkose units were named from R for top unit through S, T, U, V, W and X. The intervening mudstones were named after the arkose on top and below it, meaning that the intervening mudstone between the R and S unit is named RS. Within the individual arkose units there is a fining up sequence from pebbly conglomerate to medium or fine grained arkose.

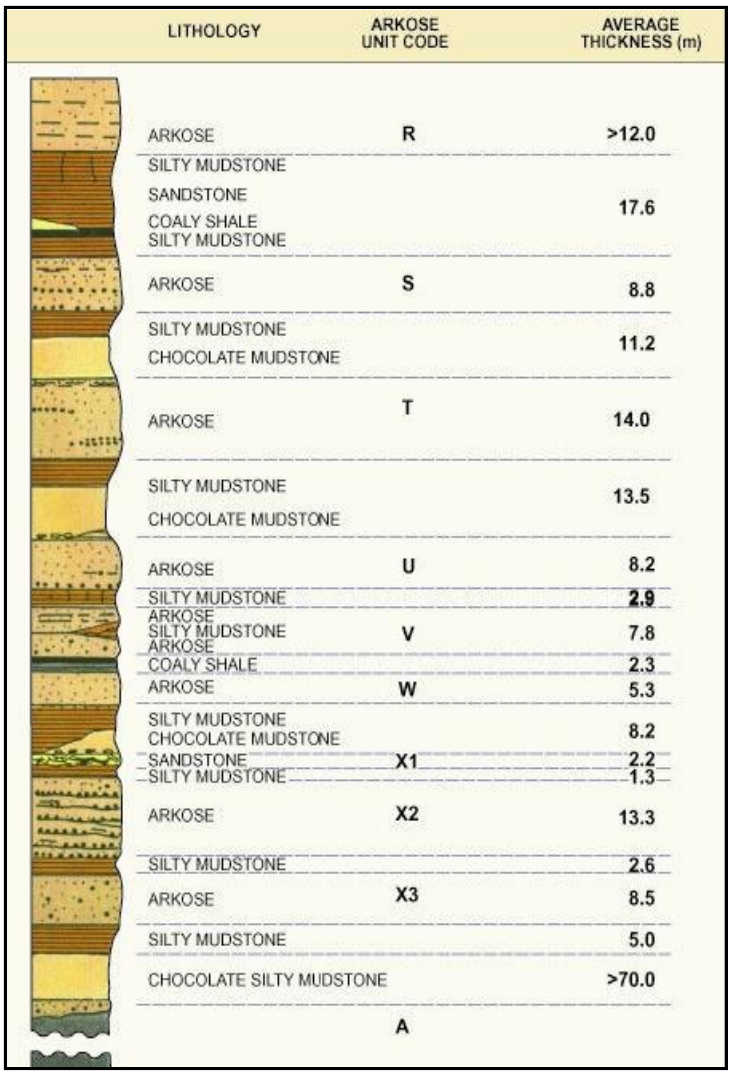


Figure 1.3: Stratigraphy of alternating arkose and mudstone forming the Kayelekera Mine Deposit (Paladin Internal Report, 2007)

In this study, sampling was mainly done from the mudstone of the RS and ST units and arkose of the S unit for Area A. On the other hand, for Area B, sampling was done from the arkose of the T unit and mudstone from the ST and TU unit.

1.3.3 Kayelekera mine geology and mineralisation

The Kayelekera deposit is a roll-front sandstone hosted Uranium deposit (Shaw, 1990). It is located in the northern edge of the North Rukuru Basin, which contains thick sequences of Permian Karoo sediments preserved in a semi-graben. The main primary uranium mineral is Coffinite. Uraninite and pitchblende are also found but in smaller quantities. Lenses of mineralisation mainly occur within arkose units which are superimposed on each other and are interbedded with mudstones. The units are superimposed vertically along the axis of a shallow north-west trending syncline. The arkose layers with interbedded mudstone are 100m deep (Brown, 1989).

Some secondary mineralisation occurs in mudstones as a result of redistribution of uranium from arkose through faulting and contact between arkose and mudstone. The mineralisation results in four types of ore which are oxidised arkose ore, reduced arkose ore, transitional arkose ore and mudstone ore. Transitional ore is mixed ore that contains both reduced and oxidised ore. Much of the uranium mineralisation occurs within the arkose units which make up 80% of the ore reserves while 20% of the ore occurrences are found in mudstones. Most of the mineralisation in the mudstone below the mineralised arkose units is preferentially developed adjacent to major faults structures that tend to offset the geology and associated mineralisation. Figure 1.4 shows a simplified cross section model of the Kayelekera deposit with the identified geological units and mineralised zones.

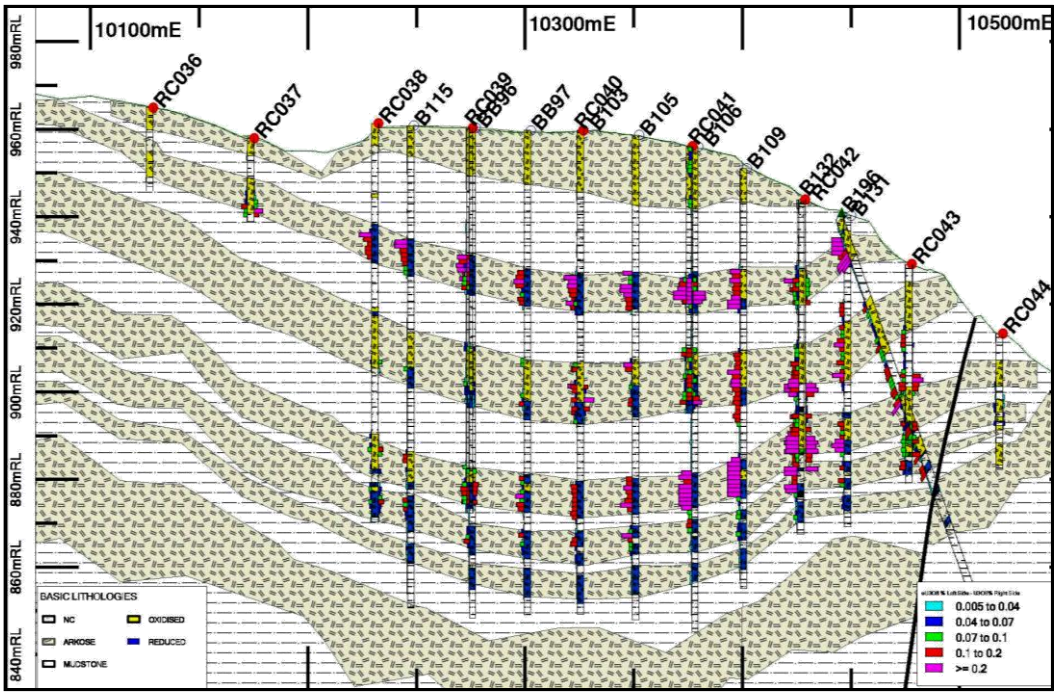


Figure 1.4: West-East Section of Geology and Mineralization for KM Deposit (Paladin Internal Report, 2007)

1.3.4 Disequilibrium state of the deposit

Early assessment of the Kayelekera deposit by Bowden and Shaw (1991) revealed a large discrepancy in some estimates of ore grade and lithology thickness as determined by the calculation of uranium equivalent-grade based on the downhole gamma-log measurements and the analytical results for uranium grade in core samples over the same intersection. It was also established that the discrepancies were highest in oxidised arkose and that the deposit is in a state of geochemical disequilibrium due to the nature of the ore. The deposit is near the surface as such it is affected by weathering as well as oxidisation by groundwater. The oxidised arkose ore shows remarkably high decay product occurrences due to the mobility of uranium in oxidising conditions (Barrett, 2005). With this mobility under oxidised environment, the uranium is leached out from the oxidised environment and re-deposited where there is reduced arkose. Although uranium itself is mobile in oxidised environment its gamma emitting daughters, Radon, tend to be less

mobile in the same oxidized environment. Consequently there is disequilibrium between uranium and its daughter product within the oxidised environment, especially oxidised arkose. This leads to misleadingly high gamma responses in Uranium depleted formations. On the other hand, there is a daughter product deficiency in reduced ore due to recent precipitation of Uranium that was leached from oxidised zones. The young age of the mineralisation coinciding with the lack of decay products leads to a lower radiometric response in reduced formations. This leads to misleadingly low gamma responses in the uranium enriched areas, especially the reduced and in mudstone that is in contact with oxidised arkose. Figure 1.5 shows a geological redox model for Kayelekera deposit showing redox fronts.

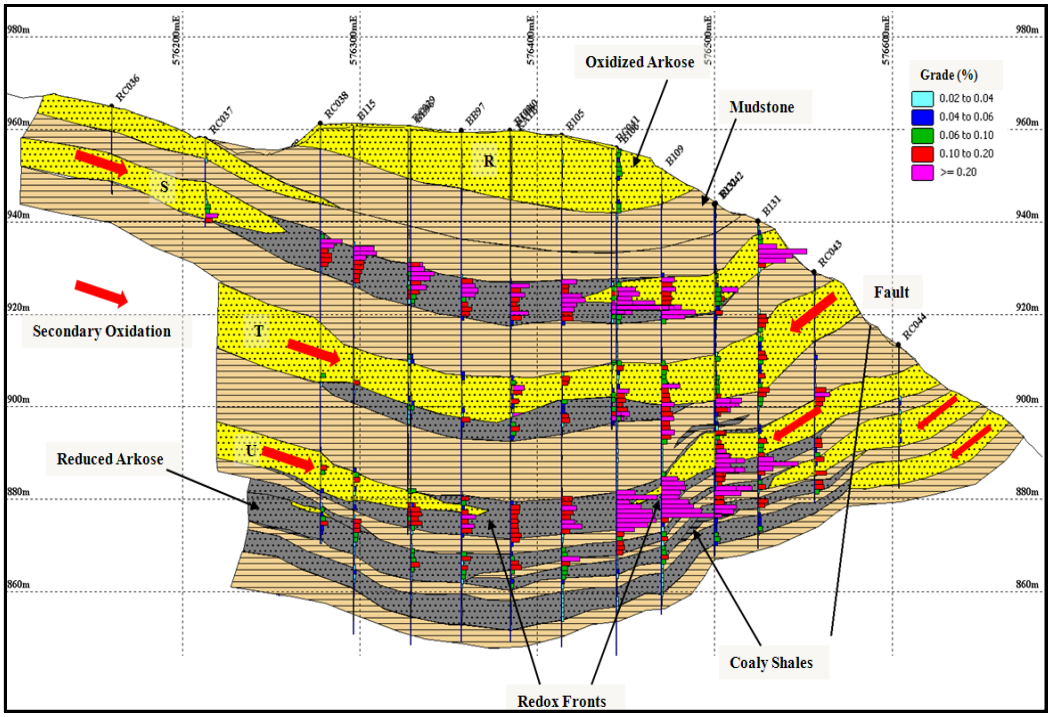


Figure 1.5: Kayelekera Ore Deposit Model (Paladin Internal Report, 2007)

1.4 Kayelekera Mine Reserves

The early estimation of Kayelekera deposit global reserves was carried out using Multiple Indicator Kriging (MIK). The use of MIK allows for a block variance adjustment factor to bring the global resource estimate more in line with grade control and potential for mining. The deposit's total reserves were estimated to be 8.01Mt. The detailed reserves as of June 2013 have been given in Table 1.1, it should be noted that figures may not add up due to rounding. A cut-off grade of 400ppm U_3O_8 was used and the figures were obtained from Paladin's 2013 financial report.

Table 1.1: KM total reserves as of June, 2013 (Paladin Financial Report, 2013)

	Mt	**Grade (ppm) U_3O_8**	**Tonnes U_3O_8**	**Mlb U_3O_8**
Proven Reserve	0.49	1,230	605	1.33
Probable Reserve	5.98	907	5,423	11.96
Stockpiles	1.54	945	1,454	3.21
Total Ore Reserve	**8.01**	**934**	**7,483**	**16.50**

1.5 Problem Statement

Mining is an expensive venture therefore the most important asset of a mining operation is the statement of its mineral reserves. As such, an accurate estimation of the recoverable reserves is necessary for proper depletion of the mineral reserves and also in determining life of the mine. With accurate recoverable reserve estimates, the long term and short term plans for the mine become more reliable. However, inaccurate estimation of the recoverable reserves makes the mine financially a risky venture. Due to the need for accurate information, the

technique used in estimating the recoverable reserves contributes to the reliability of the estimates. And there are many techniques using different software that are used to estimate the recoverable reserves. Since commissioning of the Kayelekera Uranium Mine, Sequential Gaussian Simulation has been used as the main estimation method for recoverable reserves for grade control. The technique has a less smoothing effect on data than Ordinary Kriging and also honours spatial variability of data (De-Vitry et al, 2007; Isaaks and Srivastava, 1989; Ravenscroft, 1992). Hence it provides better estimation of mining blocks as well as better ore and waste boundary delineation during mining. For these reasons it is preferred instead of the Ordinary Kriging for ore and waste selection at the Kayelekera Mine.

However, when individual simulated realizations are used, the estimate has higher variance than a Kriged estimate of the same area. Any single realization has a high degree of local error and does not give a good estimate of the grade distribution (Vann et al, 2002). This has been shown in the first four panels (realisations 1-4) from Figure 1.6 for Area B, and the panels has been colour coded by grade categories. It is further stated that any individual simulation realisation is a poorer estimate than kriging but averaging a set of several realisations can yield a good estimate, hence the average of such individual realization is used to yield a good estimate, and the average of all realizations is very similar to an Ordinary Kriged estimate as graphically shown in the last two panels of Figure 1.6.

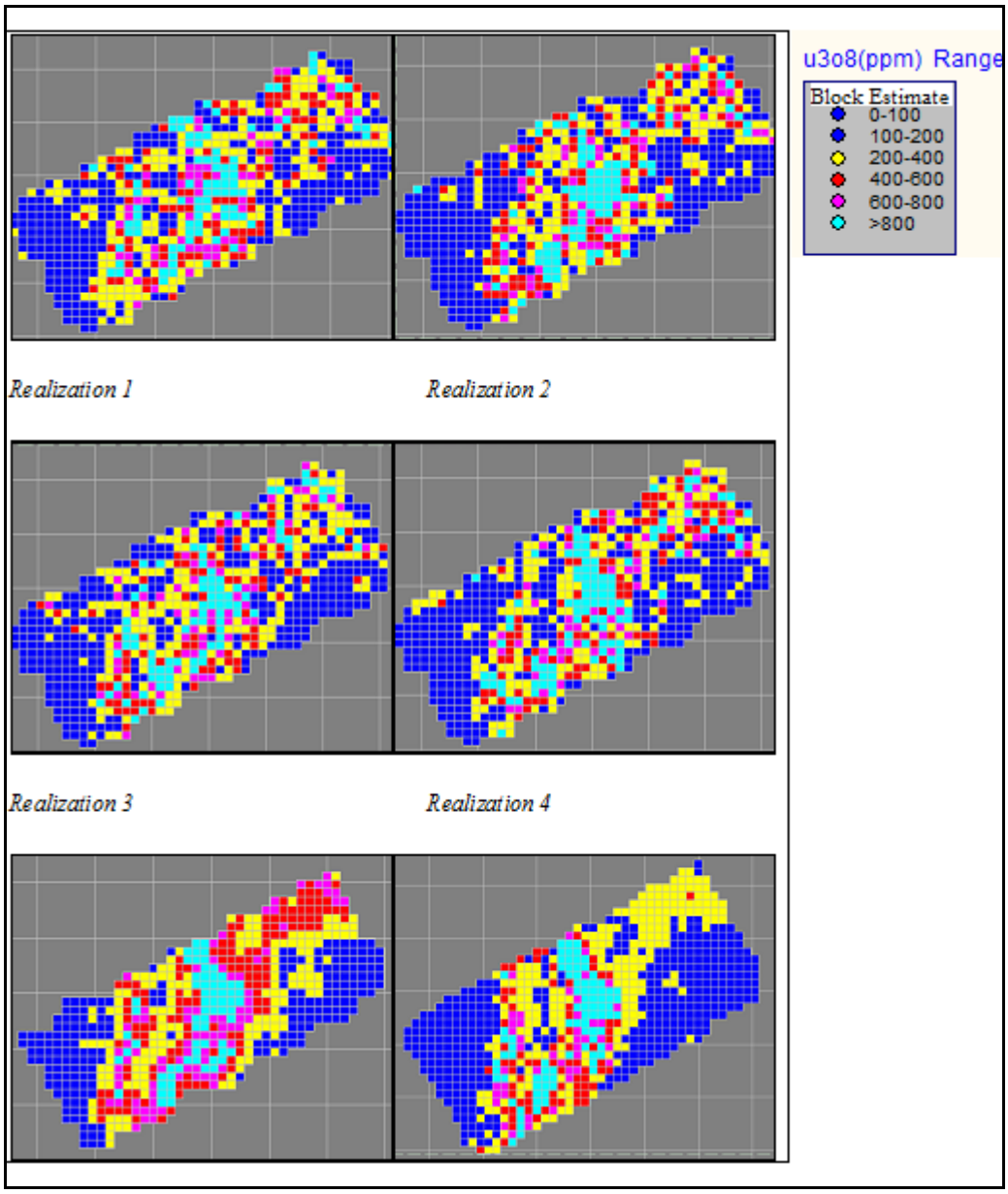


Figure 1.6: Individual simulated realizations of grade distribution at Kayelekera mine and a comparison of OK and an average of 100 simulated realizations (last two panels)

From Figure 1.6 it can be noted that any individual simulation realization is different from others and there is minimal degree of smoothing, however, the degree of smoothing in the final estimate derived from averaging 100 realizations is identical to Ordinary Kriging.

Furthermore, Samal (2008) and Schofield (2005) say that when dense sampling, such as blast hole data are available, Ordinary Kriging estimates become closer to actual values, and therefore produce more accurate estimates. Asghari et Al (2009) carried out a comparison between Sequential Gaussian Simulation and Ordinary Kriging for the Choghart iron ore deposit and found out that the estimation results were similar. The high sample density and averaging of several realizations introduces some smoothing in Sequential Gaussian Simulation output, hence similar to Ordinary Kriging.

1.6 General Objective

This research focused on a comparative analysis of estimation results derived from Sequential Gaussian Simulation and Ordinary Kriging geostatistical estimation techniques for Kayelekera Uranium Mine. The aim was to find out which of these techniques give more accurate estimate as well as investigating how the accuracy of the estimates is affected by grade continuity of the data.

Specific Objectives

The specific objectives of the study were to:

- Estimate recoverable reserves using Ordinary Kriging and Sequential Gaussian Simulation on blast hole data sets with high and low grade continuity.
- Compare estimates recoverable reserves estimates from Ordinary Kriging and Sequential Gaussian Simulation techniques using grade distribution

maps, QQ plots, correlation graphs, histograms and cumulative frequency curves.

- Create and compare grade tonnage curves from Ordinary Kriging and Sequential Gaussian Simulation estimates with blast hole data.
- Determine which of the estimation techniques gives more accurate estimates as well as replicating spatial variability of data.

1.7 Thesis Outline

In addition to the Introduction chapter, the research report is made up of six more chapters. Chapter 2 is the literature review which provides background on the theory of geostatistics and recoverable reserve estimation as well as a detailed description of Ordinary Kriging and Sequential Gaussian Simulation and their use for grade control and recoverable reserve estimation. The study compares the two techniques and the differences between the techniques have been reviewed. Chapter 3 describes the methodology and a detailed description of the data used. The chapter also looks at the statistical analysis of the data as well as creating variograms used in estimation and simulation. The estimates from Ordinary Kriging and Sequential Gaussian Simulation are presented in Chapter 4. Results from the estimation and simulation techniques are presented and discussed in Chapter 5. In this chapter, much emphasis is on comparing the two techniques. Ore boundary Maps, QQ plots and cumulative frequency plots were created for comparison purposes. However since these gave visual comparison grade tonnage curves, correlation coefficients were established to quantify comparison of the results. Finally, Chapter 7 contains the conclusions and recommendations.

2 LITERATURE REVIEW

2.1 Chapter Overview

This chapter provides a background review of literature covering geostatistics and recoverable reserve estimation pertinent to the research report. Mathematical derivations of the equations on which the geostatistical techniques are based have also been considered. Lastly, a detailed comparison between Ordinary Kriging and Sequential Gaussian Simulation has been provided.

2.2 Geostatistics and Recoverable Reserve Estimation

Estimating recoverable reserves is one of the important processes in the mining industry during production for grade control as well as mine planning. The main aim of grade control in mines is to differentiate between material that is above cut-off grade and material that is below cut-off grade (Khosrowshahi et al, 2009) through recoverable reserve estimation. Since drilling does not cover the whole area to be mined, recoverable reserve estimation aims at predicting the quality (grade) and quantity (tonnage) over an area where drilling was not done, from a limited number of data. From the estimates, a decision can be made whether to mine the material as ore (above cut-off) or waste (below cut-off). According to Sinclair and Blackwell (2002), the term local/recoverable reserve estimation is not defined rigidly, but is used in the general context of point estimation or the estimation of small blocks or units on the scale of a selective mining unit (SMU). The most important goal is to provide estimates that are accurate and reliable.

In mining, geostatistical techniques are preferred for recoverable reserve estimation compared to other techniques. Since not all areas where mining is done are drilled and sampled, geostatistical techniques were developed to aid in estimating the grade and tonnage of an area based on nearby sample values. According to Matheron (1971) geostatistics has been described as the application of the theory of regionalised variables to the estimation of mineral deposits. Daniel Krige introduced the idea of using geostatistics for local reserve estimation in the mining industry around 1951 (Krige, 1951) and around 1960s George

Matheron further developed his idea. The use of geostatistics in mining industry can be dated to as far as the 1970's (Journel and Huijbregts, 1978; Clark, 1979).

Apart from reserve estimation, geostatistical techniques are also used for mine planning as well as testing the importance of using different types of machinery on the output of the mine (Journel and Huijbregts, 1978). Currently the technique is commonly used in other disciplines like hydrogeology, meteorology and contour mapping (Delhomme and Delfiner, 1973; Royle et al, 1981). In mining, geostatistics' emphasises on the geological context of the data and the spatial relationship between data.

Compared to other methods of resource estimation, geostatistics is a better method for estimating grade and tonnage of the ore reserves. Unlike classic techniques which examine the sample data's statistical distribution, geostatistics incorporates both the statistical distribution of sample data and the spatial correlation between the sample data, hence addressing more earth science problems (Armstrong, 1998). Geostatistical techniques use the variogram, which rely on the spatial distribution and internal structure of data and not on the actual values only. If the variogram is good (robust) it provides estimates that are a good representation of spatial distribution of the input data (Samal, 2008). The technique is based on the theory of regionalised variables, which states that the interpolation from points in space should not be based on a smooth continuous object (Matheron, 1971). Unlike classical statistics that considers grade to be randomly distributed, geostatistical techniques consider the changes of mineralisation in relation to the trend direction of the ore body. It also considers the area of influence and continuity or lack of continuity of mineralisation within the ore body. Other techniques like inverse distance weighting and polygonal estimation do not provide a measure of the accuracy of estimates, geostatistical techniques provide not only the estimates but also the measure of accuracy of the estimates. Apart from estimated mean grade, it also gives the estimated variance or spread of the grade (Samal, 2008). The estimated variance is used in risk analysis of the reserve estimate especially in Conditional Simulation.

Since the technique takes into consideration spatial relationship as well as giving an estimation error, it is preferred to other classical techniques that do not consider the spatial correlation of data. Isaaks and Srivastava (1989) also mention the smoothing of predicted values based on the proportion of total sample variability that is accounted for; by random noise in geostatistical techniques. It is for these reasons that most mining companies, Kayelekera Mine being one of them, are using these techniques in recoverable reserve estimation grade control processes during mining operations

2.3 Kriging

Kriging is one of the earliest and commonly used techniques in mine operations for grade control purposes especially in estimating grade and tonnage of an area. It has been defined by Sinclair and Blackwell (2002) as a generic term that is applied to a range of methods of estimation that depend on minimising the error of estimation, commonly by a least square procedure. Just like all geostatistical techniques, the basis of the technique is on the assumption that the variable to be estimated is a regionalised variable i.e. samples are related in space. The technique is applied upon meeting underlying assumptions of second-order stationarity which implies that at a minimum the mean and variance of the sample data remain invariant in space (Journel and Huijbregts, 1978; Samal, 2008). This means that the mean for the data must be constant at any location. To ensure that the weight functions are based on the variation of the observed variable as a function of its distance, kriging makes use of the variogram (Clark, 1979)

The advantage of using kriging as an estimation technique is that, kriged estimate is accompanied by a corresponding kriging standard deviation (Clark, 1979). Furthermore, the maps and/or calculations of the standard errors can be produced without actually taking the samples. The technique relies on the spatial relationship of the data. Both kriging and inverse distance weighting rely on distance in assigning weights, however in kriging, the weights are based on both distances between points and also on the spatial relationship of the points. During estimation, kriging takes into account the relation between samples and also the relationship between the samples and the block, consequently clusters of samples

are not over-weighted (Samal, 2008). With kriging estimation, the variogram model, search parameters and sample number form the basis for assigning kriging weights (Clark, 1979). Kriging uses the variogram, which does not depend on the actual value of data, but rather on its spatial distribution and internal spatial structure. In minimizing the estimation error, it finds combination that is best for sample weights used in kriging process.

The kriging variance obtained from kriging technique can be used in classification of resources. Based on how information has been used to estimate each block, the kriging variance can be used to rank the blocks of the resource model. This is done by using relative thresholds, since the values do not have any physical or geological meaning. Alternatively visual comparison of the kriging variance can be used for defining resource categories (Rossi and Deutsch, 2014)

Universal kriging, simple kriging, indicator kriging, co-kriging and ordinary kriging are some of the type of kriging techniques (Isaaks and Srivastava, 1989). These techniques have been categorised into two, linear kriging of which Ordinary Kriging is one example and non-linear Kriging which includes indicator kriging and disjunctive kriging (Samal, 2008). However, the choice of technique to use is mainly dependent on the type of the deposit, homogeneity of the data and what one is trying to achieve i.e. is it only the mean of the data or the whole distribution of data values, is it global estimates or local estimate and is it point estimate or block estimate (Isaaks and Srivastava, 1989).

2.3.1 Ordinary Kriging

Ordinary Kriging (OK) is one of the estimation techniques commonly used in mining for grade control for mineral resource estimation. The technique is considered to be linear interpolator since it is based on the linear weighted average and assumes that the mean of the data is constant but also not known (Clark, 1979; Samal, 2008) and its equation has been defined as in equation 1:

$$Zx^* = \sum wiZ(xi) \tag{1}$$

The Zx^* is the kriged estimate and w_i is the weight assigned to the sample Z at location x_i. $\sum wi$ is the sum of kriging weights and they must sum to one to ensure that there is no biasness by filtering out the unknown local mean.

The distance from estimation point and spatial correlation of the samples greatly influence the sample weight values. In ordinary kriging, the spatial correlation structure of the data influences the weighting of neighbouring data points rather than by power of their inverted distance like in inverse distance weighting method. Upon close evaluation the kriging approach is very similar to inverse distance weighting method. However, the major difference is that Ordinary Kriging weights are assigned based on the variogram model thereby taking the spatial relationship into consideration.

The steps in Ordinary Kriging estimation have been outlined by (Clark, 1979; Isaaks and Srivastava, 1989) and are presented in the next section.

- The first step involves constructing an experimental variogram and fitting a model variogram from the data set that is to be interpolated. The constructed variogram and values at sampled locations are used to estimate values at unsampled locations.

- From the constructed variogram weights are calculated using the equations as follows:

$$w_1 S(d_{11}) + w_2 S(d_{12}) + w_3 S(d_{13}) + \ldots + w_n S(d_1 n) = S(d_{1p})$$

$$w_1 S(d_{21}) + w_2 S(d_{22}) + w_3 S(d_{23}) + \ldots + w_n S(d_2 n) = S(d_{2p})$$

$$w_1 S(d_{31}) + w_2 S(d_{32}) + w_3 S(d_{33}) + \ldots + w_n S(d_3 n) = S(d_{3p})$$

……

$$w_1 S(d_{n1}) + w_2 S(d_{n2}) + w_3 S(d_{n3}) + \ldots + w_n S(d_{nn}) = S(d_{np}) \quad (2)$$

Where $S\ (d_{np})$ is the model variogram evaluated at a distance equal to the distance between points *n* and *p*. For example, S (d_{1p}) is the model variogram evaluated at a distance equal to the separation of points *1* and *P*, w_1, w_2, w_n are weights assigned to sample at location 1, 2 and n respectively. Since it is necessary that the weights sum to one, another equation is added:

$$w_1 + w_2 + w_{3+\ \ldots +}\ w_n = 1.0 \qquad (3)$$

Since there is more than one equation and unknowns, a slack variable, λ, called Lagrange multiplier is added to the equation set. The Lagrange also helps in minimizing possible estimation error. The final set of equations is as follows:

$$w_1 S\ (d_{11}) + w_2 S\ (d_{12}) + w_3 S\ (d_{13}) + \ldots + w_n S\ (d_1 n) + \lambda = S\ (d_{1p})$$

$$w_1 S\ (d_{21}) + w_2 S\ (d_{22}) + w_3 S\ (d_{23}) + \ldots + w_n S\ (d_2 n) + \lambda = S\ (d_{2p})$$

$$w_1 S\ (d_{31}) + w_2 S\ (d_{32}) + w_3 S\ (d_{33}) + \ldots + w_n S\ (d_3 n) + \lambda = S\ (d_{3p})$$

……

$$w_1 S\ (d_{n1}) + w_2 S\ (d_{n2}) + w_3 S\ (d_{n3}) + \ldots + w_n S\ (d_{nn}) + \lambda = S\ (d_{np})$$

$$w_1 + w_2 + w_{3+\ \ldots +}\ w_n = 1.0$$

(4)

The weights w_1, w_2, and w_3 are calculated from these four equations.

- Ordinary kriging uses weights that are calculated from the variogram in estimation. Now the Z value of the interpolation point can be calculated as follows:

$$Z\ x^* = w_1 z_1 + w_2 z_2 + w_3 z_3 + \ldots + w_n z_n \qquad (5)$$

Where Z x^* is the estimated value, $w_n z_n$ is the weight assigned to sample at location *n* and z_n is the sample value at location *n*

Using the variogram in computing weights helps in minimising the expected error in least square way. It is for this reason that Ordinary Kriging is sometimes said to produce the best linear unbiased estimate and some authors (Isaaks and Srivastava, 1989; Sinclair and Blackwell, 2002; Samal, 2008) have associated Ordinary Kriging with acronym B.L.U.E. standing for **B**est **L**inear **U**nbiased **E**stimator. It is considered to be linear since the weighted linear of data being estimated make up the estimate. The unbiased comes in since there are no residual and estimation errors. Ordinary Kriging is considered to be best since the variance of errors are mostly minimised through linear combination of surrounding sample that are used to make predictions by assigning weights to surrounding samples. The estimation variance can be calculated as follows (Clark, 1979; Isaaks and Srivastava, 1989):

$$z_{\sim}^{2} = w_1 S(d_{1p}) + w_2 S(d_{2p}) + w_3 S(d_{3p}) + \lambda \quad (6)$$

Where $z_{\sim}^{2}$ is the estimation variance, w_1 is the weight and $S(d_{1p})$ is the variogram value.

Some estimation techniques like inverse distance weighting are also considered to be unbiased as well as linear like the Ordinary Kriging technique, however Ordinary Kriging aims at reducing the error variance hence distinguishes it from these techniques. However, in the process, kriged estimates tend to be smoother than the input data.

2.4 Conditional Simulation

In the context of mining simulation means imitation of conditions (Sinclair and Blackwell, 2002). It is conditional if the resulting realizations honour the actual/original data at their locations. The method is mainly used for continuous variables like grade, height and age and its basic principle is to obtain an appropriate simulation of a point and its value must be drawn from its conditional distribution given the values at some nearest points. In the mining industry, it is used in the study of grade continuity, recoverable reserve estimation, optimizing sampling plans for advanced exploration, evaluation of resource estimation

methods (Dowd and David, 1976) and also in mine planning (Sinclair and Blackwell, 2002), mill optimization (Journel and Isaaks, 1984), and financial risk analysis (Ravenscroft, 1992; Rossi, 1999). In mining, it can also be used to assess variability of the spatial distribution of the mineralization, risk sensitivity analysis in the mine planning process and effect of block size on ore variability. During mine production, Conditional Simulation can be used for reconciliation by comparing predicted grades in the resource model with the actual grades sampled at the process plant. In geostatistical simulation, a system of model realisations are generated which present a range of possibilities (Vann et al, 2002). Conditional Simulation generates maps of the grades of mineralisation at a point honouring the sample grades' histogram, the variogram or spatial continuity of the sample grades as well as the grades at sample locations (Deutsch and Journel, 1992). The calculated histogram and variogram of simulated values and sample grades should be similar. Usually it is the small scale ore variation that causes ore misclassification in mining, it is important that these small scale variations are reproduced like in Conditional Simulation, since they affect ore-waste selection process.

In mineral resource estimation, Conditional Simulation was introduced to correct the smoothing effect on estimates other techniques like Ordinary Kriging have on estimates (Matheron, 1971). As an estimation technique, it creates a pattern of values with the same statistical and spatial characteristics similar to true grades. In so doing, smoothing of data is minimised. Unlike other estimation techniques, the uncertainty attached to each estimate can be known when Conditional Simulation has been used. When assessing uncertainty attached to the prediction of a variable, or when realistic scenarios are required for post-processing algorithms, for instance, simulation of production, the spatial Model can be used for simulation purpose rather than estimation (Rambert, nd). Unlike kriging, simulation generates a series of realistic outcomes, having equal probabilities with each outcome honoring the input data, the spatial model and also the distribution model. Simulation has to reproduce statistical and geostatistical characteristics of variability (histogram and variogram) of the data (Vizi, 2008). Consequently, geostatistical simulation generates a set of values forming one of infinite possible

realizations which has simulated values having the same model of variogram as the experimental one and simulated values following the same distribution as the experimental ones.

It is not uncommon for estimates to have some error or uncertainty since predictions can be inaccurate. Some of the errors can be due to widely spaced data used, geological variability, some approximations made in the estimation process and also the limitations of the models used. Apart from resource estimation, Conditional Simulation is considered to be the best option in predicting uncertainty for estimates since the uncertainty can be predicted at different scales by simply averaging up the simulated values (Rossi and Deutsch, 2013). In addition, using a set of simulated realizations obtained by Conditional Simulation, a model of uncertainty at each location can be provided. The model can be examined by predicting the uncertainty at locations where there is data from drill holes or previous production data. Rossi and Deutsch (2013) further states that the probability intervals can then be created by counting the number of times that the true values fall within those intervals, thus determining if the predicted percentage is verified. The uncertainty model depends on the Random Function model used and can be used to characterise risk. In grade control risk analysis is used in making economic decisions, through evaluating the consequence of grade uncertainty and the best choice is considered based on the maximum profit or minimum loss choice. Furthermore, the uncertainty model as described by the realizations provides all the information required to optimize decision-making under uncertainty (Rossi and Deutsch, 2013). Techniques like Ordinary Kriging do not allow the confidence interval to be calculated using its variance. However, simulations can be used to build confidence intervals empirically, since many different simulations of a variable are calculated, there is information at each point, and there is access to a complete empirical distribution (histogram); therefore being able to evaluate the probability for a given variable to take a value belonging to a given interval (Vann et al., 2002). The main objective is to reproduce the variance of the input data, both in a univariate sense and spatiality through the histogram and the variogram or other covariance model respectively. Consequently, Conditional Simulation provides an appropriate platform to study

any problem relating to variability, in such a way that other techniques like kriging cannot (Vann et al., 2002).

Sinclair and Blackwell (2002) summarises the procedure as generating a number of realisations of the same location in space. These individual simulations at each point give a probability distribution for the grade at a specific point. These distributions are then used in many ways of which estimation of the probability that the grade is above a certain cut-off grade at a particular point is one of the uses. One of them is where the distributions in a specified block are combined and averaged to estimate the grade of that particular block or the probability that the block grade is above a certain cut-off grade. Some of the simulation techniques that are used in mining industry are Turning Bands, Sequential Gaussian and Sequential Indicator simulation. In the study Sequential Gaussian Simulation was used.

2.4.1 Sequential Gaussian Simulation

There are many simulation algorithms but Sequential Gaussian Simulation (SGS) is one of the simplest and widely used. Kriging gives estimate of both mean and standard deviation of a variable at a point, hence the variable at each point can be represented as a random variable following a normal distribution. SGS uses a random deviate from the normal distribution selected according to a uniform random number representing the probability level rather than the mean as an estimate (Bohling, 2005c).

Sequential Gaussian Simulation creates realizations of normal random variables and performs a Gaussian transformation of the data. A simulated value at a visited point is randomly drawn from the conditional cumulative distribution function, defined by the kriging mean and variance, based on neighbourhood values. At a new randomly visited point, the simulated value is conditional to the original data and previously simulated values. Finally, the simulated normal values are transformed back into the simulated values for the original variables. The process is repeated until all points are simulated for each realization throughout the grid (Deutsch and Journel, 1992).

The basic steps in Sequential Gaussian Simulation have been outlined by Sinclair and Blackwell (2002); Deutsch and Journel (1992) as:

1. Calculate histogram and statistical parameters of raw data. This helps in understanding the characteristics of data such as grade distribution.

2. Transform data into Gaussian space, this helps to preserve the global distribution of data

3. Calculate and model variogram using the normal transformed data.

4. Define a grid.

5. Choose a random path.

6. Krige a value at each node from all other values (known and simulated) to get mean ($Y^*(\mathbf{u})$) and its corresponding kriging variance ($\sigma^2_{SK}(\mathbf{u})$)

$$Y^*(\mathbf{u}) = \sum_{\beta=1}^{n} \lambda_\beta \, .Y(\mathbf{U}_\beta) \qquad (7)$$

$$\sigma^2_{SK}(\mathbf{u}) = C(0) - \sum \lambda\alpha \, C(u, u\alpha)| \qquad (8)$$

7. Draw a random value from Gaussian distribution which is known as simulated value. Draw a random residual $R(\mathbf{u})$ that follows a normal distribution with mean of 0.0 and variance of $\sigma^2_{SK}(\mathbf{u})$

8. Add the kriged estimate and residual to get simulated value:

$$Y_s(\mathbf{u}) = Y^*(\mathbf{u}) + R(\mathbf{u}) \qquad (9)$$

It should be noted that $Y_s(\mathbf{u})$ can as well be obtained by drawing from a normal distribution with mean $Y^*(\mathbf{u})$ and variance of $\sigma^2_{SK}(\mathbf{u})$. $R(\mathbf{u})$ corrects for missing variance. In essence, simulated values are kriged estimates plus random component that corrects for smoothing in data and missing variance (Deutsch and Journel, 1992)

9. The simulated value, Y_s (**u**) is added to the set of data to ensure that the covariance with this value and all future predictions is correct. This is the main idea behind sequential simulation, that is, to use previously simulated value as data so that the covariance between all simulated values is reproduced.

10. Simulate other nodes sequentially i.e. visit all locations in random order to avoid artifacts of limited search.

11. Back transform simulated value (in this step, a realization is generated).

12. To generate another realization, step 1 till 9 are repeated.

It should be pointed out that if a planned sequence is retained during simulation (step 10), there is a possibility of creating an artificial continuity. A random sequence ensures that no artificial structures are introduced in the data and that there is a significant difference to each simulation. The locations are visited randomly to avoid potential artifacts and to maximize simulation variability. Previously simulated nodes ought to be used as data values in kriging process, hence the proper covariance structure between the simulated values is preserved. To simulate another point, it is only measured data and previously simulated points that fall within the search radius that are used. Figure 2.1 shows a flow diagram of Sequential Gaussian Simulation process.

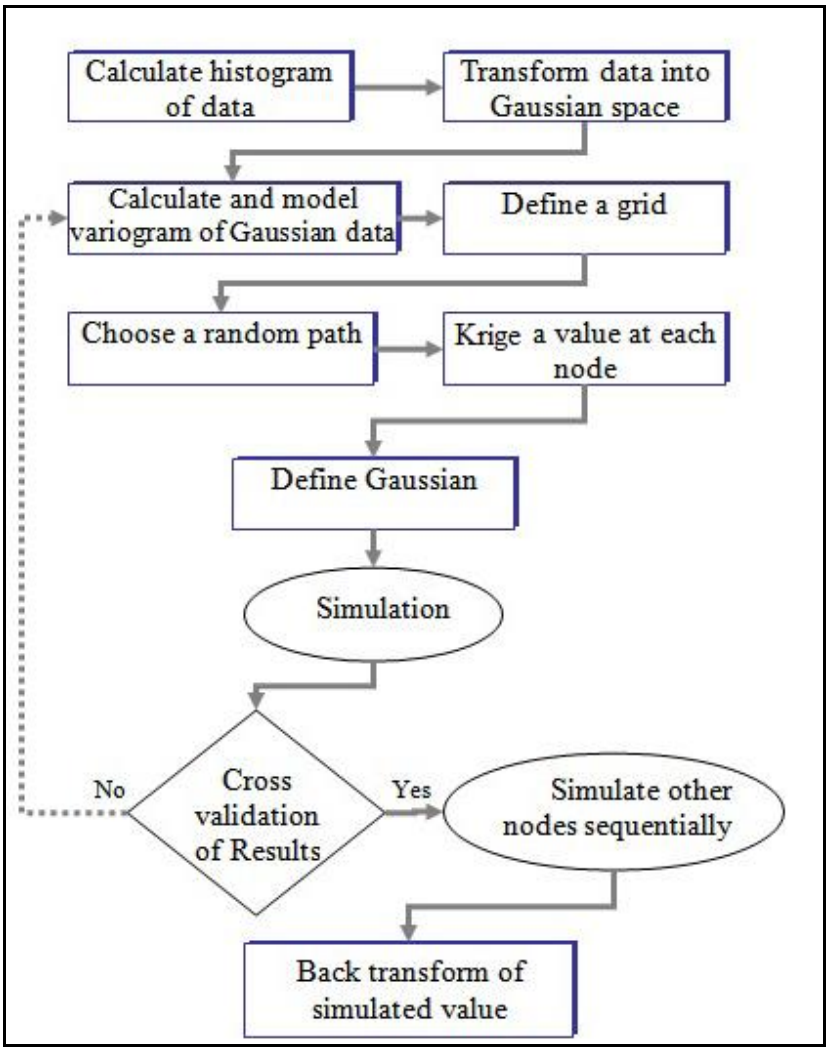


Figure 2.1: The basic steps in SGS algorithm (Deustch and Journel, 1992 and Asghari et al, 2009)

2.5 Variogram Analysis

The common characteristic of geostatistical techniques in estimation is the use of a variogram to quantify spatial variability of data under study. A variogram is an important tool used to measure spatial variability of data. It shows the variability of grade with its corresponding distance in an area of study. According to Clark (1979) a Variogram is defined as the graph (and/or formula) describing the expected difference in value between pairs of samples with a given relative orientation. Common descriptive statistics and histogram do not identify nor quantify the spatial relation (roughness) of data, which is achieved through the

variogram. The main two processes carried out during variogram analysis are calculating the experimental variogram from the data and modelling the experimental variogram by fitting it to the data. The experimental variogram is calculated by averaging one half the squared differences of the z-values over all pairs of observations with the specified separation distance and direction (Barnes, 2005; Clark, 1979). While the experimental variogram are used to measure the spatial variability of a variable in different directions, variogram map are created to find main directions of anisotropy of the data set.

Since sampling is not done in the entire area of study, the experimental variogram is only calculated where sampling was done and data is available. The results are then plotted on a two dimensional graph. After calculating and plotting the graph, a model is then fitted to the graph; in the process the spatial structure for the whole area under study is obtained including areas where data was not available. According to Clark (1979) a variogram is calculated using:

$$2\gamma^{*}(h) = 1/n \sum [g(x) - g(x+h)]^{2} \qquad (10)$$

"The '2' in front of the γ* is there for mathematical convenience. The term γ *(h)* is called the semi-variogram (although some authors would call it the variogram), and γ**(h)* is the experimental semi-variogram; γ* bears the same relationship to γ that a histogram does to a probability distribution." (Clark, 1979:8).

As the separation distance for the samples increases correlation between samples becomes less and variance increases, since the variogram measures the data's variability, its values increases as well. Three main types of variogram are Exponential, Spherical and Gaussian (Isaaks and Srivastava, 1989; Bohling, 2005a). Figure 2.2 shows the three types of variogram models (Bohling, 2005a).

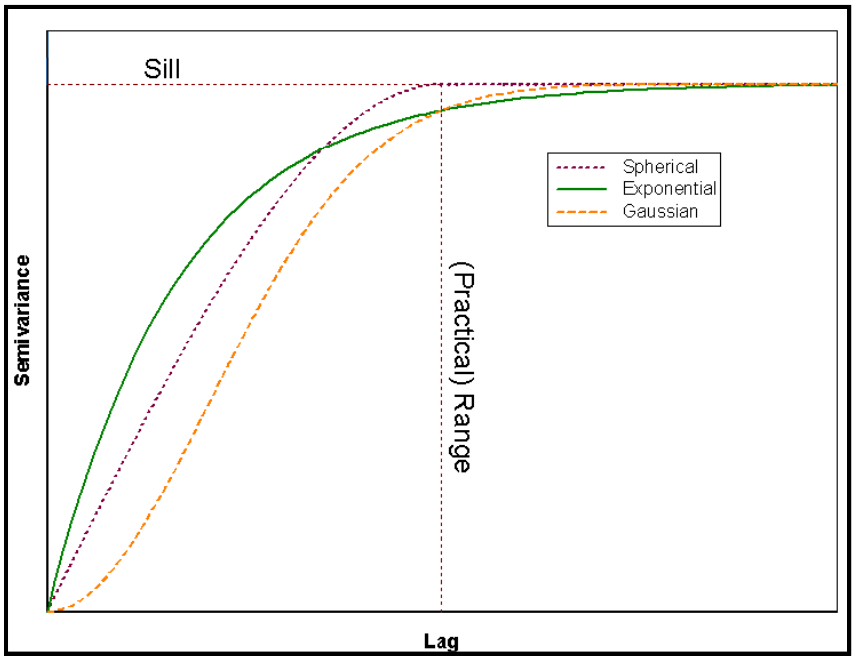


Figure 2.2: Types of variogram models

One of the differences is how they reach the sill, while exponential variogram model reaches its sill at an infinite distance, spherical model reaches its sill at a finite distance (Bohling, 2005a). Generally the spherical model indicates a high degree of spatial continuity in grades. At the beginning it has a linear shape and towards the sill it flattens out.

2.6 Comparison of Ordinary Kriging and Conditional Simulation

Conditional Simulation and Ordinary Kriging are techniques commonly used in mines for resource estimation. Just like other geostatistical techniques, both techniques use variogram in determining spatial relationship of data. Estimation errors through the kriging variance and block variance are provided along with the kriged estimates (Samal, 2008). The kriging variance forms the basis for Conditional Simulation. Although both techniques are used to provide estimates, their main goals are different. Kriging aims at providing unique estimates which minimize the local estimation variance while Conditional Simulation's purpose is to provide a set of maps of say the grade, which honours the known reality and are

likely to represent unknown reality at any location (Schofield, nd). Its ability to represent the spatial continuity of high grades and local variability of grades makes Conditional Simulation a better technique over Ordinary Kriging.

Whilst the techniques are commonly used for resource estimation, Conditional Simulation also provides a direct way of quantifying the uncertainty in knowing true grade of mining unit attached to an estimate in the form of a histogram unlike Ordinary Kriging. Since Conditional Simulation generates several simulations of the grade of the deposit, there is direct access to a histogram of possible grade for any particular point in the deposit. Furthermore each value generated is independent of other values generated in other simulations and is more likely to be the true grade value at that particular location (Schofield and Rolley, 1997). This makes Conditional Simulation a better technique than Ordinary Kriging in describing local uncertainty of the grade mineralisation through direct access to the grade distribution through averaging of simulated values. Although kriging variance may be used to provide description of the uncertainty, it requires an assumption about the shape of the histogram of possible grades which practically is not realistic (Schofield and Rolley, 1997).

Another limitation of kriging variance is that it assumes that the estimation variance is independent of the magnitude of grade being estimated, contrary to most mineral deposits which have variability of grades directly related to magnitude of grade (Schofield and Rolley, 1997). This becomes a limitation on using kriging variance to describe uncertainty in knowing the true grade of mining unit. It does not allow assessment of risk associated with the resource. Somehow, simulations attempts to sample at unknown location using constraints like statistical moments of data, thereby the requirements of stationarity are stricter than that of kriging (Vann et al., 2002)

Although Ordinary Kriging is considered to be the Best Linear Unbiased Estimator, the smoothing effect it has on estimates is one of the technique's main disadvantages. Local variability is not preserved as a result of smoothing, and does not reproduce the histograms of the original data well like Conditional Simulation.

On the other hand, Conditional Simulation honours the original data and has less smoothening effect on estimates and preserves local variability. However with increasing sampling density like that of blast hole data, maps from both Ordinary Kriging and Conditional Simulation gradually become similar to the true map of reality because they both honour the sample values at the sample locations (Asghari et al, 2009; Deustch and Journel, 1992; Schofield and Rolley, 1997).

2.7 Chapter Summary

This chapter looked at the use of geostatistical techniques in the estimation of resources, specifically Ordinary Kriging and Sequential Gaussian Simulation estimation techniques. As one of the most important tool in defining spatial variation of samples in relation to their separation distance, a variogram was discussed. One of the similarities between OK and SGS techniques is the use of variogram in determining spatial relationship of data. However, Kriging is considered to be the Best Linear Unbiased Estimator and it also has a minimum error variance hence considered to be more reliable. The smoothing effect it has on estimates is one of the technique's major disadvantages, and is also inherent in OK. Local variability is not preserved as a result of smoothing, and does not properly reproduce the histograms of the original data. On the other hand, SGS honours the original data and has less smoothening effect on estimates and preserves local variability, hence it is a preferred estimation technique at KM. Advantages and disadvantages of both OK and SGS have been summarised in Table 2.1

Table 2.1: Advantages and Disadvantages of SGS and OK

Advantages of Ordinary Kriging	**Disadvantages of Ordinary Kriging**
• Gives minimum error variance	• Produces smoothed estimates
• Gives estimation error/kriging variance for the estimate	• Does not reproduce histograms and does not preserve local variability
• Helps to compensate for the effects of data clustering by treating clusters like single points	• Does not allow assessment of the risk associated with resource-estimation
• Locally accurate and appropriate for visualisation of trend	• Inappropriate for evaluation where the extreme values are important
• Honours local data with discontinuity	
Advantages of SGS	**Disadvantages of SGS**
• Less smoothing of estimates	• High estimation error when individual simulation is used
• Reproduces histograms and better representation of local variability in so doing provides more realistic estimates	• If large number of realisations are to be used, it can create a problem with data management
• Honours spatial variability of data sets	• There is wide range of variability between simulations if conditioning data used is inadequate
• Assessment of global uncertainty can be done	• Needs caution in interpreting confidence limits calculated from post processing simulation since uncertainty in the conditioning data can sometimes be large
• Appropriate for data with extreme values since it reproduces the extreme values as well as their variability	• Selection of small search neighbourhood can lead to poor conditioning and replication of variogram

3 METHODOLOGY

3.1 Chapter Overview

As part of this research two separate areas, with slightly different elevations, Area A and Area B (shown in Figure 3.1), within the Kayelekera pit were selected in which to carry out the comparison between the local reserve estimation techniques using Ordinary Kriging and Sequential Gaussian Simulation. The grade distribution of uranium mineralisation in the pit is controlled mainly by the geology, the conditions of geochemical disequilibrium in the host rocks, the local concentration of uranium along fault lines, and the cross-cutting structural features. As a result, Areas A and B (Figure 3.1) have quite dissimilar uranium grade distributions. As a result of the combination of geology, lithology and structural features, Area A has better grade continuity than Area B. Area A shows better grade continuity with minimal change in grade between adjacent holes. Area B displays less grade continuity with abrupt changes in grades between adjacent blast holes being evident.

The study involved comparing the outcomes for Conditional Simulation and Ordinary Kriging estimation techniques on Areas A and B which demonstrate different grade continuity. Hellman and Schofield's MP software was used for the geostatistical analyses, while some of the spatial displays and image manipulations were done using Microsoft Excel and Micromine software.

3.2 Data Collection

The areas were located on different elevations, Area A was from 930rl while Area B was from 912rl. The pit locations of these areas have been shown in Figure 3.1. The drill spacing for both areas was 3m by 4m with an average depth of 7.2 meters including sub drills. All drill holes were vertical and sample collection was done at every meter down the hole.

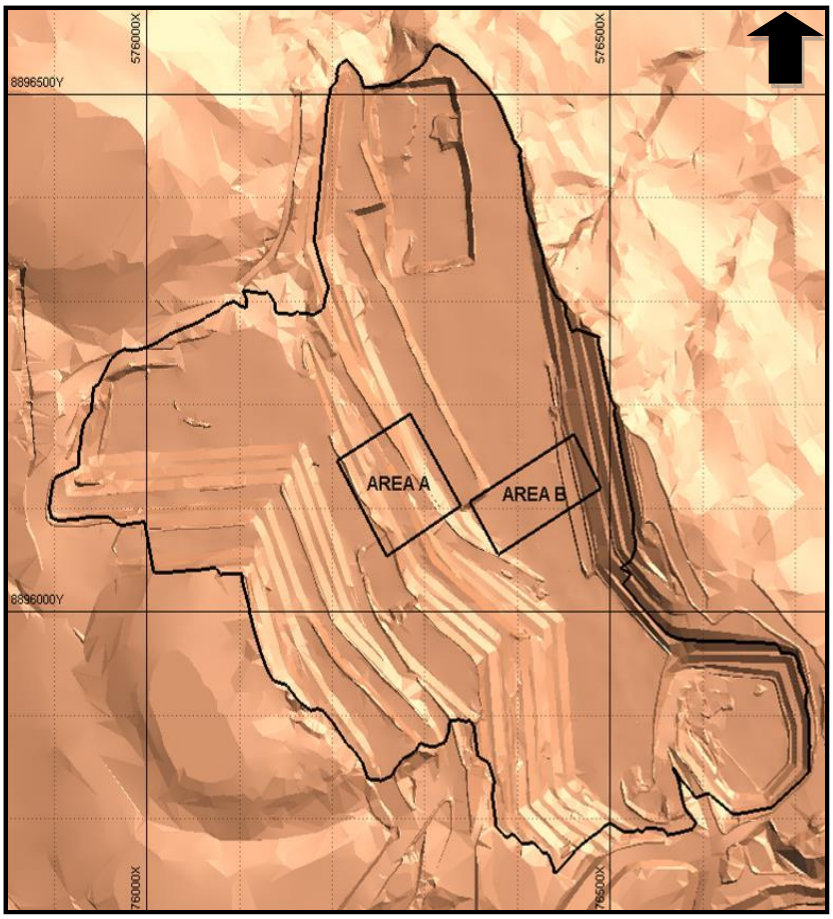


Figure 3.1: Location of Study Areas A and B within the open pit mining operations

The choice of these areas was largely dependent on the continuity of uranium grade. Uranium is mobile in an oxidised environment leaching out and re-depositing in a reduced environment. This leaching of the oxidised arkose leads to inconsistent uranium distribution and less continuity of grades. In contrast the lower mobility of uranium in reduced arkose means that uranium grades are more consistent and continuous. For these reasons, three different variables were collected from each blast hole. The variables measured included gamma radiation data, XRF assay data and lithology data.

Gamma radiation, measured in counts per second (CPS) over 5cm intervals in drill holes in both areas was logged and converted to the equivalent Uranium Oxide (eU_3O_8) grade concentrations. An Auslog detector attached to a probe was used for measuring the total Gamma radiation (counts) emitted by uranium in the

holes. The machine measures gamma every 5 cm, this was composited into one meter using Micromine software to have one meter interval equivalent uranium grade data like lithology and XRF data.

A handheld X-Ray Fluorescence (XRF) machine was used to collect a second data set consisting of assay data gathered from samples taken in the pit to determine the Uranium content of each sample. Unlike the gamma logging tool, the XRF machine measures the actual uranium (U) in the sample. The XRF machines were calibrated using certified standard material before the sample analysis.

Equivalent Uranium grade gamma logging was compared with the XRF assay values. The scatter plots in Figure 3.2 indicate a positive linear relationship between gamma values and XRF values for both Area A and Area B. As the Gamma value increases, XRF assay values also increase, indicating a positive correlation.

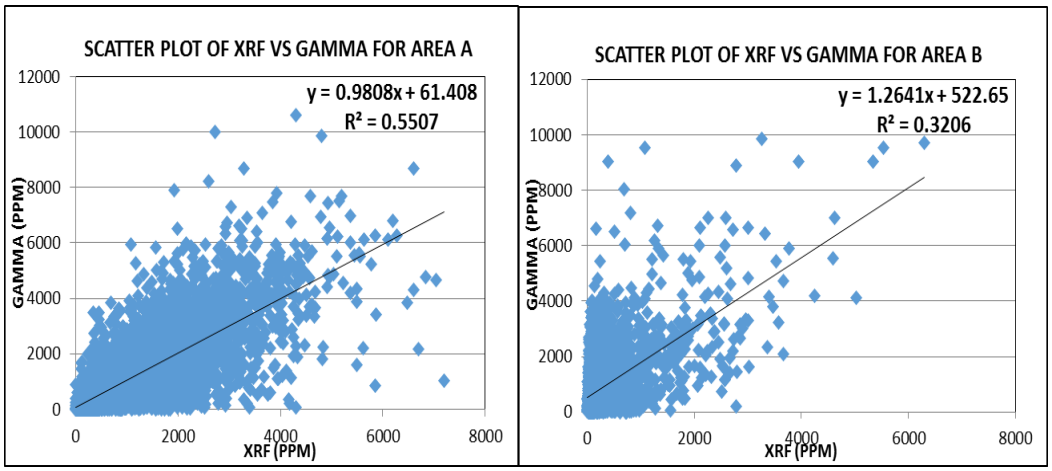


Figure 3.2: Gamma vs. XRF Scatter Plots for Area A and Area B

Area A data shows a large error component due to the broad spread of the data, but very little in the way of a bias. Area B data contains error and strong positive bias because the data is shifted off to one side of the 45 degree line. The third variable collected was lithological information. Geological logging was carried out on each sample, describing lithology type and the redox state of each sample, i.e. if it is reduced (AR), oxidised (AO) or mudstone (MD). The geological information collected was used to determine which type of data and which

conversion factors in case of Gamma data have to be applied in each sample. Table 3.1 shows the number of samples and ore type for both areas.

Table 3.1: Lithology of Samples from Area A and B

AREA A	
Ore Type	**Number of Samples**
AR	3054
AO	93
MD	1139
AREA B	
Ore Type	**Number of Samples**
AR	138
AO	2302
MD	1452

A cross sectional view of the geological description of the rock samples for Area A and Area B have been shown in figure 3.3 and 3.4 respectively. The figures shows drill holes with total depth of 6 meters, and in some cases where there are some sub drills, it shows a depth of more than 6 meters. Area A contained more reduced arkose (AR) and Mudstone (MD) than Area B which contained more oxidised arkose (AO).

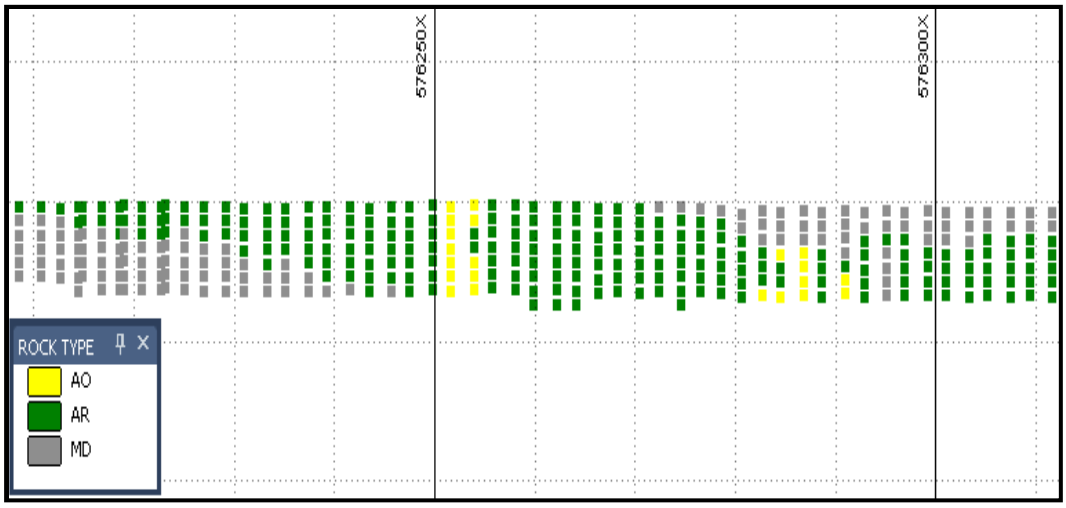


Figure 3.3: Geology sectional view of drill holes samples for Area A

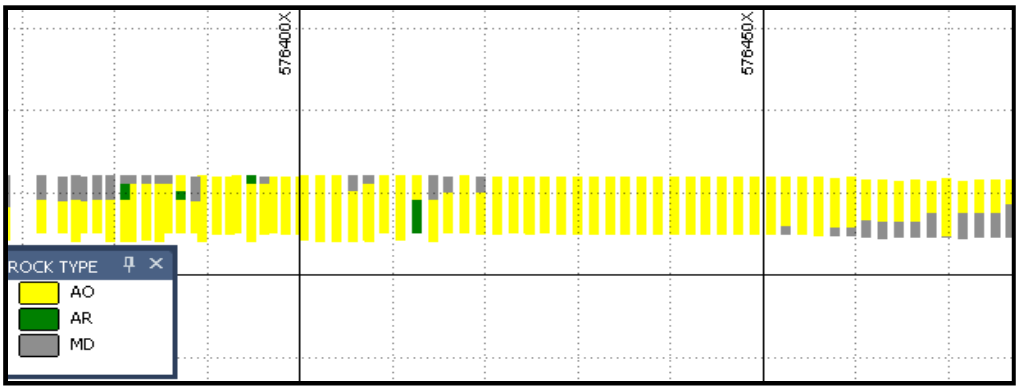


Figure 3.4: Geology sectional view of drill holes samples for Area B

Since three variables were collected, each sample had geological description and was also measured for XRF (assay) data and Gamma (equivalent Uranium grade) data as illustrated in Figure 3.5 taken from three drill holes.

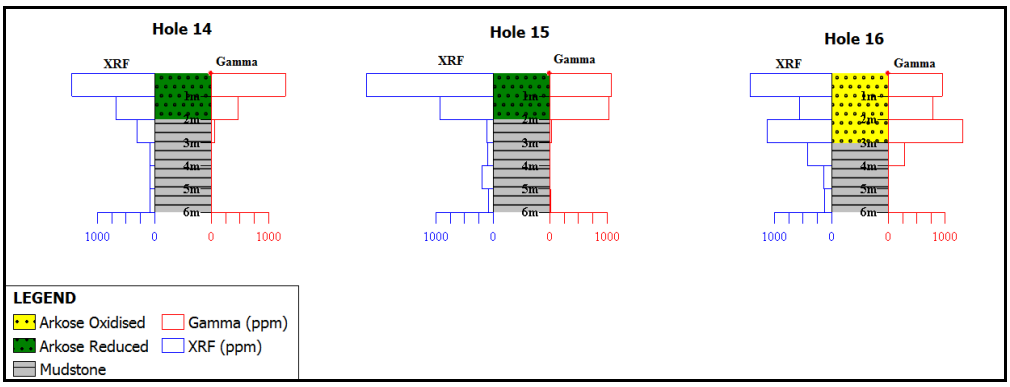


Figure 3.5: **Drill hole with geology, XRF and Gamma logged for each depth**

The lithological data was used to determine if, within a particular depth, XRF or Gamma data should be used in the analysis. When the lithology of the associated sample showed oxidised arkose (AO), XRF data was used, whereas when it was found to be reduced arkose (AR) or mudstone (MD), the gamma data was used. Due to leaching out of uranium in oxidised arkose, there is an increase in uranium daughter products. These are more readily detected by the probe during gamma logging than actual uranium. As a result, the gamma data returns misleadingly high grade "uranium" values and consequently XRF data is preferred since it measures the actual uranium in the sample (Bowden and Shaw, 1991; Barrett, 2005).

The Lithology, XRF and Gamma data were combined into one Micromine file, called Consolidated File as in Table 3.2, to calculate final grade (U_3O_8) to be used in estimation. The table shows different factors that were applied to the reduced arkose and mudstone to achieve the correct U_3O_8 value. These were standard factors used at the mine and were developed by (Barrett, 2005) in his study of disequilibrium state of the Kayelekera deposit.

Table 3.2: Sample of Consolidated file

Hole ID	From	To	Rock Type	XRF (ppm)	Gamma (ppm)	Conversion Factors	Final U_3O_8
14	0	1	Reduced Arkose	1449.55	1299.03	Multiply Gamma by **1.2**	1558.8
	1	2		678.54	465.60	Multiply Gamma by **1.2**	558.72
	2	3	Mudstone	300.79	59.71	Multiply Gamma by **1.4**	84.20
	3	4		81.91	5.64	Multiply Gamma by **1.4**	7.95
	4	5		84.65	0.41	Multiply Gamma by **1.4**	0.58
	5	6		82.19	1.80	Multiply Gamma by **1.4**	2.54
15	0	1	Reduced Arkose	2223.23	1076.85	Multiply Gamma by **1.2**	1292.2
	1	2		926.35	1033.41	Multiply Gamma by **1.2**	1240
	2	3	Mudstone	102.95	29.90	Multiply Gamma by **1.4**	42.15
	3	4		86.91	2.00	Multiply Gamma by **1.4**	2.82
	4	5		191.49	3.60	Multiply Gamma by **1.4**	5.08
	5	6		79.79	8.98	Multiply Gamma by **1.4**	12.66
16	0	1	Oxidised Arkose	1432.62	946.44	Multiply XRF by **1**	1432.6
	1	2		564.97	778.94	Multiply XRF by **1**	564.97
	2	3		1127.26	1312.05	Multiply XRF by **1**	1127.2
	3	4	Mudstone	421.71	287.52	Multiply Gamma by **1.4**	405.40
	4	5		140.58	4.04	Multiply Gamma by **1.4**	5.70
	5	6		115.40	0.92	Multiply Gamma by **1.4**	1.30

DATA SET FOR AREA A

A total of 3901 samples obtained in 487 blast holes were collected from Area A where there was better grade continuity and less spatial variation. Sinclair and Blackwell (2002) provide an example of 'value continuity', meaning that grades are said to be continuous over distances for which they show recognizable degree of similarity. There are more continuous high grade (non-blue) areas and low grade (blue) zones in Area A. Figure 3.6 and Figure 3.7 show the location of blast holes with colours indicating different grade categories in plan and east - west views, respectively. The colour shown in plan view in Figure 3.6 is the grade of the first meter sampled on that particular location. Spatial continuity can be observed from the locations of high and low grades whereby the high grades are located close to each other and low grades are also located close to each other for a large area. The same trend applies to down hole grades as seen from Figure 3.7, it can be observed from the map that from one meter to another the grades are similar, indicating the high continuity of grade.

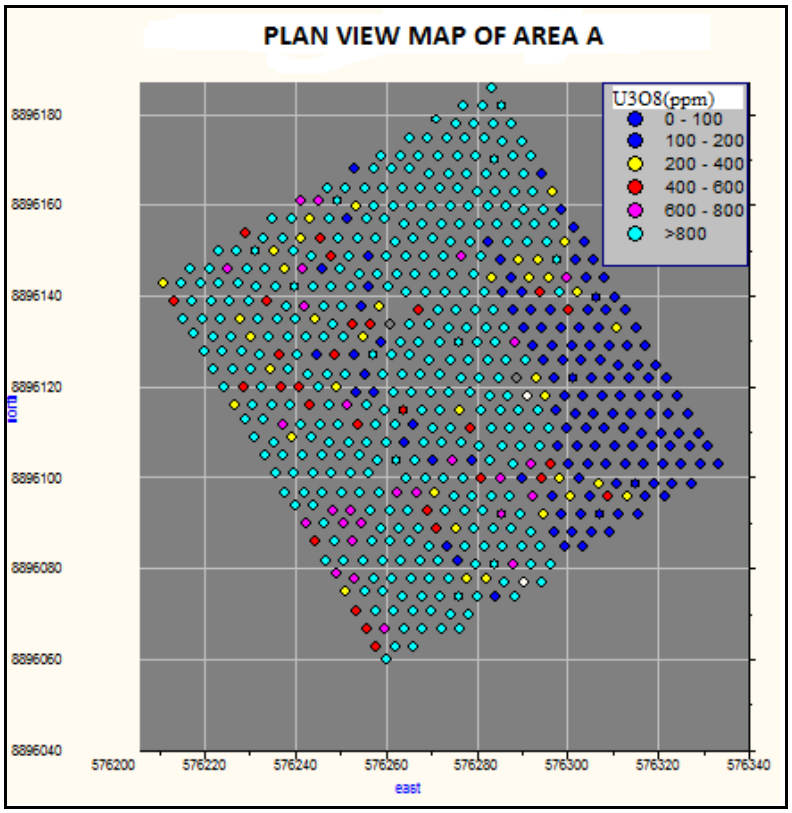


Figure 3.6: Area A drill hole data locations colour coded by U_3O_8 grades

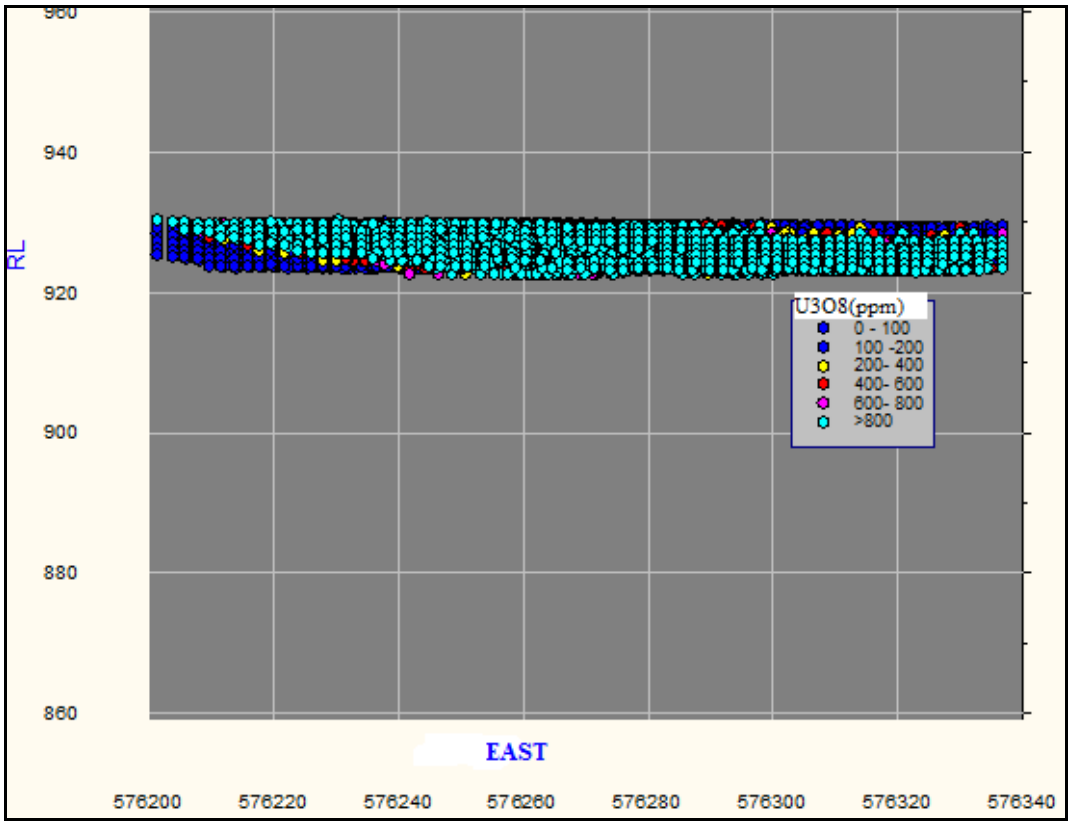


Figure 3.7: Area A drill hole data East – West view(Cross-sectional View)

DATA SET FOR AREA B

The total samples used were 3892 obtained from 480 blast holes. Locations of the blast holes with corresponding grades have been shown in Figures 3.8 and Figure 3.9 in plan and east – west view respectively. From the maps it can be observed that overall grades in Area B are less continuous than in Area A. The change in sample grades from high grade (non-blue) to low grade (blue) is abrupt, as a result of the lithological control of the mineralisation. It can be observed that extremely high grades are close to extremely low grades, this indicates high spatial variability of the grades.

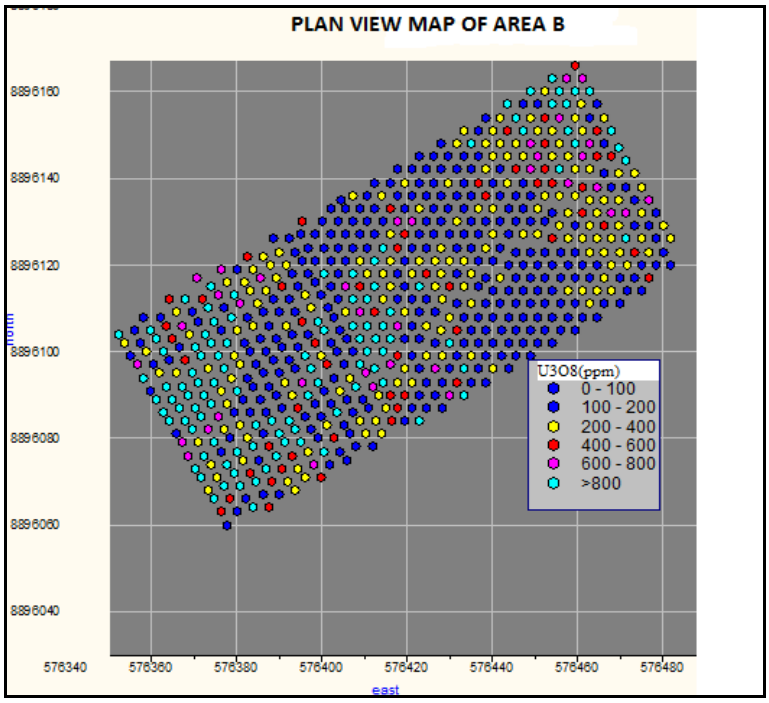


Figure 3.8: Area B drill hole data locations colour coded by U_3O_8 grades

Looking in the Z direction from Figure 3.9, it can be observed that the change in grades from one sample to another down hole is quite significant. Further, the grades are not similar looking at holes close to each other, hence the data was considered to be discontinuous in grade.

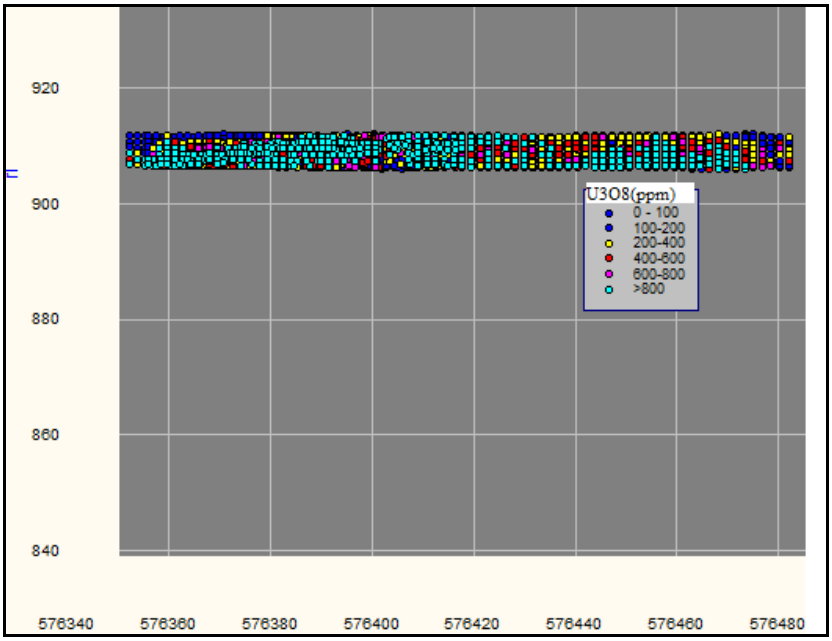


Figure 3.9: Area B drill hole data East – West view (Cross-sectional View)

3.3 Data Validation

Basic errors can be made when collecting data as well as entering the data. These errors may include duplicate records, overlapping intervals, missing records as well as wrong interval length being recorded and these can affect the quality of estimates obtained. Before the estimation process, both data sets were thoroughly checked and edited for errors using Micromine. The data was also plotted to check for points outside the data limits. There were few errors, mainly due to duplicate records from XRF data and it was established that this was a result of analysing the same sample twice.

3.4 Statistical Data Analysis

Statistical analysis of data for Area A and Area B was carried out. Mainly, it included producing histograms, cumulative frequency curves, calculating statistical parameters as well as producing probability plots from the data.

3.4.1 Histograms and Cumulative Frequency Curves

As one way of assessing grade characteristics and distribution of the data sets histograms and cumulative frequency curves were computed. Graphs in Figure 3.10 for Area A and B indicates a positive skewed distribution. The grade distribution indicates high proportion of low grade values and low percentage of high grades with high values which is common in most heavy metals like Uranium.

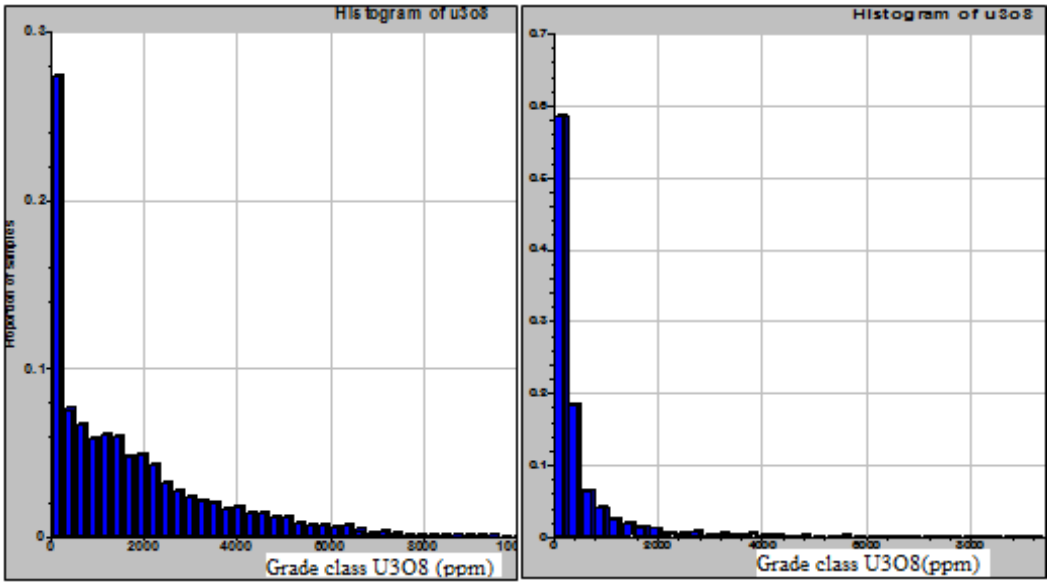


Figure 3.10: **Histograms for U_3O_8 for Area A (Left) and Area B (Right)**

Cumulative frequency curve in Figure 3.11 shows that Area B has a higher proportion of grades below cut off than Area A. At cut-off grade of 400ppm, 30% of the data points are below this grade for Area A, on the other hand 70% are below 400ppm cut-off grade for Area B. These proportions indicate a better mineralisation in Area A than Area B. From the histograms, the data was observed to have a positive skewed distribution which is also why the cumulative curve is not S shaped.

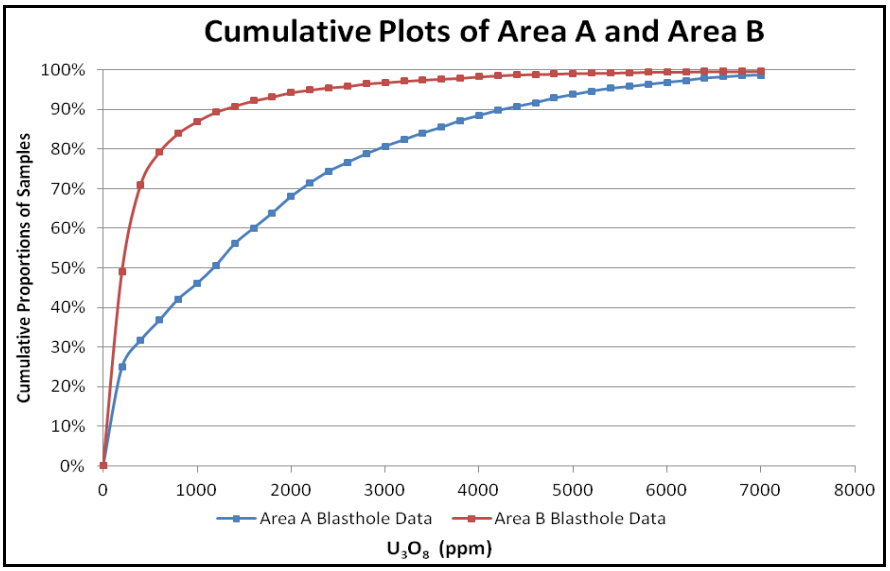


Figure 3.11: Cumulative Histogram of U_3O_8 for Study Area A and Area B

3.4.2 Descriptive statistics

A calculation of statistical parameters for the two areas are summarised in Table 3.3. The median and mode for both data sets were lower than their means confirming the positively skewed distribution of the data sets. The coefficient of variation for Area B is higher than that of Area A, which indicates a higher variability in Area B than A. The higher mean, standard deviation and Median for Area A also indicate that there is a much richer concentrations of U_3O_8 mineralisation than in Area B.

Table 3.3: Descriptive statistics for U3O8 for Area A and B

Statistic Parameter	Area A	Area B
Mean	1663	529
Variance	3172584	885274
CV	1.07	1.78
Minimum	0.03	0.30
Q1	213	109
Median	1165	204
Q3	2466.00	477
Maximum	12721	9831
IQR	2253	368
Std dev	1781	941

3.5 Probability Plots

Probability Plots for the data from Areas A and B were plotted and have been shown in Figures 3.12 and 3.13 respectively. The probability plot for data in Area A is clearly divided into two areas one above 800ppm and one below 800 ppm U_3O_8. These two areas are shown in Figure 3.12. This could be due to data having very low grades and very high grades mineralisation as compared to Area B which had mostly lower grades. The probability plot for Area B suggests that there is only one distribution and therefore only one domain unlike data for Area A.

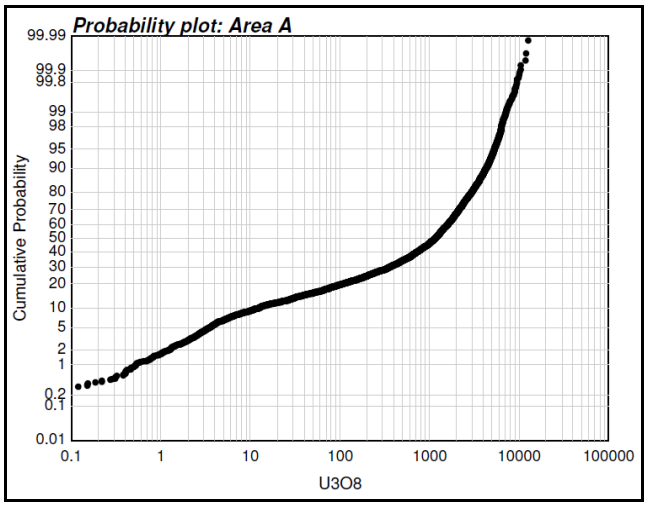


Figure 3.12: **Probability plot for Area A**

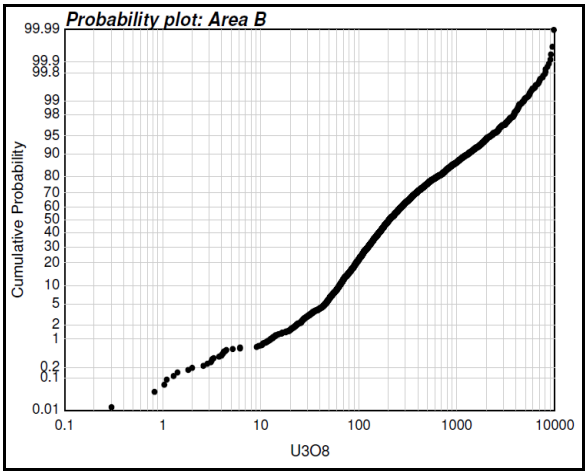


Figure 3.13: Probability Plot for Area B

3.6 Data Domaining

It is not uncommon for data to have different zones of mineralisation in which the average grade and data characteristics are different. If these different mineralisation zones are not separated, they can lead to misinterpretation of mineralisation controls (Coombes, 1997). Probability plots for Area A indicated two distributions, consequently data for the area was domained. Mainly two domains were observed, which are Domain 1 (Dom1) and Domain 2 (Dom2) for grades below 800ppm and grades above 800ppm respectively as in Figures 3.14. To take into account the grade variation in the data, domaining was done in 2 meters benches not the whole drilled six meters. The six meter blast hole data was cut into 2 meters benches, on

which low and high grade domaining was done. Consequently, this means that data was cut into three benches, i.e. 930 to 928rl, 928 to 926 RL and 926 to 924 rl. The domained ore and waste categories from each bench was appended into one file called domained file which was later used in modelling. Data for Area B was observed to have a single distribution and domaining was not required.

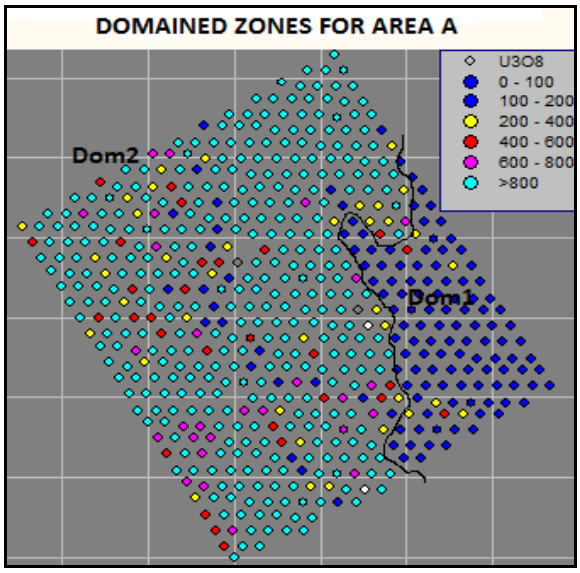


Figure 3.14: Map showing domained zones for Area A

3.7 Declustering

In some cases, spatial location of data collection sites are irregularly spaced. There might be more sampling done in some areas than in others. This creates some bias in the data statistics due to preferential spatial position (e.g. many close-spaced holes in a high grade area), thereby affecting the mean value of data. Therefore, it is essential that declustering of data points be implemented to remove any potential bias. However, in the study since in both areas drilling was done on regular grid, the sample spacing was uniform and declustering was not required.

3.8 Data Transformation

Successful implementation of Sequential Gaussian Simulation requires that the data used in the procedure is normally distributed. Normal score transformation of

data aims at getting a mean of 0 and variance of 1. In order to achieve this both of the highly skewed data sets were transformed into standard normal score distributions. In this case, the mean and variance of the distribution obtained were 0 and 0.999 respectively for both Area A and Area B. Figure 3.15 to 3.18 show frequency cumulative plots and histograms for untransformed and transformed U_3O_8 for both Areas. The median value in both Areas was 0, which was an indication of symmetric distribution hence acceptable for variography and SGS.

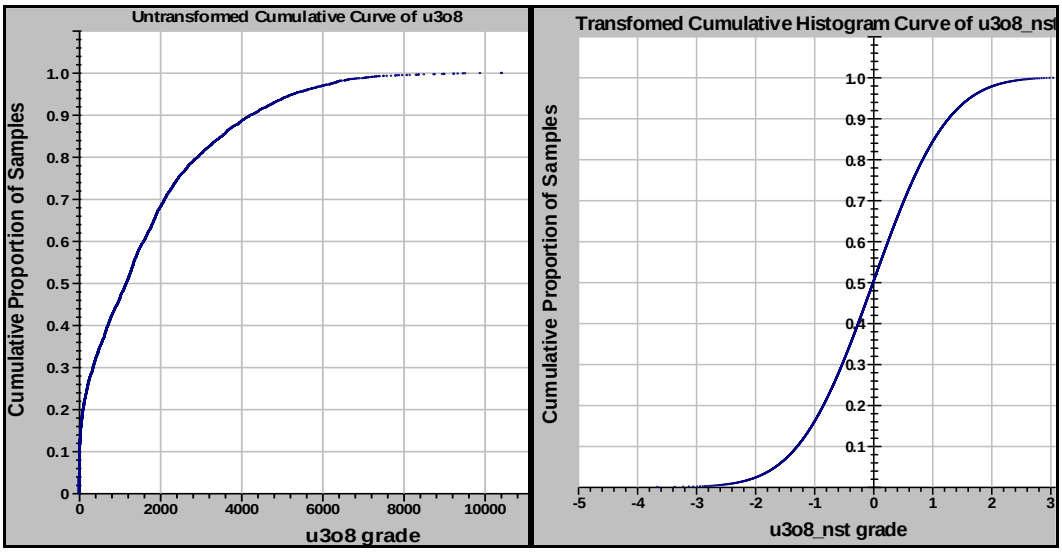


Figure 3.15: **Cumulative Curves for Untransformed (Left) and Transformed (Right) U_3O_8 for Area A**

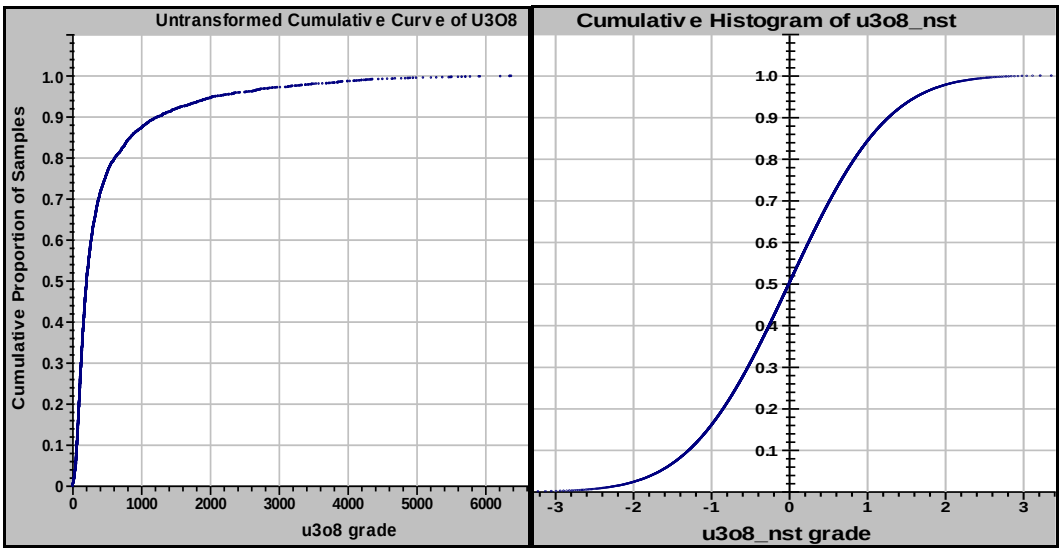


Figure 3.16: **Cumulative Curves for Untransformed (Left) and Transformed (Right) U_3O_8 for Area B**

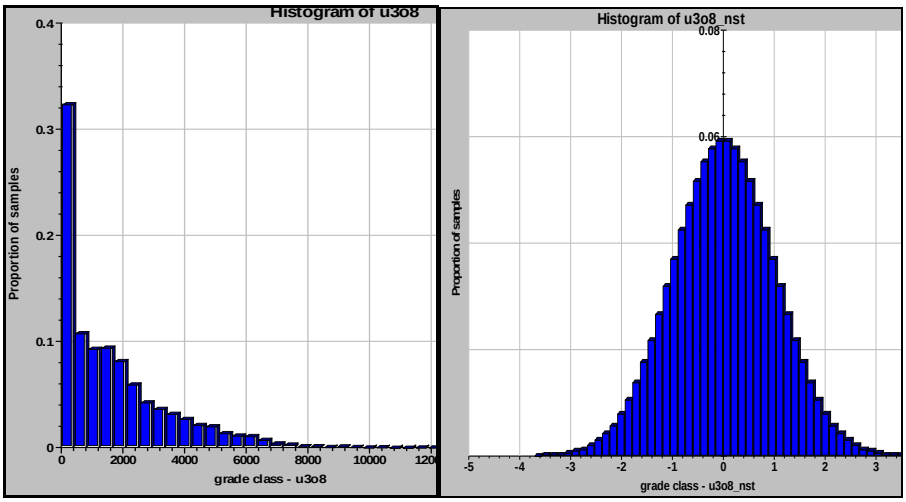


Figure 3.17: Area A non-transformed and transformed U_3O_8 distribution

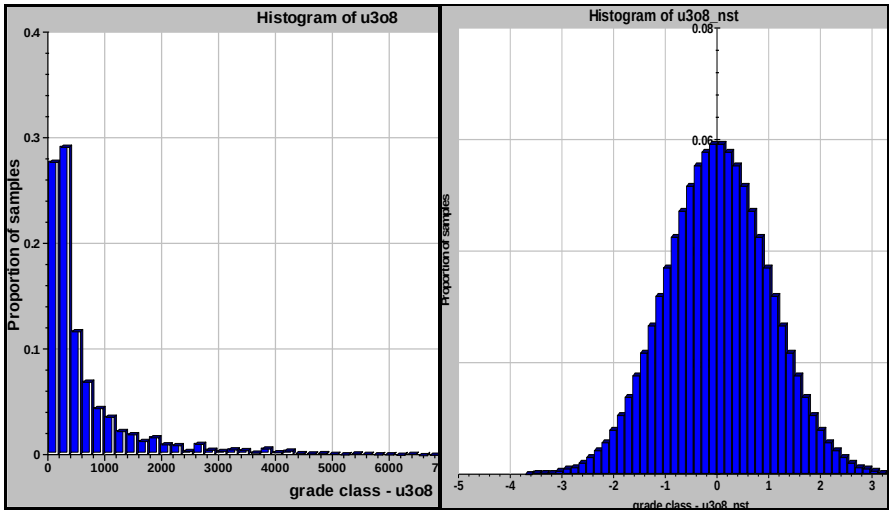


Figure 3.18: Area B non-transformed and transformed U_3O_8 distribution

3.9 Variogram Analysis

Data was read into the MP Grade control system from where the variography was performed. The version of MP grade control system was developed by Hellman and Schofield in early 90's and is mainly used for geostatistical analysis of grade control data for Kayelekera Mine. Variograms were calculated for the whole 6m in the Z direction (downhole). Three steps were followed, which are creating variogram maps, calculating experimental variograms and finally a model was fitted to the experimental variograms.

3.9.1 Variogram maps

Variogram map helps in assessing spatial continuity and also assessing the degree of anisotropy in the data set. Mainly it is used to study how strong the spatial continuity is as well as the direction properties of the spatial continuity of the data set. Since SGS uses normal score transformed data and OK uses non-transformed data, variogram maps were created for both transformed and non-transformed data.

It can be observed from variogram maps in Figures 3.19 and 3.20 that Area A has a strong continuity of U_3O_8 in the North North West (NNW) to South South East (SSE) in which the azimuth is 120° for both normal score transformed and non-transformed data. A similar observation was made for geology, the change from one lithological unit to another was smaller in the North North West to South South East direction, changes were observed in the West-East directions. Since mineralisation is mostly controlled by the geology, this implies that for this Area, the grades in sample locations in NNW-SSE will be similar and will result in lower variance values. Similarly, Area B indicated a strong U_3O_8 continuity in the North to South direction, which was same direction as the strike.

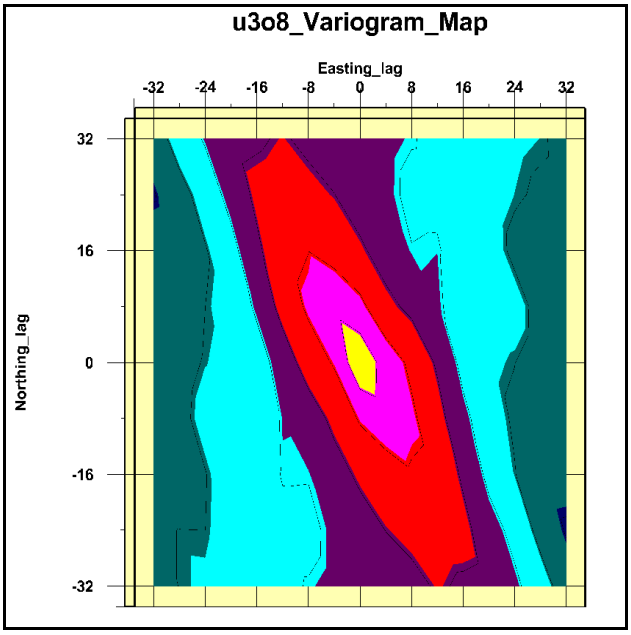


Figure 3.19: Plan View U_3O_8 Variogram Map for Area A

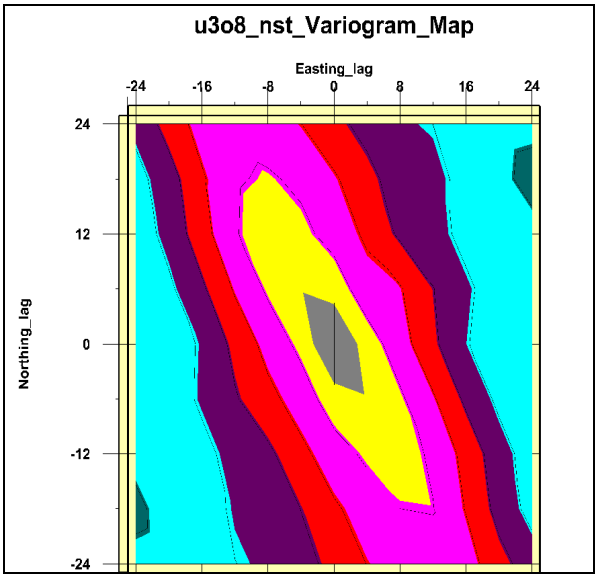


Figure 3.20: Plan View U_3O_8_normal score transformed Variogram Map for Area A

On the other hand, Area B was observed to have a North – South (Azimuth 90°) directional trend for both transformed and non-transformed data as it can be seen in Figure 3.21 and Figure 3.22. Area A unlike Area B indicates that samples in the North-South direction will be more similar than in the east to north direction, especially for transformed data set.

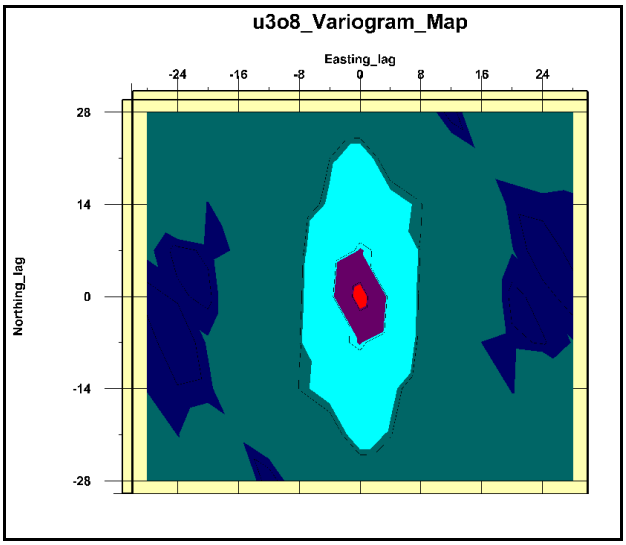


Figure 3.21: Plan View U_3O_8 Variogram Map for Area B

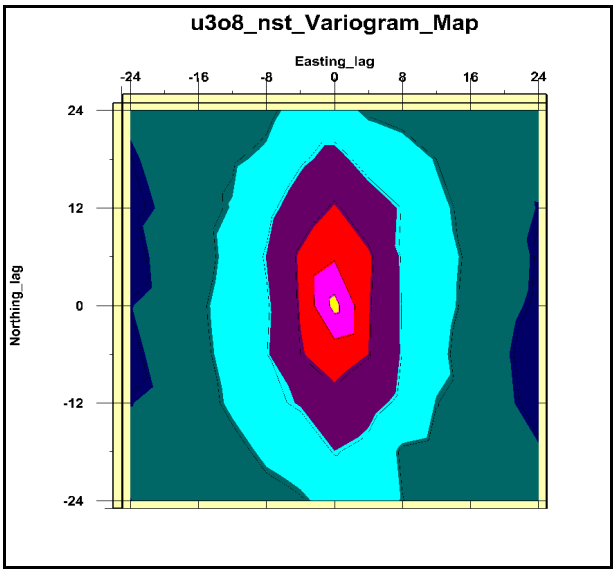


Figure 3.22: Plan View U_3O_8_normal score transformed Variogram Map for Area B

3.9.2 Variogram modelling

After determining anisotropy and spatial continuity, experimental variograms were calculated for the data sets. This was done to provide a description of the spatial correlation of the data. Since Area A indicated NNW-SSE continuity from the variogram map, this means that U_3O_8 is spatially correlated along NNW-SSE orientation. Consequently, eexperimental variograms were calculated for four directions, East-West, North-South, vertical and NNW-SSE. Lag tolerance was calculated as half of the lag distance as it can be seen from Table 3.5

Table 3.4: Area A directional variogram parameters

Direction	AZM	Azimuth Tolerance	Plunge	Plunge Tolerance	Lag Distance	Lag Tolerance
Along Strike (N-S)	0	45	0	45	4	2
Along Dip (E-W)	90	45	0	45	8	4
Vertical	0	45	-90	45	1	0.5
NNW-SSE	120	45	0	45	5	2.5

On the other hand, variogram for Area B was calculated for three directions as shown in Table 3.6. Only three directions, North –South, East-West and vertical, were considered since the variogram map for Area B showed a preferred orientation in the same direction as the direction along strike (N-S).

Table 3.5: Area B directional variogram parameters

Direction	AZM	Azimuth Tolerance	Plunge	Plunge Tolerance	Lag Distance	Lag Tolerance
Along Strike (N-S)	0	45	0	45	4	2
Along Dip (E-W)	90	45	0	45	6	3
Vertical	0	45	-90	45	1	0.5

Using parameters indicated on the variogram maps, experimental variograms were calculated and model variograms were fitted. A spherical model was identified as the best fit for the experimental variograms. Data sets from both Area A and Area B produced good omnidirectional variograms. One reason for the good variogram model could be due to large amount of data used. Figures 3.23 to 3.36, show transformed and untransformed variogram models for both Area A and Area B.

3.9.3 Variogram modelling for non-transformed data

Since Ordinary Kriging uses non-transformed data, variograms from raw data were created for both Area A and Area B and have been shown in Figures 3.23 to 3.29. Spherical model was found to be the best fit for the models. Area A variogram has nugget (C_0) of 0.04 m^2 lower than that of Area B which was 0.30 m^2. The range values were higher for Area A than B, which can be attributed to high spatial continuity of grades.

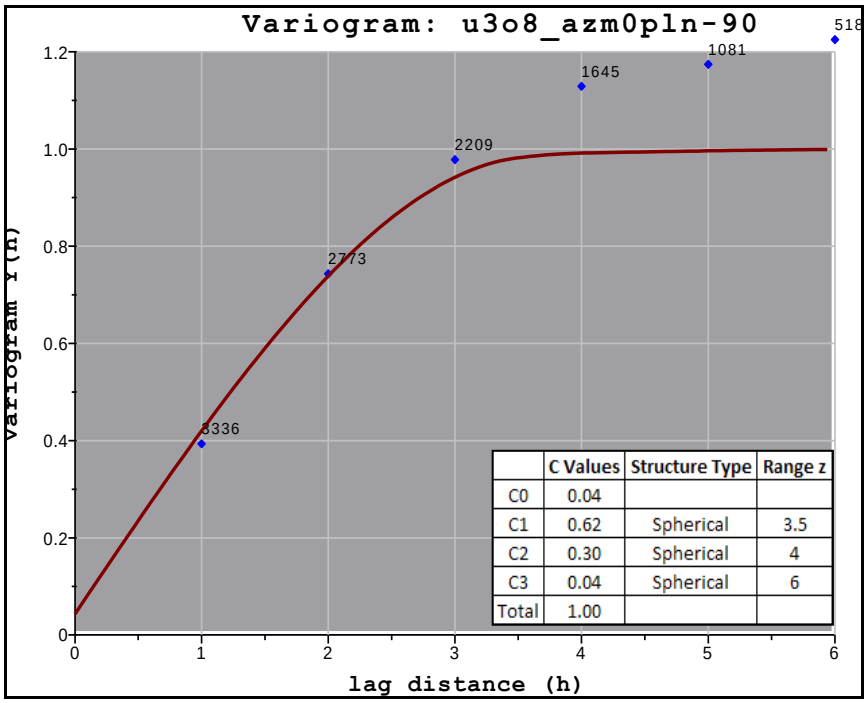


Figure 3.23 : **Area A Vertical Variogram model using Non-transformed Data (max of 6m downhole data)**

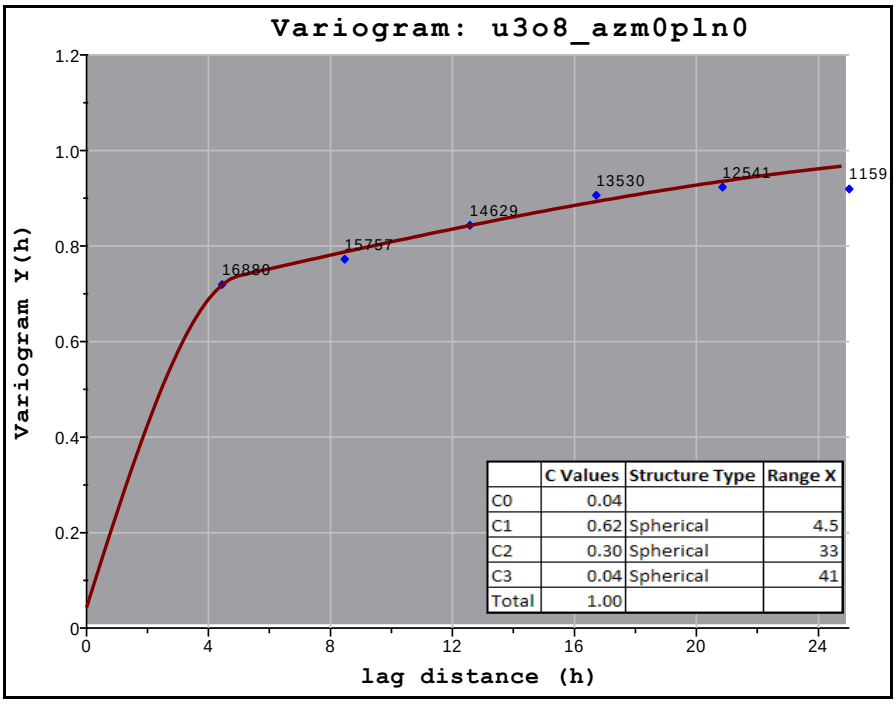


Figure 3.24: **Area A East-West Variogram model using Non-transformed Data**

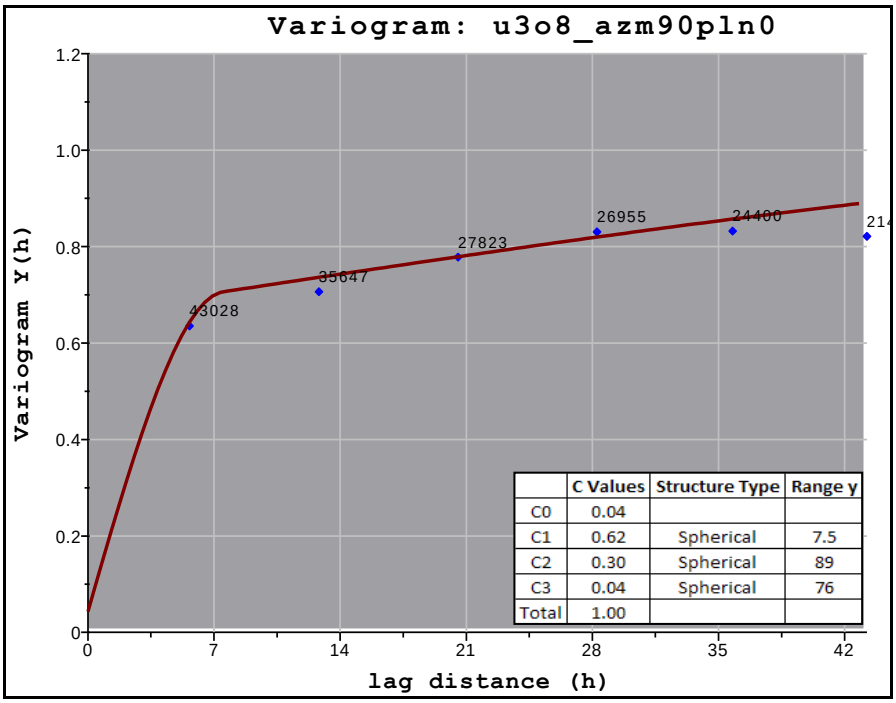


Figure 3.25: Area A North-South Variogram model using Non-transformed Data

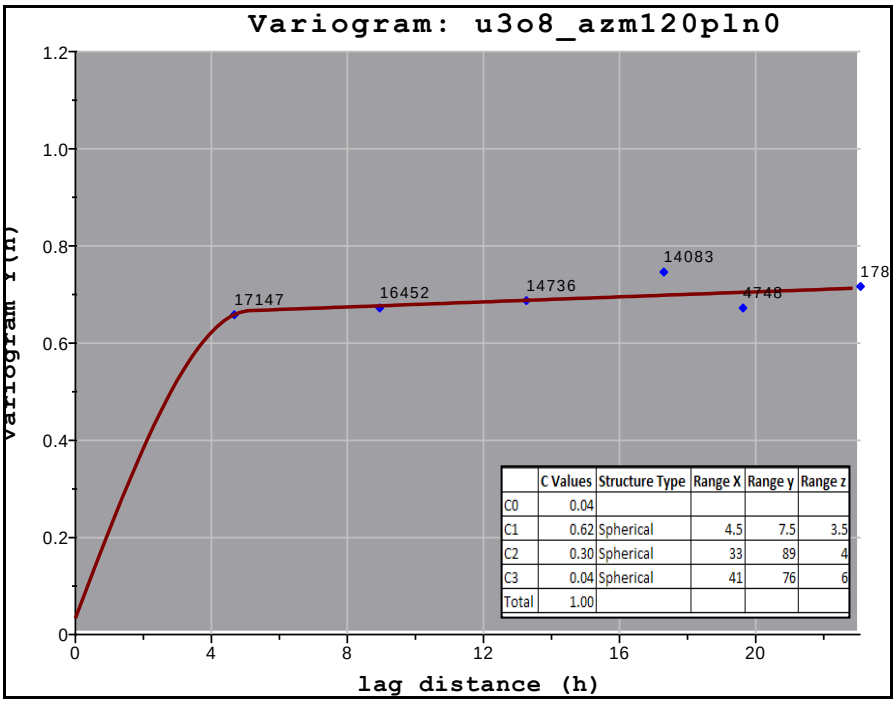


Figure 3.26: Area A NNW-SSE (AZM 120º) Variogram model using Non-transformed Data

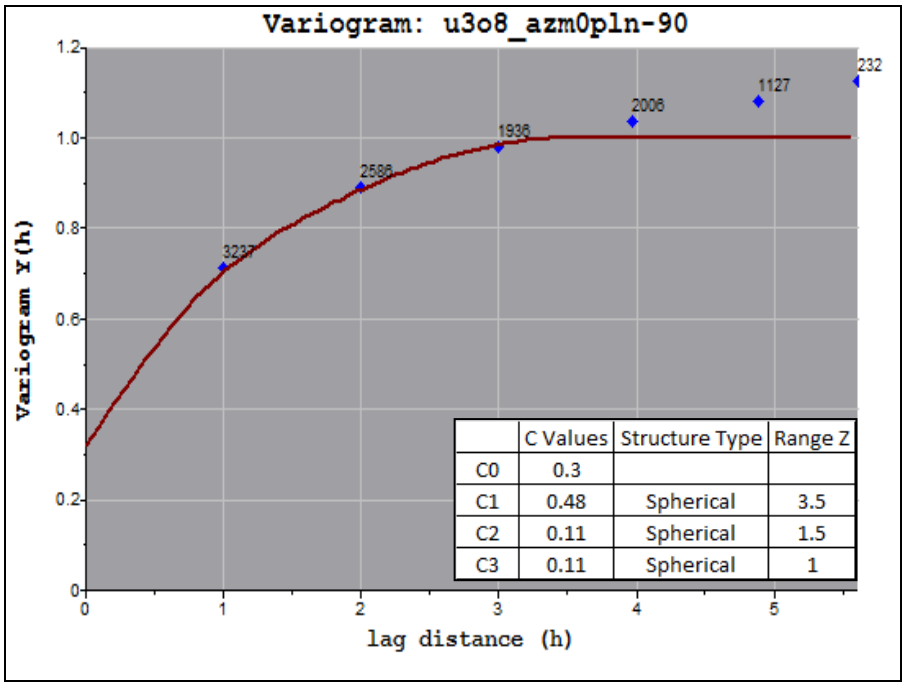


Figure 3.27 : Area B Vertical Variogram model using Non-transformed Data (max of 6m downhole data)

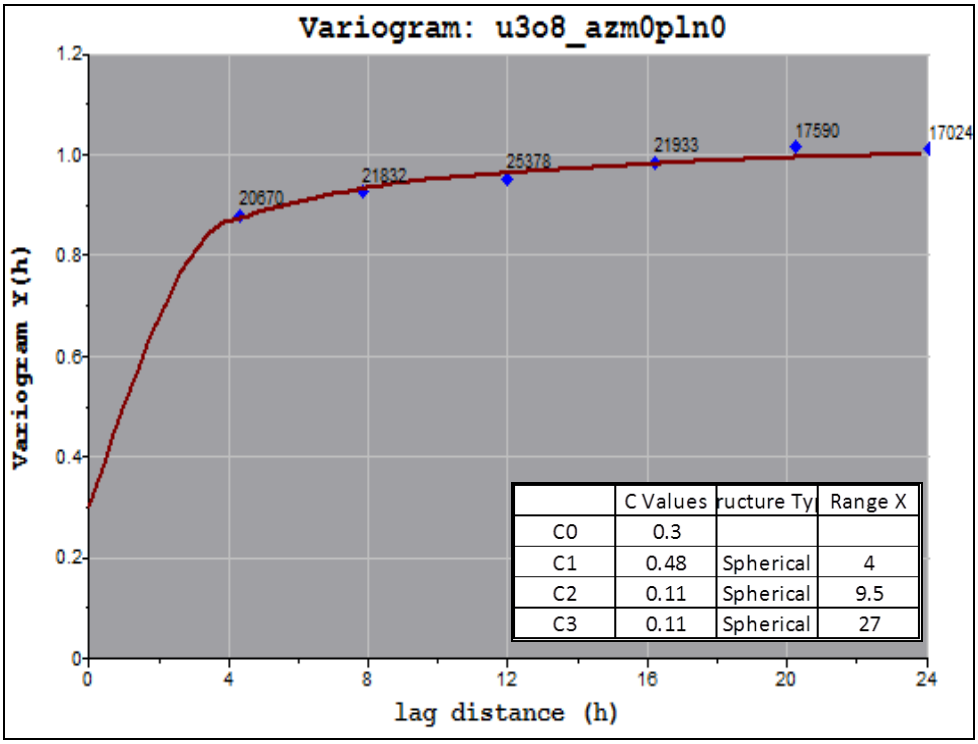


Figure 3.28: Area B East-West Variogram model using Non-transformed data

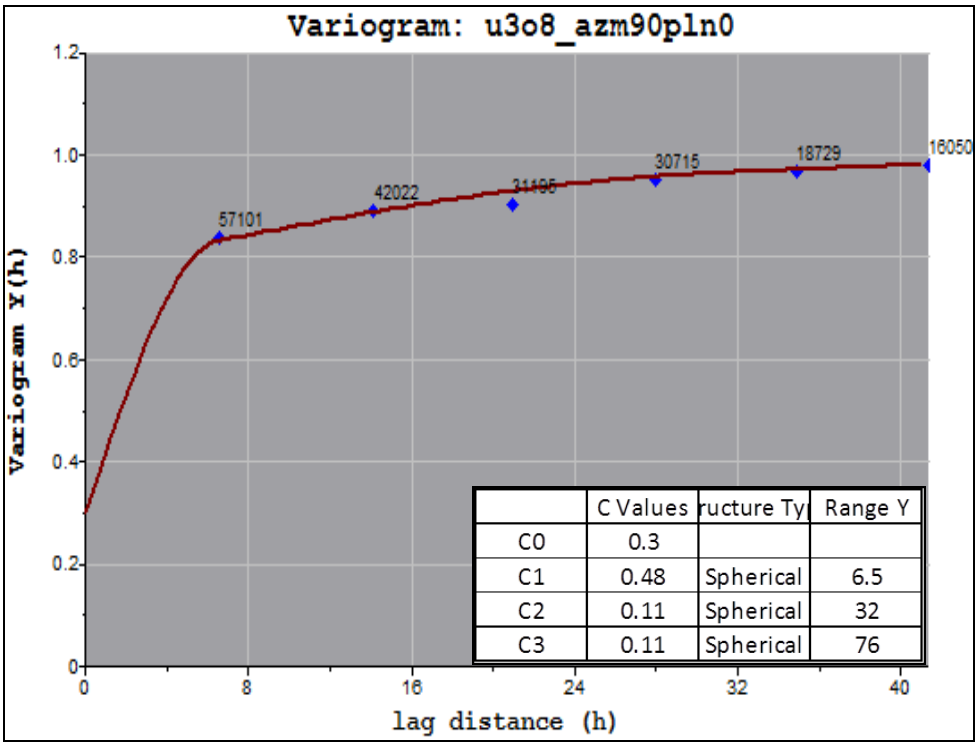


Figure 3.29: Area B North-South Variogram model using Non-transformed Data

3.9.4 Variogram modelling for transformed data

Similar observations as in non-transformed model variograms were made for the transformed data variogram models as in Figures 3.30 to 3.36 for both Area A and Area B. All variograms were structured and a spherical model was found to be the best fit. Area A variogram has nugget (C_0) of 0.05 m^2 lower than that of Area B which was 0.23 m^2. The range values for Area A were higher than for Area B indicating more grade continuity in Area A than Area B.

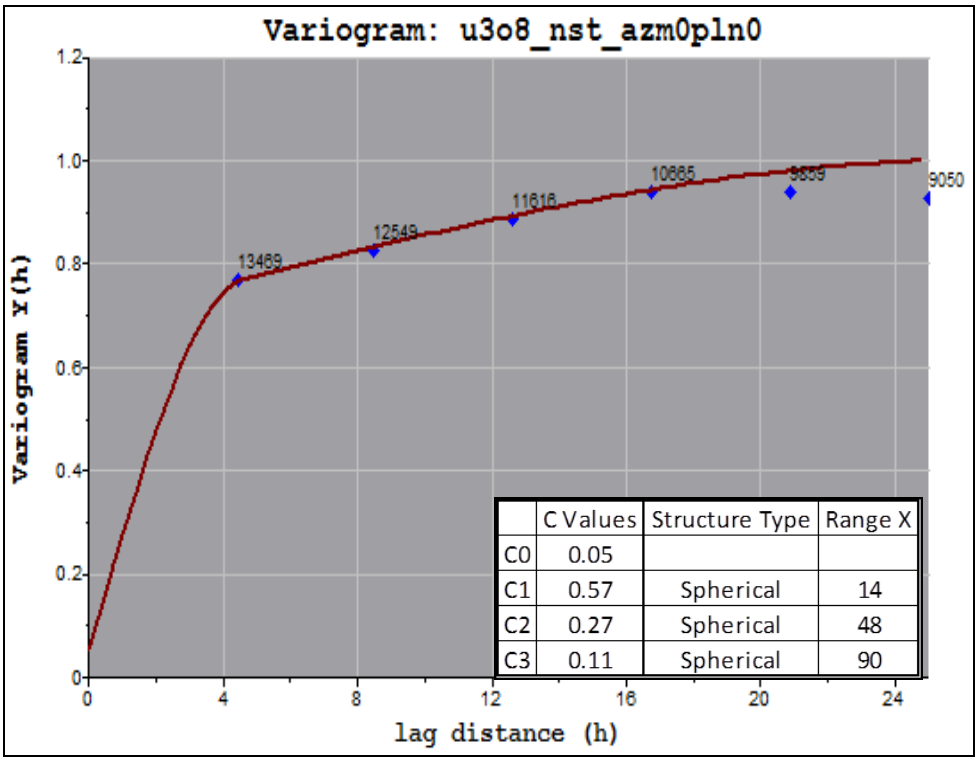


Figure 3.30: **Area A East-West Variogram model using transformed data**

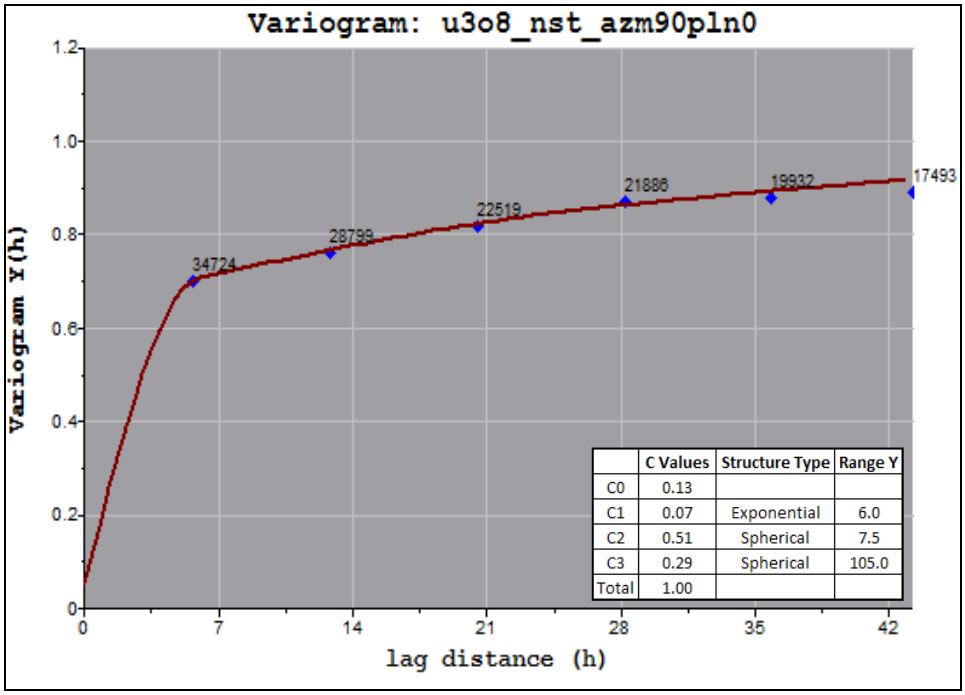


Figure 3.31: Area A North-South Variogram model using transformed data

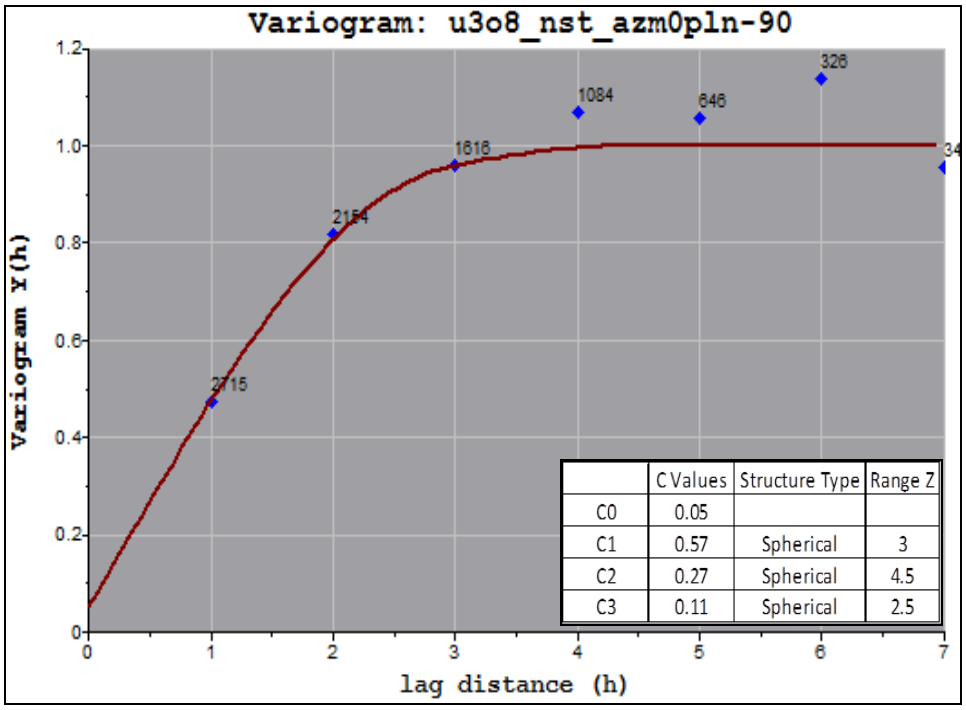


Figure 3.32: Area A Vertical Variogram model using transformed data (max of 6m downhole data)

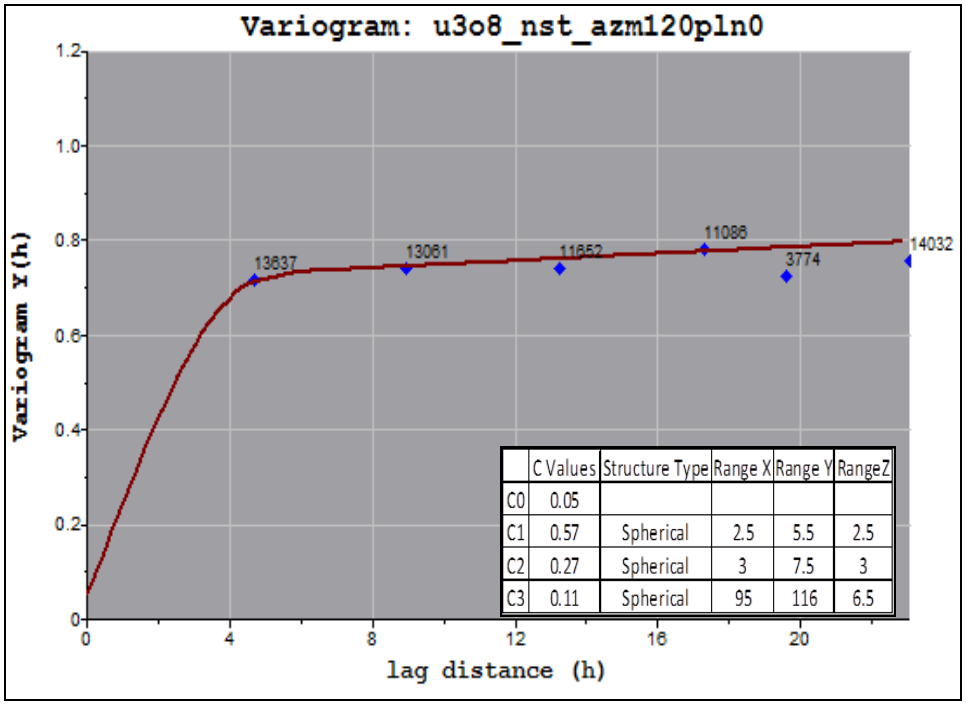


Figure 3.33: Area A NNW-SSE (AZM 120º) Variogram model using transformed data

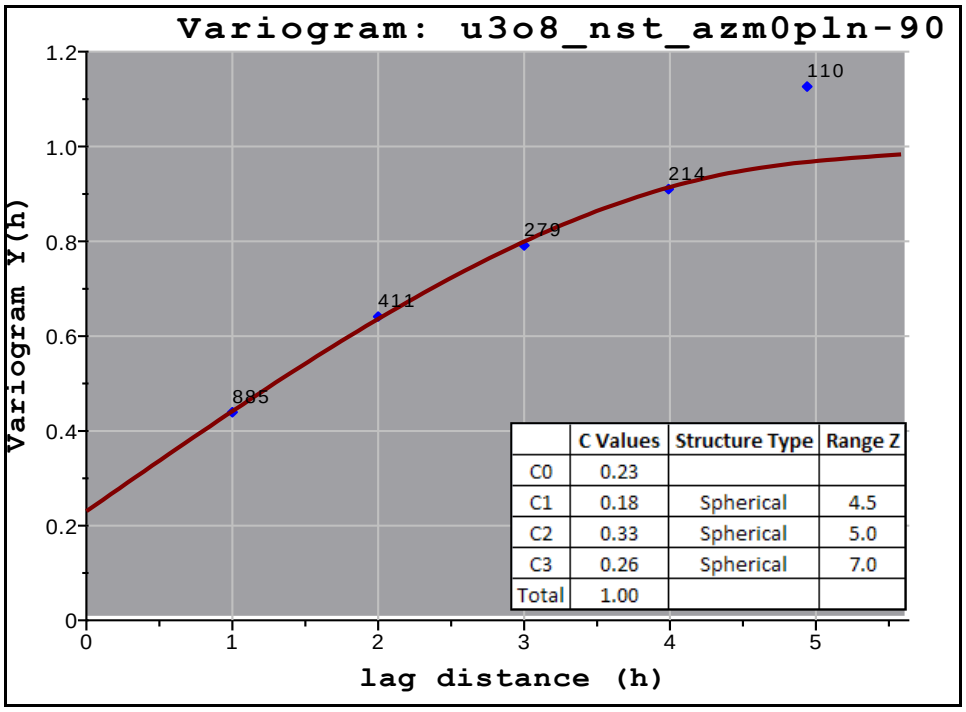


Figure 3.34: Area B Vertical Variogram model using transformed Data (max of 6m downhole data)

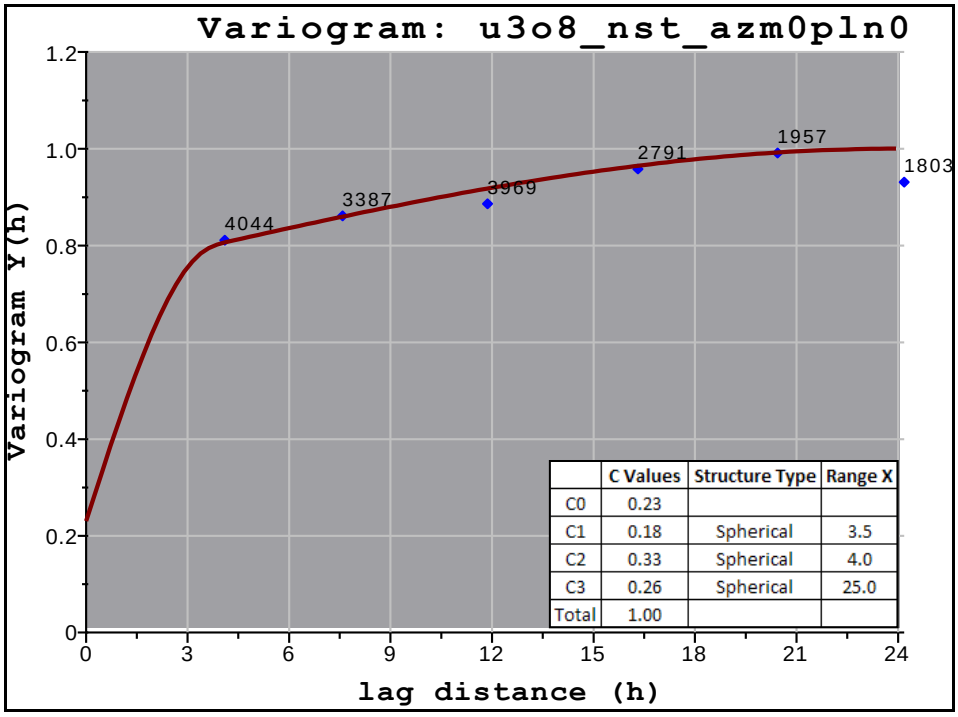


Figure 3.35: Area B East-West Variogram model using transformed data

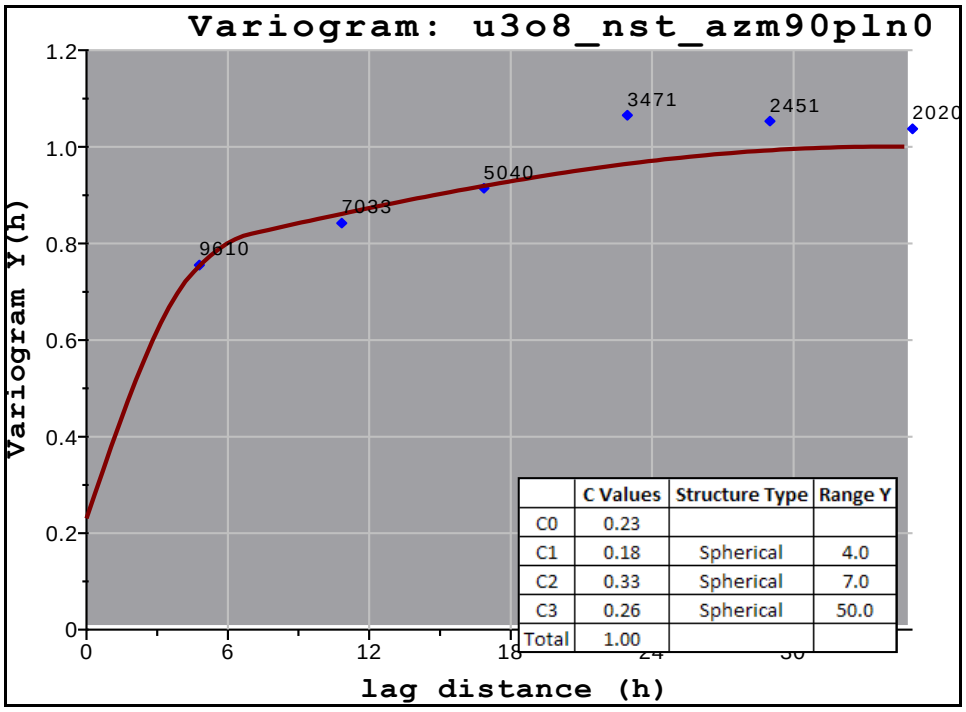


Figure 3.36: Area B North-South Variogram model using transformed Data

The mineralisation at KM has a North-South strike direction and this has also been reflected in the N-S direction variogram model as it shows more continuity. Consequently the North-South direction models were the best fit. It can also be noted that, due to N-S mineralisation style, the experimental variograms in the East-West direction were only reliable for a shorter lag distance, specifically for the first three to four lags. For this reason, emphasis was also placed on fitting models for the North-South direction.

Furthermore, the structural setting of the geology at Kayelekera Mine is syn-formal and not flat lying, as reflected in the short East to West ranges. The syn-formal structural setting of the geology tends to shorten the ranges, hence the values of ranges of the variograms are small specifically in the West to East direction since it is in the directions in which the geology tend to gently dip.

4 ESTIMATION OF RECOVERABLE RESERVES USING ORDINARY KRIGING AND SEQUENTIAL GAUSSIAN SIMULATION

4.1 Chapter Overview

Local recoverable reserve estimates were developed using SGS and OK. Having established the spatial continuity of the mineralisation for both Area A and Area B through variogram analyses and modelling, local grade estimation using OK and SGS was carried out. The search radius was defined in relation to drill spacing, and it was calculated as one and half times the drill spacing, hence the search radius used was 6m in X direction, 9m in Y direction and 3m in Z direction. In all cases, a minimum of 16 samples were used to obtain an estimated value. The model variograms were used to compute the weights which were modelled in the kriging process in data sets from both Area A and Area B.

4.2 Ordinary Kriging Recoverable Estimates

Estimates from ordinary kriging for Area A and Area B are shown in Figure 4.1. The figures show kriged estimates in plan view from the two data sets with the block size of 3m by 3m by 2m. Each block indicates estimated grade colour coded by different cut off grades and it is for the first layer of the estimated blocks.

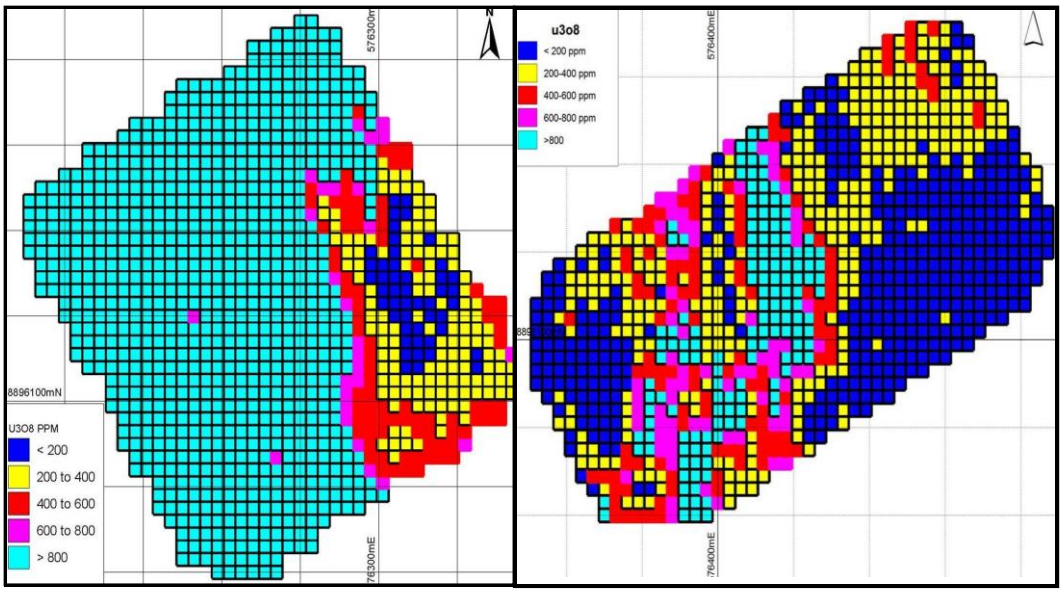


Figure 4.1: OK block estimates for Area A (Left) and Area B (Right)

Table 4.1: Ordinary Kriging Estimates at 400ppm cut-off grade

	OK estimates above cut-off grade (400ppm) for Area A	OK estimates above cut-off grade (400ppm) for Area B
Grade	1,961ppm	947ppm
Tonnes	119,681t	51,623t
Metal	235Mt	49Mt

4.3 Sequential Gaussian Simulation (SGS) recoverable reserve estimates

The second recoverable reserve estimation method is the SGS. The application of this method involves using data that has been transformed to Normal Score distribution. After variogram analysis and modelling, Sequential Gaussian Simulation was also carried out on both data sets using Normal Score Transformed data. The search radius, minimum and maximum data and block size were the same as previously discussed in OK estimation. The transformed data and calculated variograms were the input data for the simulations. Considering that the number of simulations used to produce estimates of a variable affects the outcome of the estimates, 100 simulations were considered to be appropriate and used in the study and are also currently used at KM.

Since the simulation was carried out on transformed data, the SGS estimates were in Gaussian values, were then back-transformed to original units. This was done using Histogram Transformation algorithms of the MP grade control software and back-transformed estimates have been displayed in Figures 4.2. The results shows the first layer of the estimated block on each location. Each individual block is an average grade of 100 realisations on a 3m by 3m by 2m block size.

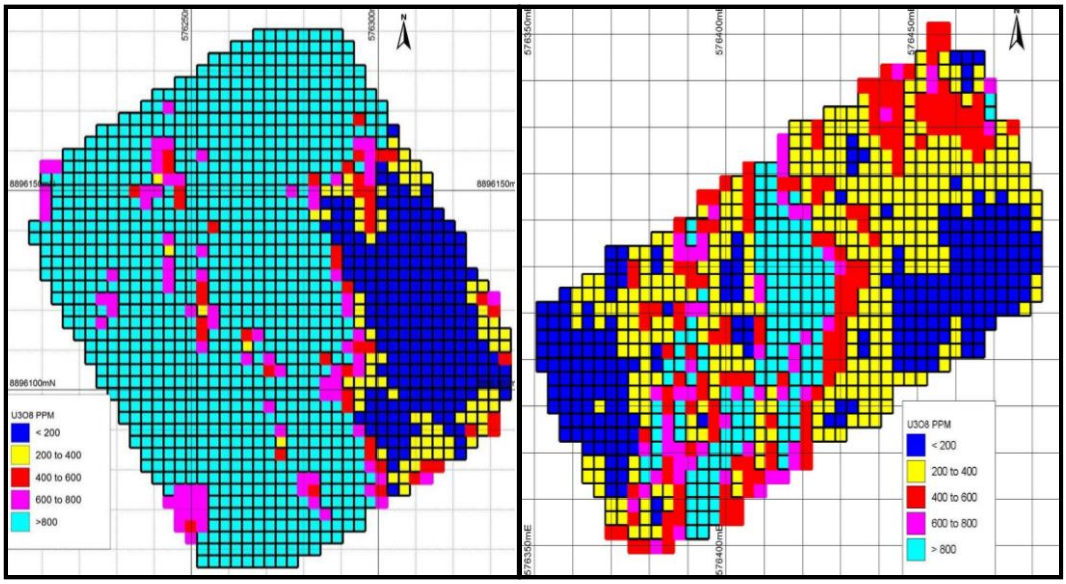


Figure 4.2: SGS block estimates for Area A (Left) and Area B (Right)

Table 4.2: SGS Estimates at 400ppm cut-off grade

	SGS estimates above cut-off grade (400ppm) for Area A	SGS estimates above cut-off grade (400ppm) for Area B
Grade	2,049ppm	908ppm
Tonnes	110,283t	53,982t
Metal	226Mt	49Mt

4.4 Summary

From the maps (Figure 4.1 and Figure 4.2), both estimates appear to have maintained the portions of high and low grades. The low grade area in the south eastern part of the Area A, remained low. However, OK appears to have slightly smoothed the data as it can be observed from the low grade patches that were within the high grade area, which have been maintained and are well defined for SGS estimates. Altogether, Ordinary Kriging and Sequential Gaussian Simulation estimates showed slight disparities to the blast hole data.

Results of estimates using both OK and SGS techniques are summarised in Table 4.3. The results indicate that OK has higher tonnage than SGS for Area A. Although OK has more tonnage than SGS, it has underestimated the grade for Area A. The metal content appears to be very similar and Area B has same total metal content. Overall, little difference was observed in terms of Grade, Tonnes and Metal content from the two techniques for both Area A and Area B. Detailed comparison of the estimates with the actual values has been given in the next section.

Table 4.3: Grade, tonnage and metal estimates from OK and SGS

AREA A			
Technique	**Grade(ppm)**	**Tonnes (t)**	**Metal (Mt)**
Actual	2,194	108,372	226
OK	1,961	119,681	235
SGS	2,049	110,283	226
AREA B			
Technique	**Grade(ppm)**	**Tonnes (t)**	**Metal (Mt)**
Actual	1,027	45,765	47
OK	947	51,623	49
SGS	908	53,982	49

5 COMPARISON OF ORDINARY KRIGING AND SEQUENTIAL GAUSSIAN SIMULATION ESTIMATES

5.1 Chapter Overview

The aim of the study was to compare the estimates from Ordinary Kriging and Sequential Gaussian Simulation (SGS) and identify which technique produces a more accurate estimate of the mineral reserves. Several criteria for comparing estimation methods are described in literature, such as the correlation between estimates and true values, grade and tonnage curves (Ravenscroft, 1992), degree of smoothing achieved by the interpolation methods or the precision of the methods as measured by mean square error or mean absolute error (Marcotte and Asli, 1995) and profit and loss (Verly, 2005). In this study grade tonnage curves, scatter plots, profit and loss analysis, visual comparison with the blast hole data and correlation coefficients were the main comparison methods used and have been explained in the following sections. In addition the measures of uncertainty associated with both estimation techniques is discussed.

5.2 Visual Examination of Estimates

Visual comparison of estimates with the actual data was used for checking the quality of model estimates. The visual comparison although highly qualitative also helps in understanding variability of results compared to actual data. This was done by using maps from estimates, histograms, QQ plots, grade profiles and cumulative frequency curves.

5.2.1 Comparison of maps of estimates with adjacent blast holes

A plan view of the grade estimates are superimposed on the blast hole locations. Standard practice at Kayelekera Mine is that estimates are generated in 6m benches, but the mining is done on 2m benches. The plan view maps were also displayed in 2m benches and named Bench 1, Bench 2 and Bench 3 for top bench, middle bench and bottom bench respectively, as illustrated in Figures 5.1 to 5.12. Estimates (displayed as blocks) from both OK and SGS techniques closely reflect samples from the blast hole data (displayed as circles). Conditional Simulation

seems to overestimate most of the lower grades (blue), than Ordinary Kriging especially for data set A (Figures 5.1 and 5.2). Both estimates appear to reflect the input values with Ordinary Kriging performing better than the SGS model for Area B. The spatial patterns of SGS estimates and OK estimates did not considerably differ from that of blast hole data.

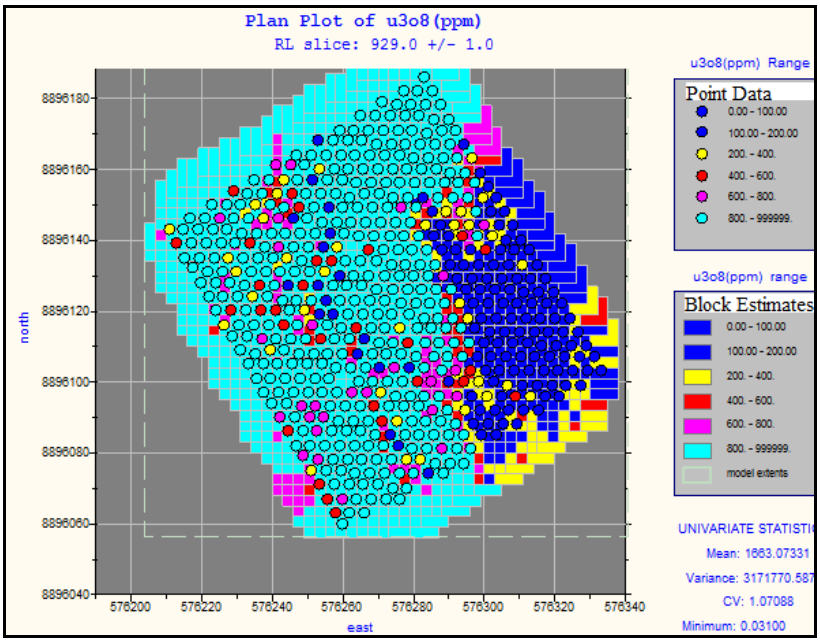


Figure 5.1: Area A comparison of blast hole data with OK model, bench 1

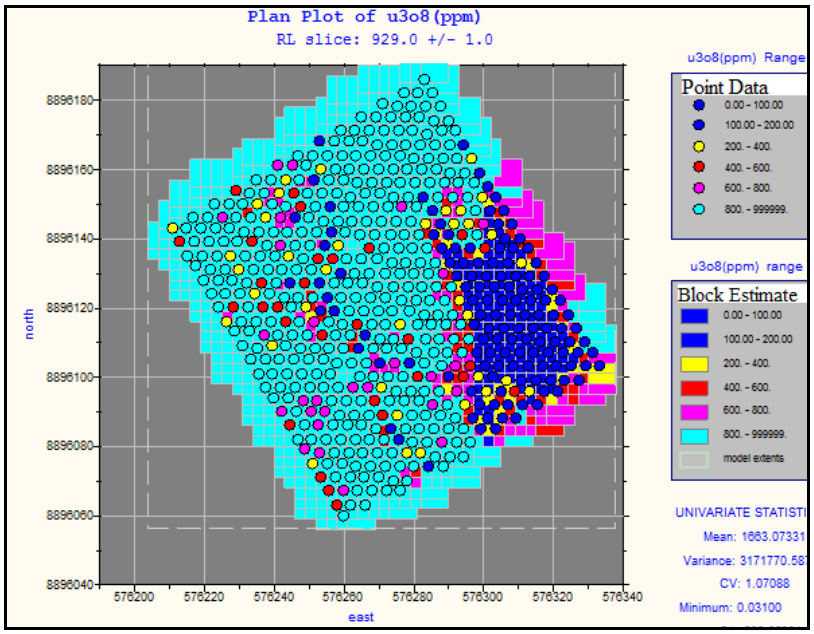


Figure 5.2: Area A comparison of blast hole data with SGS model, bench1 1

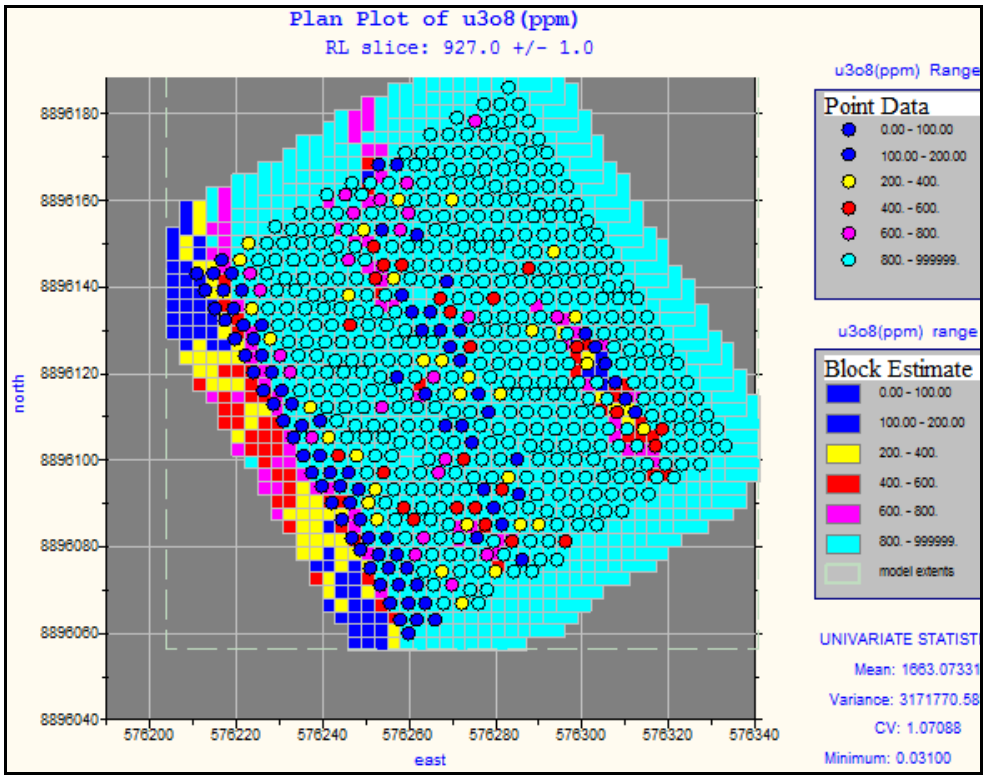


Figure 5.3: Area A comparison of blast hole data with OK model, bench 2

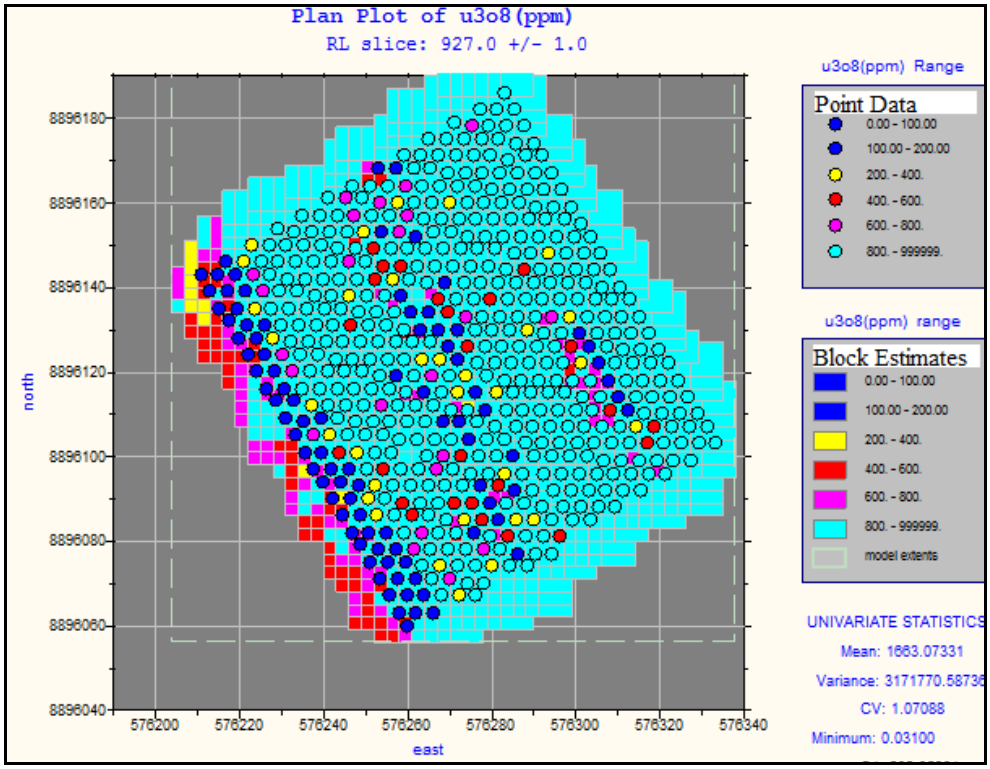


Figure 5.4: Area A comparison of blast hole data with SGS model, bench 2

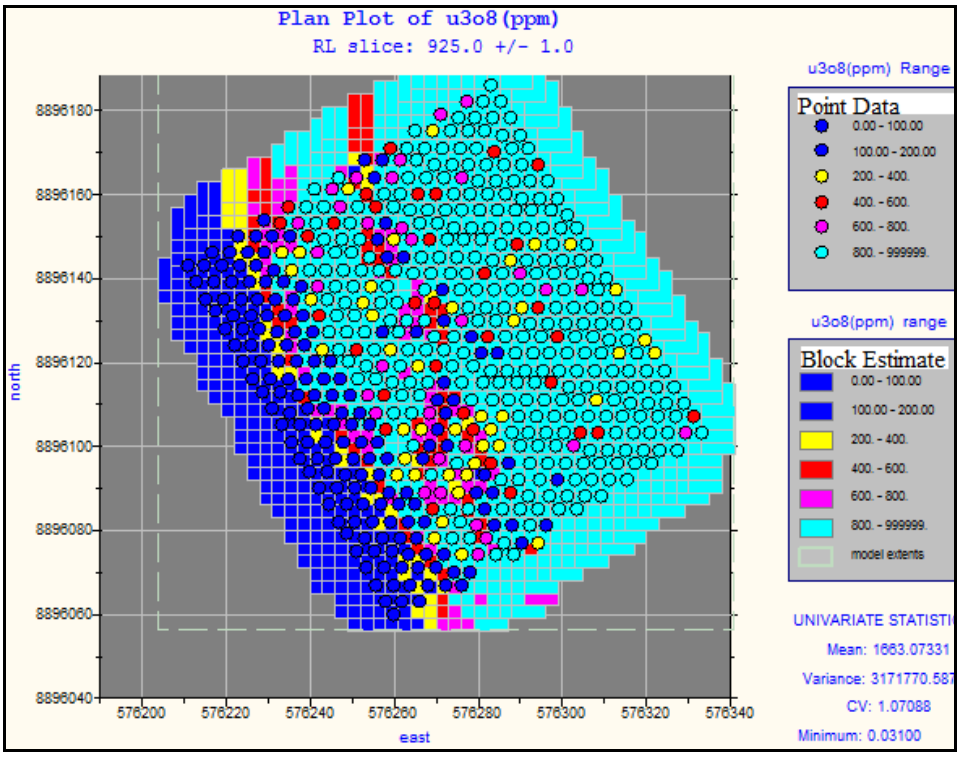


Figure 5.5: Area A comparison of blast hole data with OK model, bench 3

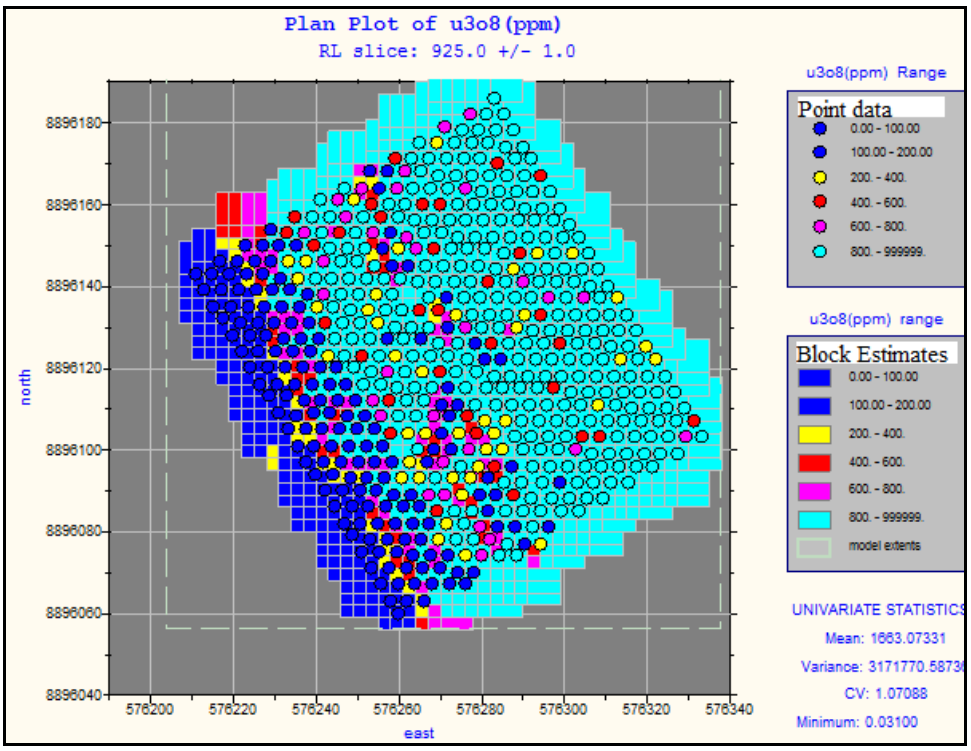


Figure 5.6: Area A comparison of blast hole data with SGS model, bench 3

Despite local estimates closely reflecting samples from the nearest blast holes, where grade for adjacent blast holes differ substantially (especially for Area B), grade change in estimates is also abrupt and in many cases does not reflect the observed blast hole data. Local portions of high and low grades reflects blast hole data well for Area A OK model estimates. However, OK estimates do not preserve the grade variation properties of the data in Area B where there is less grade continuity.

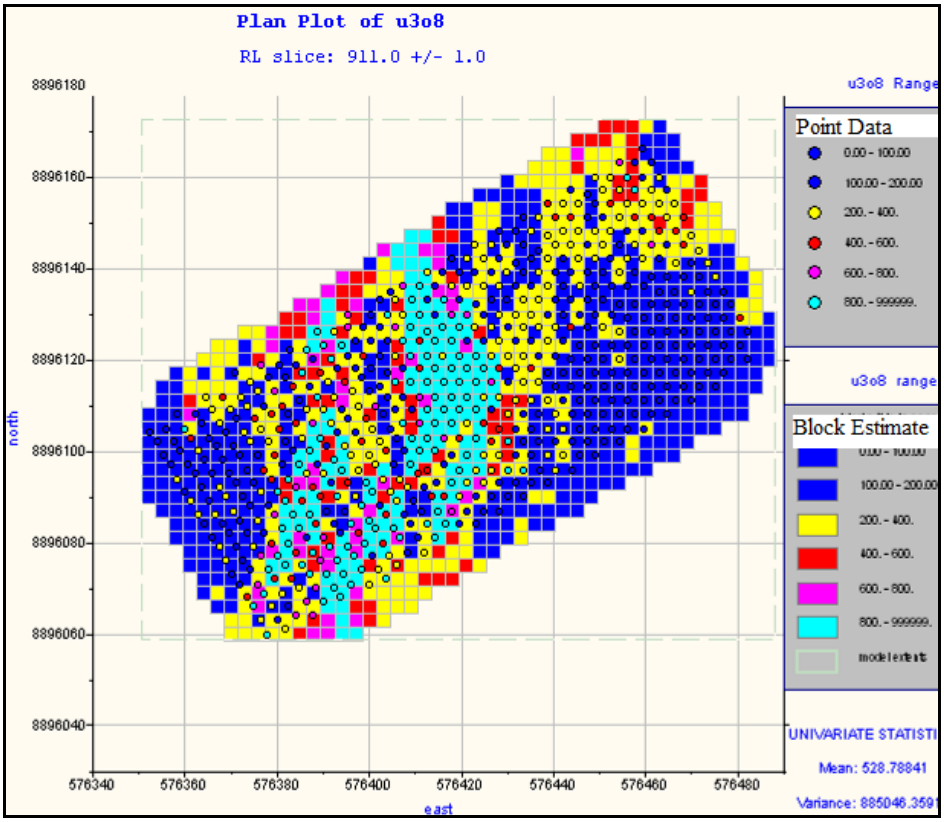


Figure 5.7: Area B comparison of blast hole data with OK model, bench 1

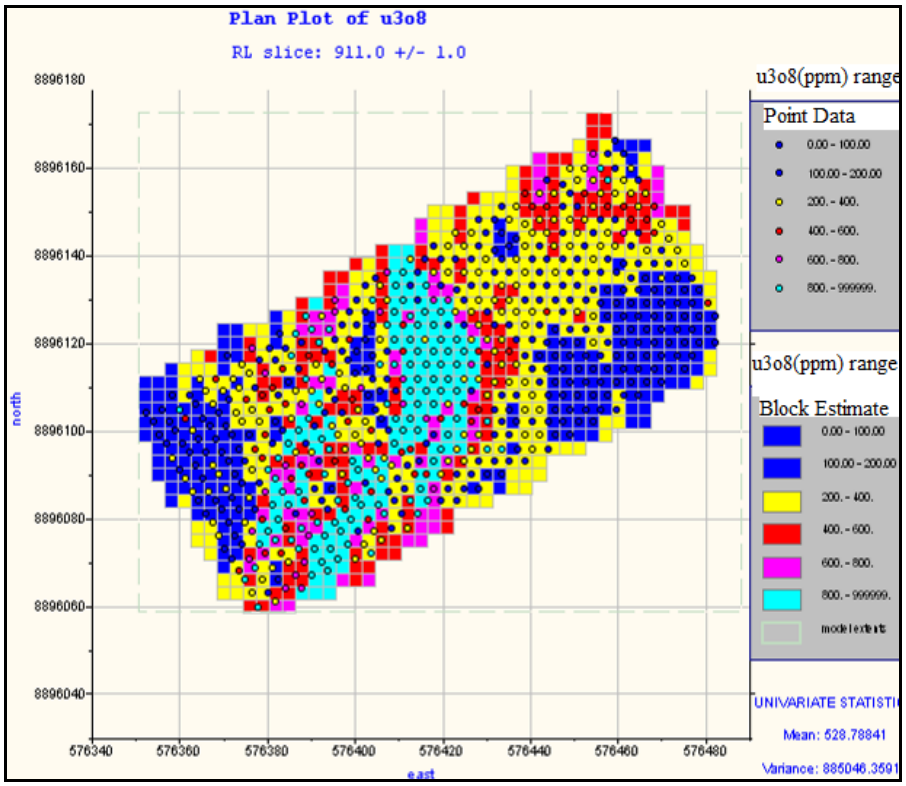


Figure 5.8: **Area B comparison of blast hole data with SGS model, bench 1**

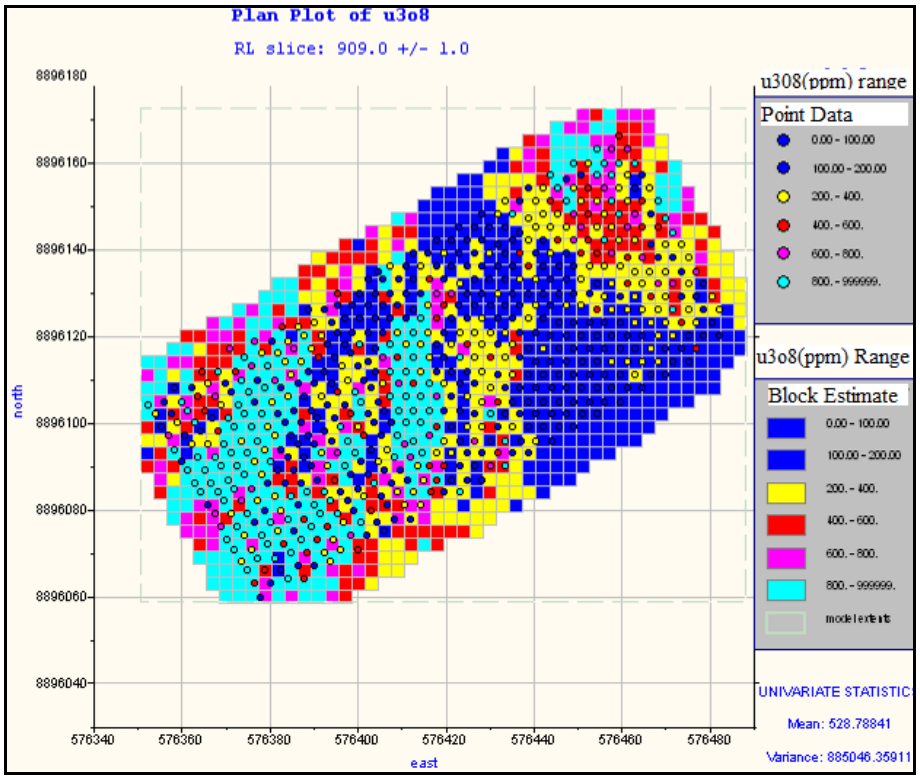


Figure 5.9: Data set B comparison of blast hole data with OK model, bench 2

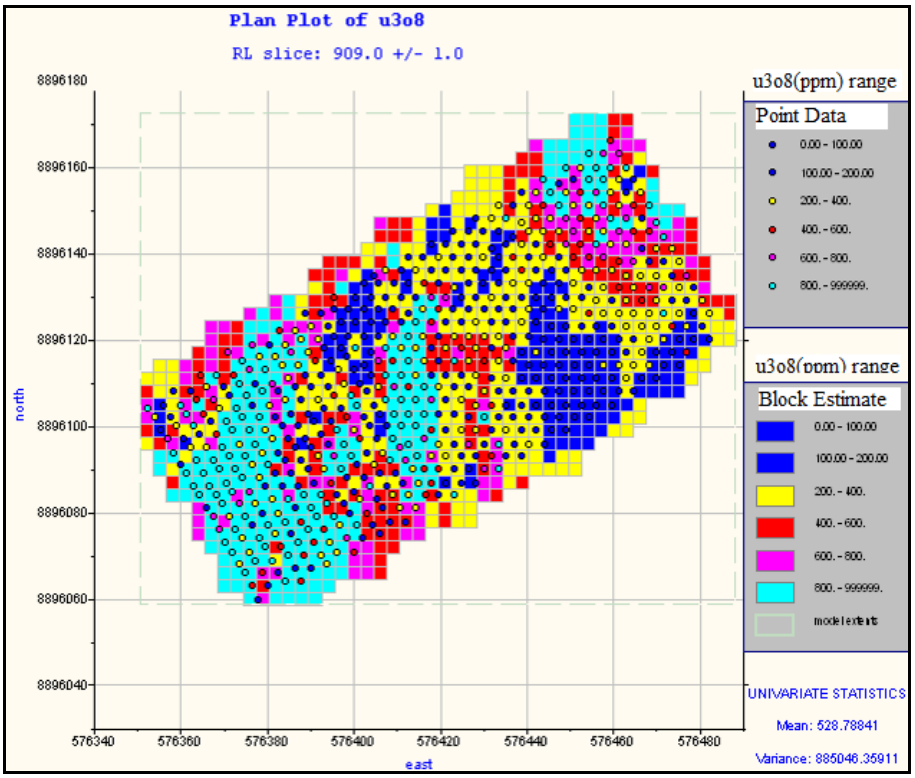


Figure 5.10: Area B comparison of blast hole data with SGS model, bench 2

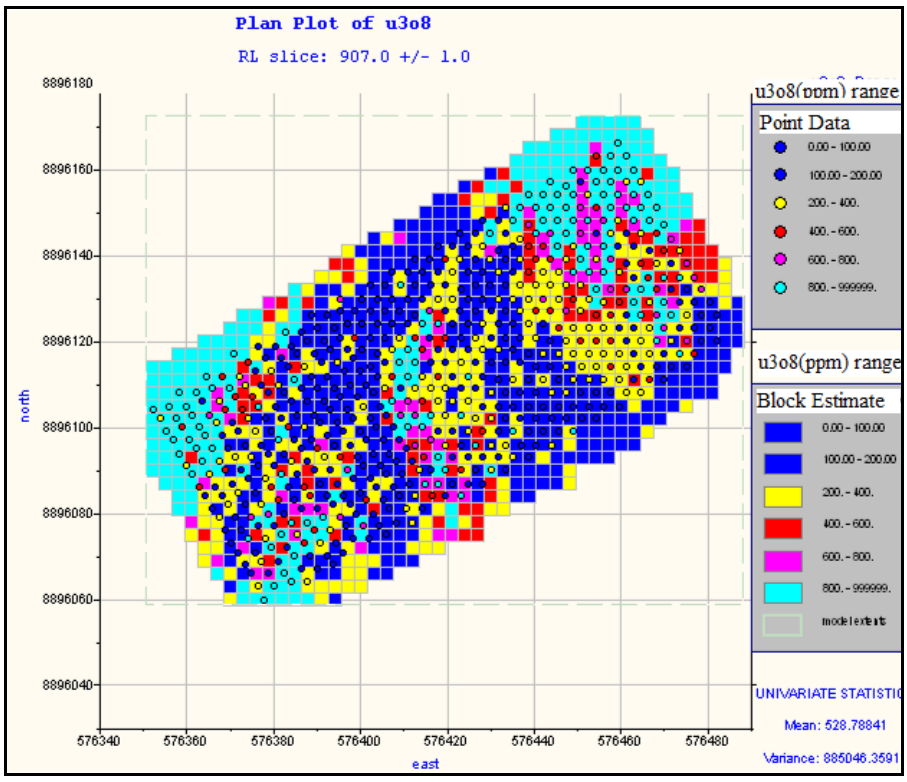


Figure 5.11: Area B comparison of blast hole data with OK model, bench 3

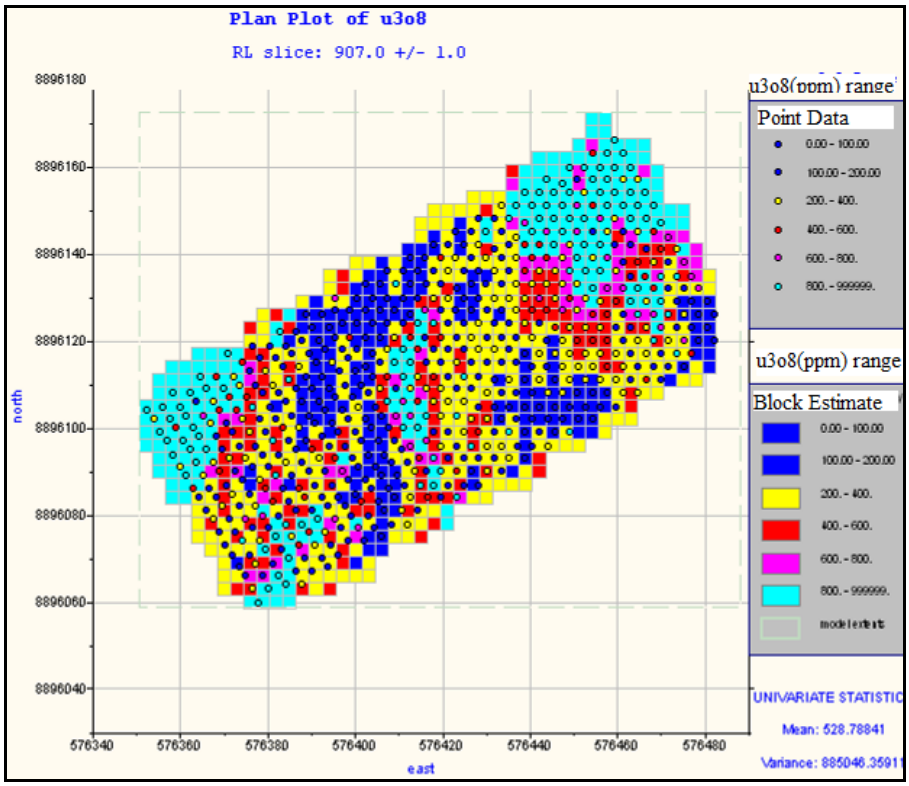


Figure 5.12: Area B comparison of blast hole data with SGS model, bench 3

5.2.2 Comparison of cumulative frequency plots

The cumulative frequency plots of the estimates were compared with those of the input data. Figure 5.13 and Figure 5.14 show a comparison of cumulative plots for Actual data, OK and SGS for Area A and Area B respectively. The results indicate similarity of estimates' cumulative frequency curves of both techniques with that of raw data. It can be noted that, for Area A, at cut-off grade of 400 ppm the proportion of grade is 10%, 24% and 23% for SGS, OK and actual data respectively. The sample proportion for OK and actual data are similar for lower grades (up to 1000ppm), as the grade increases the proportion of OK estimates are larger than the blast hole data. On the other hand, sample proportions of less than 3000ppm for SGS are lower than that of actual values this indicates that SGS has overestimated the lower grades than OK.

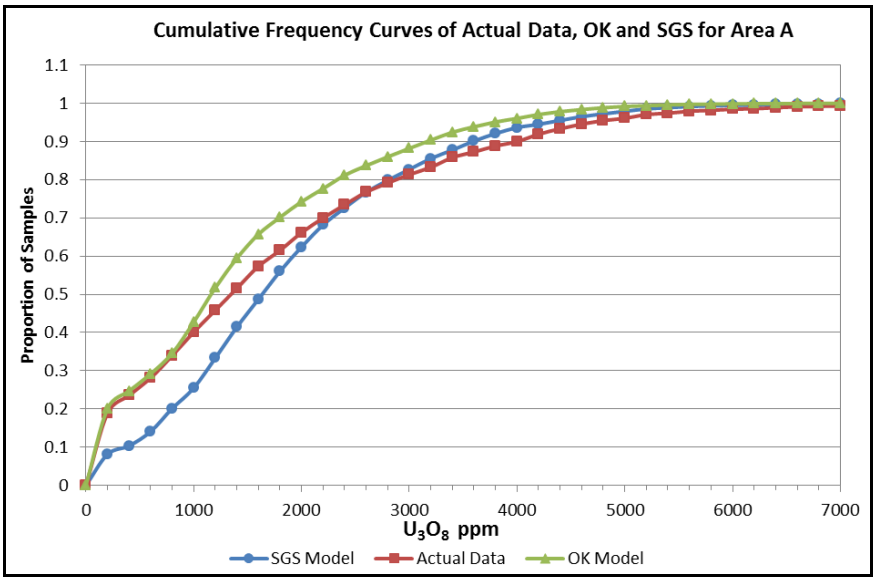


Figure 5.13: Comparison of cumulative frequency plots of Actual data, OK and SGS estimates for Area A

On the other hand, there is a minimal difference between cumulative plots for the actual data and both estimates for Area B, as plotted in Figure 5.14. Overall, OK has a cumulative plot closer to the input data than SGS, but the difference between the two methods is minimal as they both produce cumulative plots similar to the actual data. This indicates a similarity between the estimates, the techniques give similar estimates.

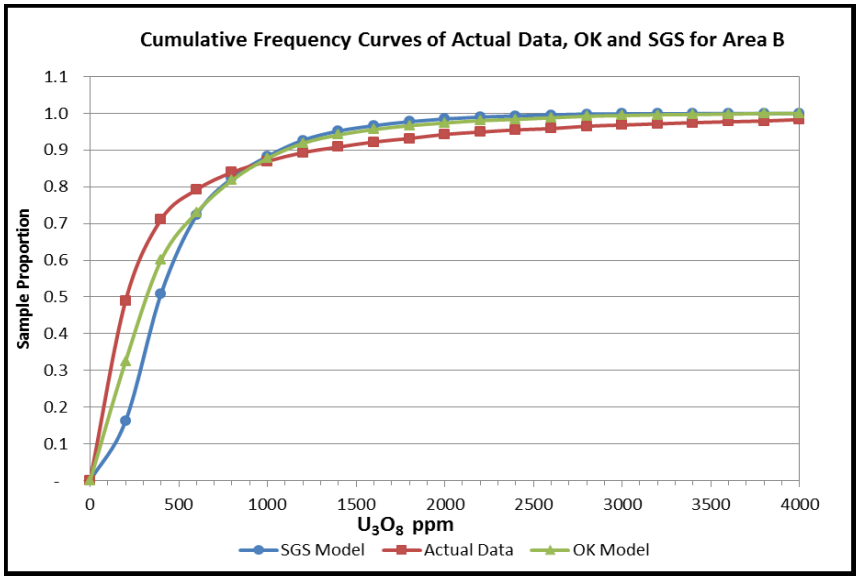


Figure 5.14: Comparison of cumulative frequency plots of Actual data, OK and SGS estimates for Area B

5.2.3 Comparison of histograms

Histograms from estimates were compared with histograms from actual data. Figures 5.15 to 5.18 shows how well the histogram of the estimates compare with the histogram of actual data. In both cases, the positively skewed shape of the original data has been maintained. In all cases, both Ordinary Kriging and Sequential Gaussian Simulation have successfully reproduced the histograms and are quite similar to that of actual data.

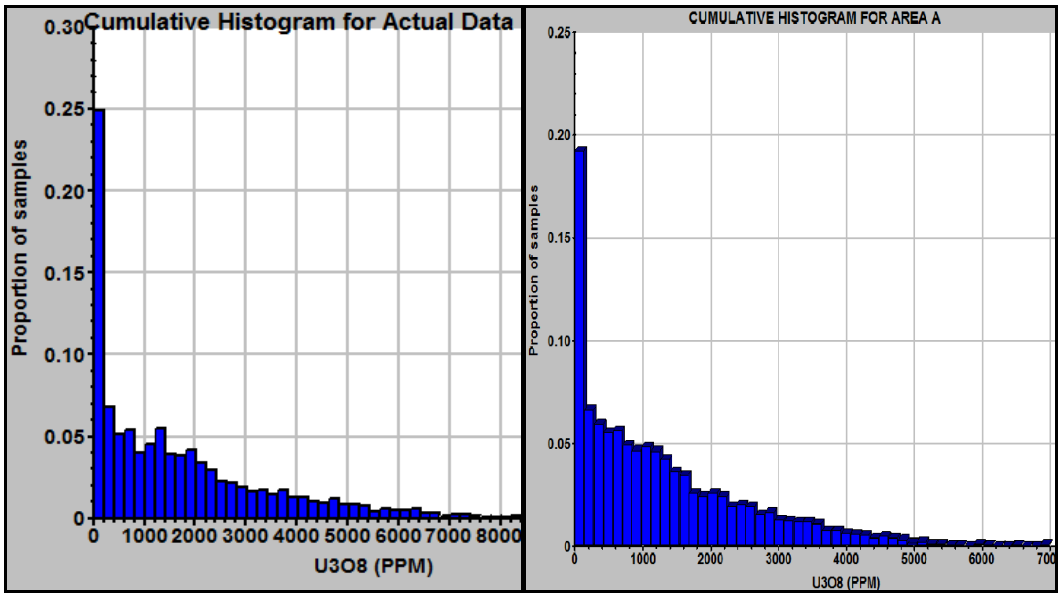


Figure 5.15: Histograms of actual data versus OK model for Area A

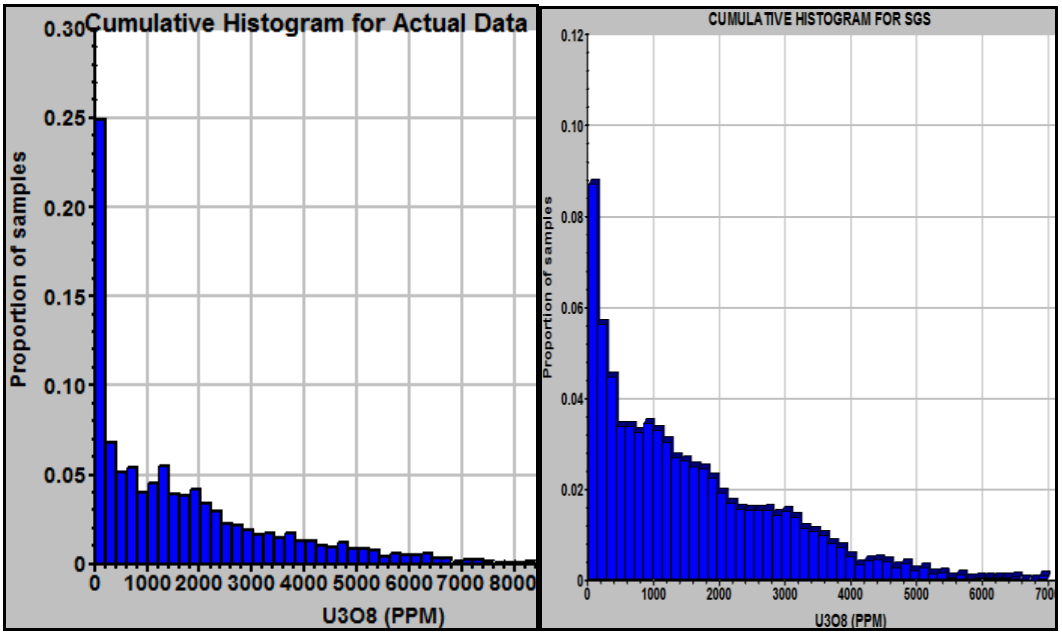


Figure 5.16: Histograms of actual data versus SGS model for Area A

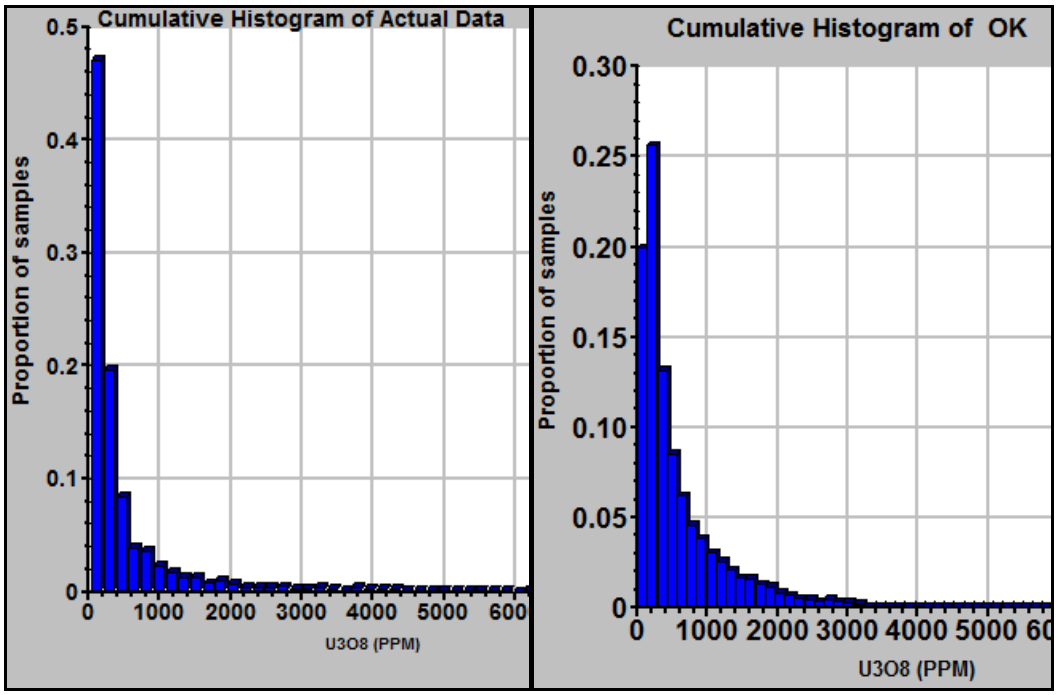


Figure 5.17: Histograms of actual data versus OK model for Area B

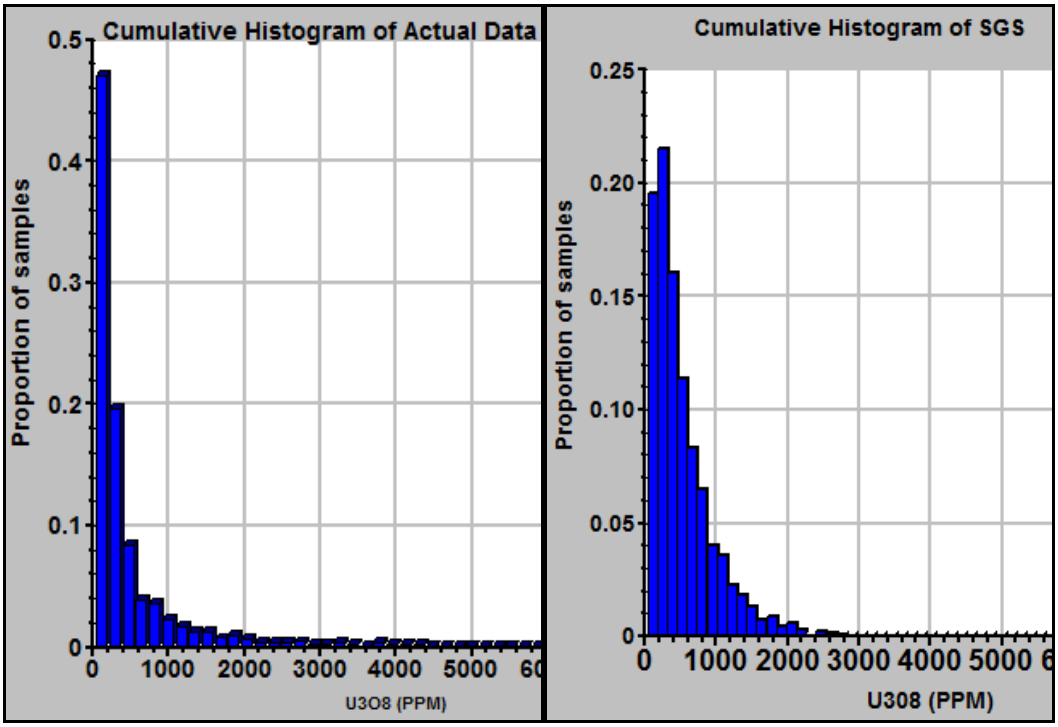


Figure 5.18: Histograms of actual data versus SGS model for Area B

5.2.4 QQ Plots comparison

QQ plots for comparing actual data and estimates were created and Figures 5.19 and 5.20 illustrates how the QQ plots from estimates compare with that of actual data. Both techniques indicate an overestimation of the input data, although OK appears to have a closer correlation with the blast hole data than the SGS estimates for Area A. Higher grades (above 2300 ppm) appear to have been underestimated as shown in the graphs. The correlation between actual data and model estimates for Area B seems to be better for lower grades, for higher grades there is poor correlation. Overall there is better correlation for Area A than Area B for both techniques. The poor results can be attributed to difference in support that was used, whereby for actual data, point support (from drill holes) was used while for estimates it was the block support used.

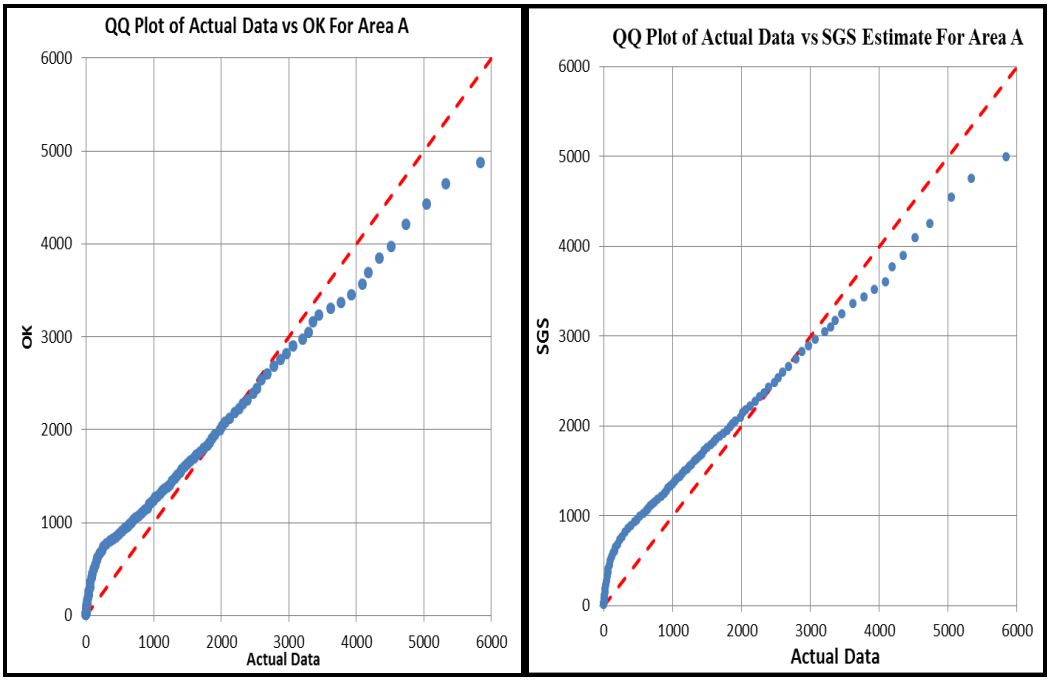


Figure 5.19: QQ plot of Actual data versus OK and SGS estimates for Area A

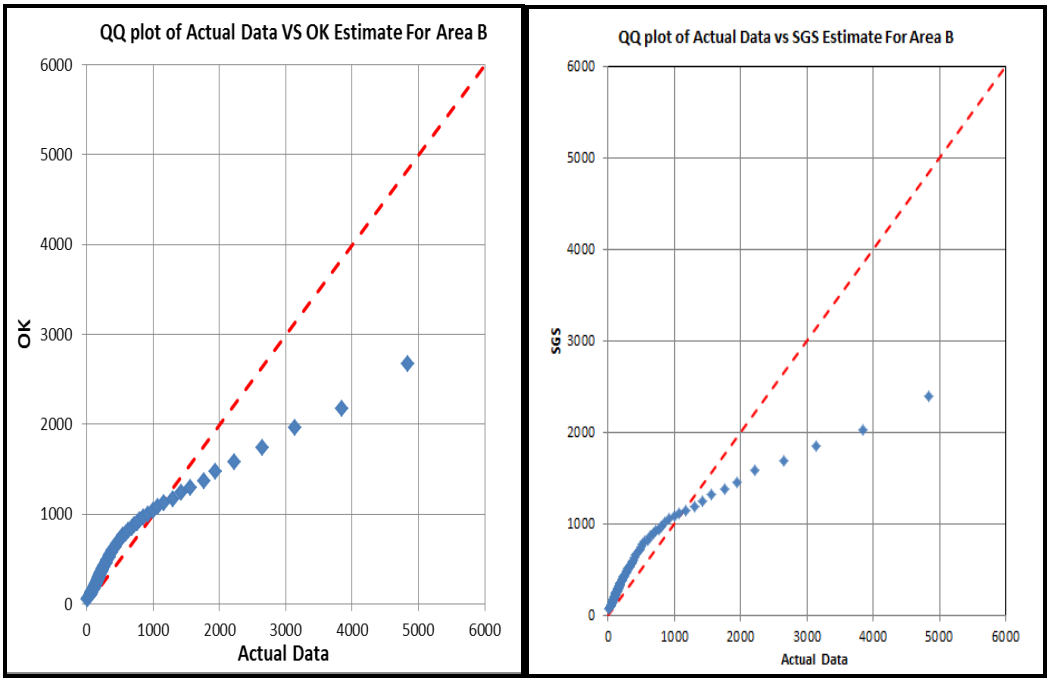


Figure 5.20: QQ plot of Actual data versus OK and SGS estimates for Area B

5.3 Quantitative Comparison of Estimates with Actual Values

Examination of the grade maps, histograms, QQ plots and cumulative frequency curves gave the visual comparison of data. These helped to understand spatial difference between the estimates and the actual data and it is more qualitative. There was no quantification of the differences therefore other methods were also used to compliment the visual comparison of data. Such methods include grade tonnage curves, statistical parameters, correlation coefficients, profit and loss analysis.

5.3.1 Comparison of descriptive statistics

The descriptive statistics for the actual data and estimates are shown in Table 5.1. Averages of estimates for both Area A and Area B appears to be similar to raw data, except for OK estimates for Area A. OK method has reproduced the median values for both data sets while SGS has slightly increased the median values, which indicates an overestimation of low values. The maximum values for both methods are similar, but have been underestimated due to smoothing effect on the

data by both methods. Standard deviations for both techniques are lower than the actual values also indicating smoothing of data and reduced variability in the estimates than the actual data.

Table 5.1: Comparison of statistics for actual data, OK and SGS estimates

AREA A					
	Mean	**Minimum**	**Median**	**Maximum**	**Std. dev.**
Actual Data	1,663	0.03	1,165	12,721	1,781
SGS	1,654	0.2	1,171	7,957	1,290
OK	1,698	0.5	1,163	7,292	1,206
AREA B					
	Mean	**Minimum**	**Median**	**Maximum**	**Std. dev.**
Actual Data	529	0.3	204	9,832	941
SGS	526	0.9	392	4,328	542
OK	496	0.7	301	4,312	523

Estimates have statistical parameters closer to actual data. The estimated means of OK and SGS estimates are in good agreement with the actual data. However, the statistic parameters, through low standard deviation show that there is less grade variability of estimates from both techniques than the actual data. The parameters also show a decrease in maximum values for the estimates than the actual data. Less variation and less maximum values indicate some degree of smoothing in the estimates. The difference in standard deviation can be attributed to difference in size and volume of the unit under consideration, since in estimates blocks are being used while in actual data drill hole sample support is being used.

5.3.2 Grade tonnage results and curves

Grade Tonnage Curves are tools frequently used in mines during planning and production. They are used to relate tonnage of mineable ore to its grade production to determine the volume and grade of ore that can be profitably mined at a given cut-off grade. Ravenscroft (1992) carried out a comparison of grade

tonnage curves from discrete gaussian model, Ordinary Kriging and Conditional Simulation for comparing recoverable reserve estimates. In the study, further examination of the estimates was made using a comparison between the grade tonnage curves of actual data and the estimates. Since there are three main ore categories used to delineate ore i.e. 400 ppm for low grade, 600 ppm for medium grade ppm and above 800 ppm for high grade, the grade, tonnes and metal, the results in Table 5.2 and Table 5.3 have been calculated based on these grade categories. It can be observed that for Area A, the estimates are almost identical, with SGS producing slightly lower values than OK. When total estimates are considered, results are even very similar. Examination of the metal content from the estimates above each cut-off grade shows similar amount of metal content between the estimates and they are close to actual metal content.

Table 5.2: Grade, tonnes and contained U3O8 (metal) above cut-off grades by actual data, OK and SGS estimates for Area A

AREA A					
Technique		**Cut-off Grade**			
		400 ppm	**600 ppm**	**800 ppm**	**ALL**
Actual	**Grade(ppm)**	2,194	2,301	2,442	1,896
	Tonnes	108,372	100,276	91,774	158,693
	Metal (Mt)	226	224	218	227
OK	**Grade(ppm)**	1,961	2,044	2,144	1,630
	Tonnes	119,681	113,212	105,402	145,960
	Metal (Mt)	235	231	226	238
SGS	**Grade(ppm)**	2,049	2,116	2,223	1,847
	Tonnes	110,283	105,687	98,283	123,138
	Metal (Mt)	238	231	224	301

The results for Area B in Table 5.3 show the similarity between OK, SGS estimates with Actual data, for both grade and tonnes. Examination of the contained metal at each cut-off grade shows similar metal content from estimates and actual data.

Table 5.3: Grade, tonnes and contained U3O8 (metal) above cut-off grades by actual data, OK and SGS estimates for Area B

AREA B					
Technique		**Cut-off Grade**			
		400 ppm	**600 ppm**	**800 ppm**	**ALL**
Actual	**Grade(ppm)**	1,027	1,248	1,469	348
	Tonnes	45,765	32,910	25,466	112,327
	Metal (Mt)	47	41	37	39
OK	**Grade(ppm)**	947	1,158	1,370	307
	Tonnes	51,623	35,432	24,327	119,192
	Metal (Mt)	49	41	33	37
SGS	**Grade(ppm)**	908	1,144	1,312	329
	Tonnes	53,982	34,537	25,140	113,294
	Metal (Mt)	49	40	33	37

Furthermore, grade and tonnage from estimates were calculated for each grade interval, Tables B1 and B2 in the appendix shows the results and these formed the basis from which grade and tonnage curves were established. Grade tonnage curves in Figure 5.21 show that tonnage for both OK and SGS estimates are close to that of actual data for Area A, however, both techniques consistently predicts lower grade than actual data at each cut off. There is a bigger margin in grades between SGS and OK estimates with the actual values, however the estimated grade from both techniques appear to be very similar. The results are even very similar for Area B, as it can be observed from Figure 5.22, with both grade and tonnage from estimates being close to that of actual values. The difference in the results is also due to difference in support, for actual data, points were used whereas for OK and SGS, block data was used.

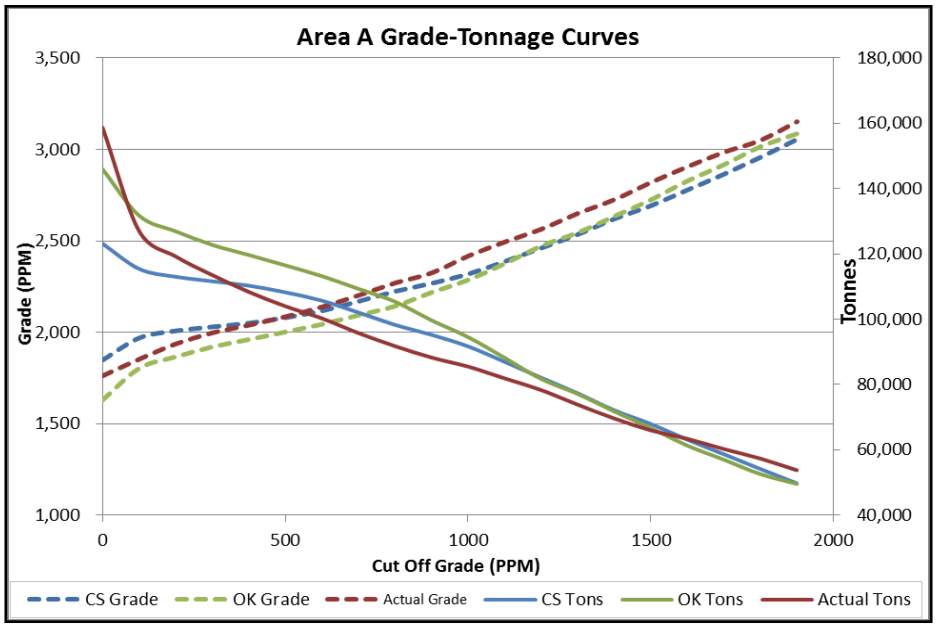


Figure 5.21: Grade tonnage curves for Area A

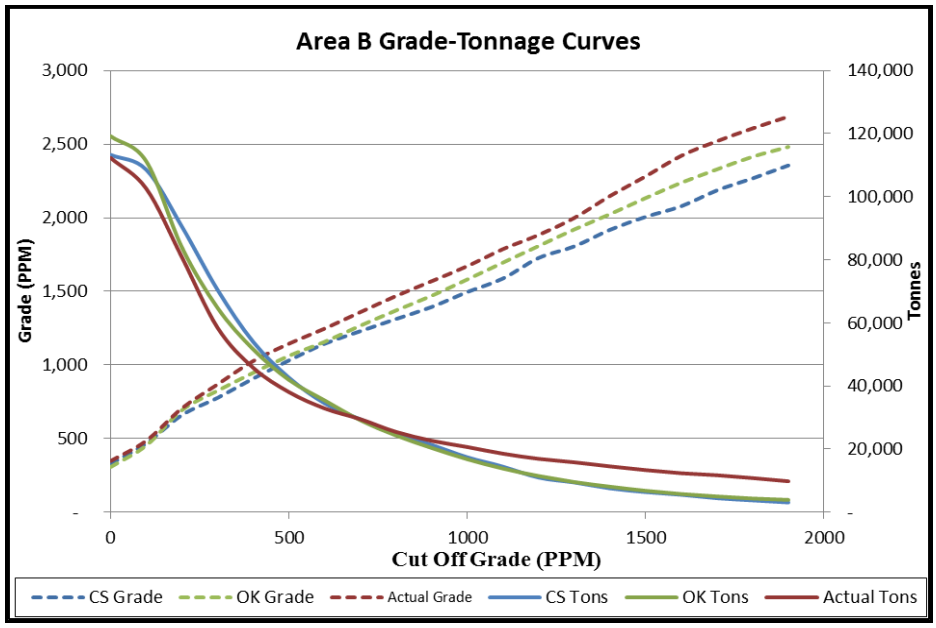


Figure 5.22: Grade tonnage curves for Area B

Overall, from the grade tonnage results and curves, it has been established that actual data, OK and SGS estimates are similar. This means that the techniques reproduced the data quite well. The results are similar even at high cut-off grade, except for grade for Area A which has tonnage slightly different for medium grades.

5.3.3 Correlation coefficients and correlation graphs

As another way of finding out how well the estimates matched with the original data, scatter plots were plotted and correlation coefficients calculated from the scatterplots. A positive correlation can be observed from scatterplots in Figure 5.23 and 5.24 for Area A and Area B respectively. From the trend line fitted to the scatterplots, correlation coefficients were calculated and have been summarised in Table 5.4. The correlation coefficients indicate a good correlation between model estimates from both techniques and blast hole data. However a strong bias can be observed from both techniques in Figures 5.23 and 5.24. Grades from estimates are observed to be lower than the actual values, probably due to difference in support used. Similarly with grade-tonnage curves, point support inform of blast hole data was used for actual data, while for estimates the block support was used.

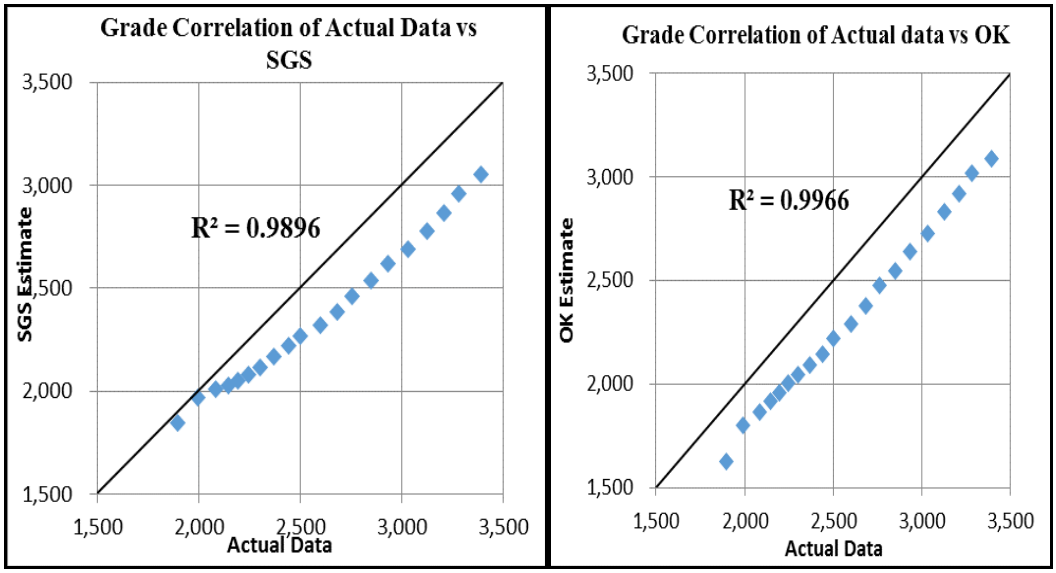


Figure 5.23: Comparison of correlation plots for Area A

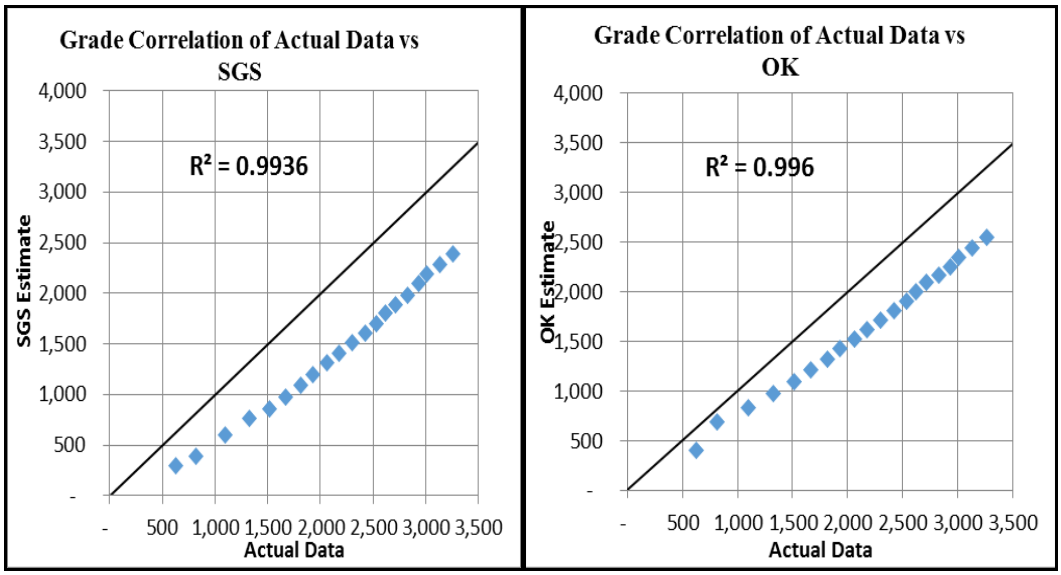


Figure 5.24: Comparison of correlation plots for Area B

Table 5.4: Correlation coefficients of blast hole data, OK and SGS estimates

	Area A	Area B
	Actual Data	Actual Data
SGS	0.9896	0.9936
OK	0.9966	0.996

5.3.4 Profit and loss from the estimates

As one way of reviewing grade control classification of ore and waste, Verly (2005) used a profit/loss approach to compare different grade estimation techniques, similar approach was used in the study. The formulas used to calculate profit have been displayed in equations 1 and 2. The economic parameters in Table 5.5 and the formulas used are also the ones used by the Paladin Energy LTD in calculating profit and losses.

Profit = Revenue – Cost (1)

Profit = (Recovery*metal*price) – ((processing cost*tonnes processed) + (ore mining cost*tonnes of ore) + (waste mining cost*tonnes of waste) (2)

Table 5.5: Economic parameters for calculating profits/loss

Economic parameter	Price
Processing Cost ($/t)	45
Recovery (%)	85
Ore Mining Cost ($/t)	3
Waste mining cost ($/t)	1
Uranium price ($/t)	132,277

Profits were calculated at main four ore grade categories as used during mining and Table 5.6 and 5.7 shows the results for Area A and Area B respectively. At all cut offs, estimates give profits that are very similar and are close to actual data. As the cut off increases, the profits are decreasing and the profits from estimates are becoming very similar.

Table 5.6: **Profits and losses from Actual, OK and SGS estimates for Area A**

AREA A					
Technique		**Cut-off Grade**			
		All	**400 ppm**	**600 ppm**	**800 ppm**
Actual	**Profit ($ 000's)**	22,558	21,499	21,094	20,746
	Grade (ppm)	1,860	2,194	2,301	2,442
	Tonnes	31,690	4,393	4,515	3,498
OK	**Profit ($ 000's)**	19,737	20,616	20,555	20,307
	Grade	1,630	1,961	2,044	2,144
	Tonnes	14,238	3,173	3,905	5,736
SGS	**Profit ($ 000's)**	19,665	20,103	20,059	19,824
	Grade (ppm)	1,847	2,049	2,116	2,223
	Tonnes	1,180	3,621	2,197	2,888

Table 5.7: Profits and losses from Actual, OK and SGS estimates for Area B

AREA B					
Technique		**Cut-off Grade**			
		All	**400 ppm**	**600 ppm**	**800 ppm**
Actual	**Profit ($ 000's)**	-997	3,023	2,957	2,896
	Grade (ppm)	348	1,027	1,248	1,469
	Tonnes	112,327	45,765	32,910	25,466
OK	**Profit ($ 000's)**	-1,606	2,952	2,827	2,486
	Grade (ppm)	307	947	1,158	1,370
	Tonnes	119,192	51,623	35,432	24,327
SGS	**Profit ($ 000's)**	-1,247	2,862	2,707	2,414
	Grade (ppm)	329	908	1,144	1,312
	Tonnes	113,294	53,982	34,537	25,140

Profits at all cut-off grades were calculated and have been presented in Table C1 in appendix, and graphs in Figure 5.25 and 5.26 were plotted from the results. From the graphs it can be noted that maximum profit will be realised at cut-off grade of 400 ppm for both techniques. It can be noted that estimates and actual data match very closely. Overall, there is little difference in profits between the estimates and they are close to actual profits. This means that both techniques have produced accurate estimates as the profits that can be obtained from estimates are similar to actual data.

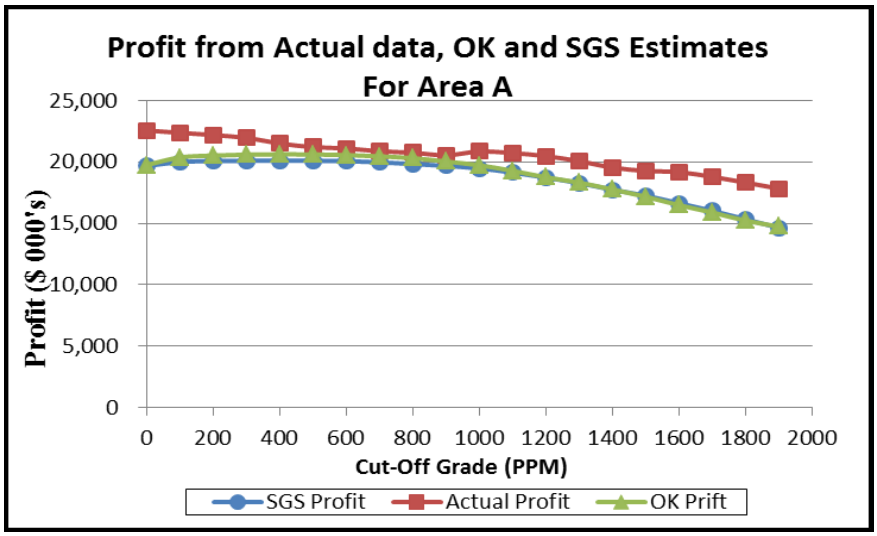


Figure 5.25: Profits from Actual data, OK and SGS estimates for Area A

As with Area A, the maximum profit will be realised at 400 ppm for Area B. Unlike Area A, when everything is mined there can be a significant loss of up to $1606 since there are more low grades which are probably so low with respect to mill cut-off grades. Since processing each and every material going through mill is part of processing cost, in this regards the waste material will increase the cost while having no financial value, hence negative profits. There is little difference in profits between the estimates from OK and SGS techniques. However, estimates and actual data profits are similar for only up to where maximum profits are realised, beyond which there is a significant difference in profits whereby the estimates profits decreasing more than the actual data.

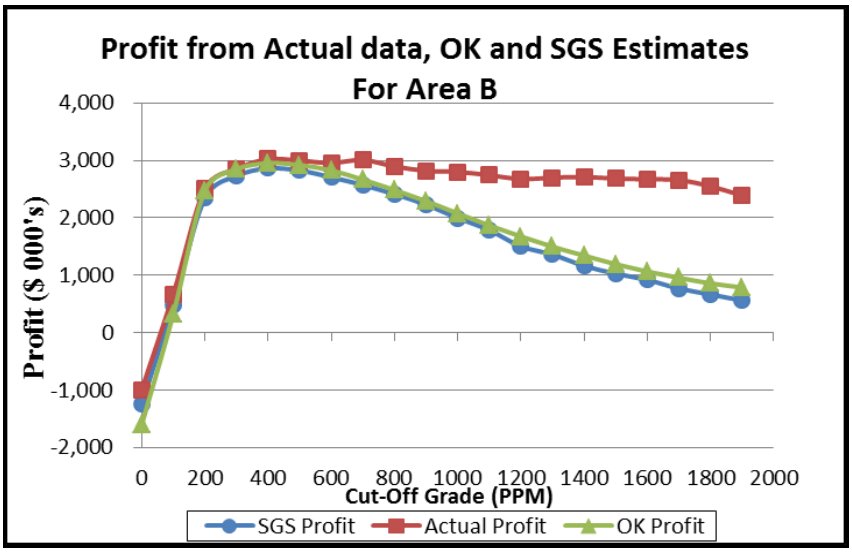


Figure 5.26: Profits from Actual data, OK and SGS estimates for Area B

A comparison of profits and actual data shows that estimates give similar profits that are close to actual data, especially for Area A and lower grades of Area B. The similarity in profits among the estimates implies that both techniques produce accurate estimates and similar profits will be realised by using either OK or SGS. However, there is a significant drop in profits by both techniques for Area B, which is due to the grade distribution of Area B which was less continuous, hence lower grades were found together with high grade. With lower cut-off grade there is less selectivity but as the grade increases there will be more selectivity and less

tonnage, hence a drop in profits. As expected Area A has more profits than Area B since the grade mineralisation was high. From these profit graphs, it can be concluded that the techniques gave similar estimates that can be said that they reflect blast hole data.

Additionally, Verly (2005) compared the profits from different techniques with that Average simulation which was considered as the truth. Similar approach was also used in the study, in this case scatter plot of profits from estimates were plotted. There is a good correlation between estimates themselves for both Area A and Area B as can be observed from Figure 5.27. However, a minor difference can be observed for very high profits, whereby Ordinary Kriging tends to outperform SGS for Area A.

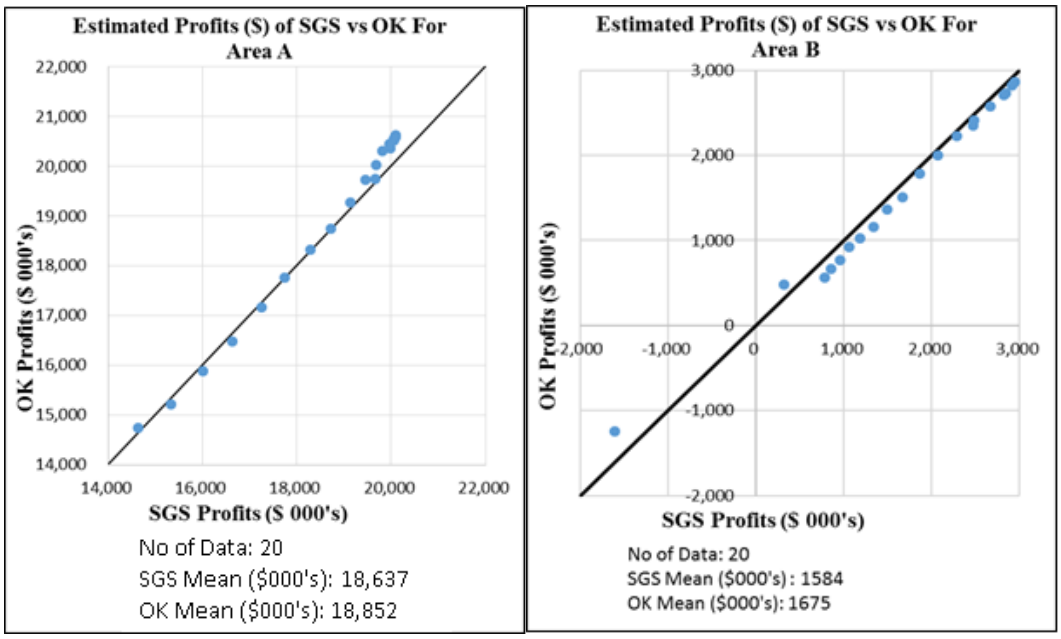


Figure 5.27: SGS versus OK Profits for Area A (left) and Area B (Right)

5.4 Chapter Summary

Two estimates were prepared one using Ordinary Kriging and another using Sequential Gaussian Simulation. This chapter presented the results of the study. Discussed were the comparisons between actual data and estimates from OK and

SGS and different methods were used to compare these estimates. The estimations were checked in plan views against the raw data. From the visual observation it was found that both techniques gave grade results close to actual values especially for data set A. When the estimates were compared with adjacent blast holes, it was noted that model estimates reflected blast holes quite well. From profits generated, it was established that the estimates were similar, both techniques gave profits close to actual data. Through grade tonnage curves, it was found that OK performed better than the SGS, but the differences between the estimates themselves were minimal, both techniques were close to actual data. Correlations coefficients from both techniques were within acceptable range (close to one). Good correlation could be due to large amount of data used which makes it more similar to raw data. Additionally, the profits generated and correlation coefficients gave similar results and both acceptable, implying that both techniques are accurate. However scatterplots from grade estimates and actual data, indicated some bias, which was due to point support used for actual data and block support for estimates

Not only were the estimates similar, but both also introduced some minor smoothing in estimates, observed through less variability of grades. This was observed from descriptive statistics that model estimates had higher minimum and low maximum values than the actual data. Through the coefficient of variation and standard deviation, it was identified that both techniques have slightly lower variability than actual data, especially for Area B. This could be due to the grade distribution which was more variable.

6 CONCLUSION AND RECOMMENDATIONS

The study was carried out to compare Ordinary Kriging and Sequential Gaussian Simulation for recoverable reserve estimation at Kayelekera mine. Estimates were generated for two areas with different grade distributions within the pit using Hellman and Schofield's MP software. From the generated estimates a comparison was carried out which included examination of descriptive statistics, histograms, profit and loss analysis, cumulative curves, grade tonnage curves, correlation coefficients and correlation graphs.

Overall, no significant differences could be established, due to grade distribution. However for Area B, the profits dropped substantially after reaching maximum cut-off grade, which was due to less grade continuity for the area. In addition, the SGS model may benefit from some basic form of data domaining to limit the influence of high grade populations on lower grade areas and vice-versa, particularly given the restricted low grade distribution.

The results show that Ordinary Kriging and Sequential Gaussian Simulation methods give similar estimates from grade and tonnage above cut-off grade results. Similarity in results was also observed through the profits analysis of the estimates as well as the descriptive statistics for both techniques. However, from correlation plots, a huge bias was apparent, which was mainly attributed to the fact that point and block support was used for actual data and estimates respectively.

Despite both techniques providing geologically sensible recoverable reserve estimates, some degree of smoothing was observed. The results from descriptive statistics and histograms showed less variability through increased mean and decreased maximum and less variability was also observed through the decreased range in the histograms. Less variability in grades was found to be due to smoothing of data by both techniques. It is important to note that one of the contributing factors for smoothing in the SGS was due to the averaging of simulations. In the study, since hundred realisation were averaged to give an

estimate at a single location, there is a possibility that this introduced some smoothing in the data. Consequently, the averaging of 100 realisations was equivalent to Ordinary Kriging estimates.

In spite of the similarities in grade and tonnage between the estimates, through observation from the grade maps it was observed that Sequential Gaussian Simulation maintained spatial variability of data better than Ordinary Kriging. OK does not reproduce the variability of data and cannot be used where local variation in grades is significant. SGS seems to better reproduce sharp and gradual grade contacts much better than OK, which has smoothing effect on grade especially where the grades values change abruptly. On this basis, therefore, it can be concluded that SGS is a more appropriate technique for local reserve estimation than OK. In situation where local variation is insignificant, e.g. large mining blocks, Ordinary Kriging can give equally good results like Sequential Gaussian Simulation.

Since two sets of software are used at KM mainly for grade estimation using Sequential Gaussian Simulation and another one for data check as well as creating ore grade maps, this increases costs in paying licence fee for the software. The software used for creating maps cannot be used in estimation because one cannot run Sequential Gaussian Simulation but it is used for creating maps and data validation only. It will be financially beneficial at KM to try using Ordinary Kriging in ore modelling since it has been observed that there is minimal difference between SGS and OK. The method ought to be compared with the current technique since using a single software package for both modelling and creating ore block boundary maps would have a positive financial effect. In this case, smoothing from Ordinary Kriging ought to be quantified to decide if it can be used instead of Sequential Gaussian Simulation.

Additionally, a study needs to be done to quantify the differences through actual ore recovered from the mill. In this regard, reconciliation should be done between OK estimates, SGS estimates and actual material recovered from the mill.

REFERENCES

Armstrong, M. (1998) "Basic Linear Geostatistics." Berlin: Springer.

Asghari, O., Soltni, F. and Amnieh, B. (2009) "The Comparison between Sequential Gaussian Simulation (SGS) of Choghart Ore Deposit and Geostatistical Estimation through Ordinary Kriging." Australian Journal of Basic and Applied Sciences, vol 3, no1, pp 330-341

Barrett, DM. (2005) "Kayelekera Uranium Deposit Malawi. Preliminary Investigation of High Background Radiation Levels Sometimes Recorded on Downhole Gamma Logs." Unpublished internal report, Paladin Energy Ltd.

Barnes, R. (2005) "Variogram Tutorial." Golden Software Inc.

Bohling, G. (2005a) "Introduction to Geostatistics and Variogram Analysis." Kansas geological survey. INTERNET. Http://people.ku.edu/~gbohling/cpe940/. Cited 3 October 2013.

Bohling, G. (2005b) "Kriging." Kansas geological survey. INTERNET. Http://people.ku.edu/~gbohling/cpe940/. Cited 3 October 2013

Bohling, G. (2005c) "Stochastic simulation and reservoir modelling workflow." Australian Journal of Basic and Applied Sciences, vol. 3, no1, pp 330-341.

Bowden, RA and Shaw RP. (1991) "The Kayelekera Uranium Deposit, northern Malawi. Past exploration activities, economic geology and decay series disequilibrium" Unpublished CEGB project report

Brown, LR. (1989) "Kayelekera Uranium Project, - In-situ Geological Reserves." Unpublished CEGB project report

Clark, I. (1979) "Practical geostatistics." London: Applied Science Publishers.

Coombes J. (1997) "Handy Hints for Variography" AusIMM National Conference on Iron Making Resources and Reserves Estimation

David, M. (1977) "Geostatistical Ore Reserve Estimation." Amsterdam: Elsevier pp 2-48

Delhomme, IP and Delfiner, P. (1973) "Application du krigeage a l'optimisation d'une champagne pluviometrique en zone a ride" Symposium on the design of water resources Projects with inadequate data. Madrid, pp 191-210

Deutsch, CV. (2002) “Geostatistical Reservoir Modelling.” New York: Oxford University Press

Deutsch, CV and Journel AG. (1992) “GSLIB: Geostatistical Software Library and User’s Guide.” New York: Oxford university press. pp340

De-Vitry, C., Vann J and Arvidson, H. (2007). “A Guide to Selecting the Optimal Method of Resource Estimation for Multivariate Iron Ore Deposit.” Iron ore conference. Perth

Dowd, PA and David, M. (1976) “Advanced Geostatistics in the Mining Industry. Dordrecht: D. Reidel Pub. Co.

Isaaks, EH and Srivastava, RM. (1989) “An introduction to applied geostatistics.” New York: Oxford University Press.

Journel, AG and Huijbregts, CJ. (1978) “Mining geostatistics.” London: Academic Press.

Journel, AG and Isaaks, EH. (1984) “Conditional indicator simulation: Application to a Saskatchewan uranium deposit.” Mathematical Geology, vol 16, no 7, pp 685-718.

Khosrowshahi, S., Shaw, WJ and McKevitt MB. (2009) “Ore Block Optimisation for Open Pit Grade Control.” Seventh International Mining Geology Conference. Perth

Krige, DG. (1951) “A statistical approach to some basic mine valuation problems on the Witwatersrand. Journal of the Chemical, Metallurgical and Mining Society of South Africa. Dec 1951, pp 119-139

Lipton, IT., Gaze, RL, Horton, JA and Khosrowshahi, S. (1998) “Practical application of multiple indicator kriging and conditional simulation to recoverable resource estimation for the Halley’s lateritic nickel deposit.” Beyond Ordinary Kriging: Non-Linear Geostatistical Methods In Practice. Perth, Geostatistical Association of Australasia.

Marcotte, D and Asli, M. (1995) “Comparison of approaches to spatial estimation in a bivariate context.” Mathematical Geology, vol 27, pp 641–658

Matheron, G. (1971) “The theory of regionalise variables and its application.” Cahier no 5, Centre de Morphologie Mathematique de Fontainebleau

ND, (2007) “Paladin Energy Annual Report” unpublished Paladin Energy report

Rambert, F. (ND) “Introduction to Mining Geostatistics.” Geovariances. Avon, France

Ravenscroft, PJ. (1992) **“**Recoverable reserve estimation by conditional simulation.” Geological Society, London, Special Publications, vol 63, pp 289-298

Rossi, ME. (1999) “Improving the Estimates of the Recoverable Reserves” Mining Engineering, Society for Mining, Metallurgy and Exploration (SME), vol 51, pp. 50-54.

Rossi, ME., and Deutsch, CV. (2013) “Mineral Resource Estimation.” Springer, New York.

Royle, AG. Claussen, FL and Frederiksen, P. (1981) “Paractical Universal Kriging and Automatic contouring” Geo-Proc, vol 1, pp 377-394

Samal, A. (1998) “Issues about kriging.” 25th Annual Mineral Exploration Roundup, Vancouver, B.C., Canada

Schofield, N., and Rolley, P. (1997) “Optimisation of ore selection in mining: Method and case studies.” 3rd International Mining Geology Conference, AusIMM-AIG, Series 6.97, p. 93–97.

Shaw, RP (1990) “The Geology of the Kayelekera Uranium Deposit.” Unpublished CEGB project report.

Sinclair, AJ and Blackwell, GH. (2002) “Applied Mineral Inventory Estimation.” UK: Cambridge University Press

Vann, J., Bertoli, V. and Jackson, S. (2002) “Geostatistical Simulation for Quantitative Geoscience.” Geostatistical Association of Australasia symposium.

Verly, G. (2005) “Grade Control Classification of Ore and Waste: A Critical Review of Estimation and Simulation Procedures.” Mathematical Geology, vol 37, no 5

Vizi, L. (2008) “A Case Study in Uniform Conditioning of Local recoverable Reserves Estimation for Jelsava Magnetite Deposit-level 220.” Geoscience Engineering, vol. LIV, no.1 pp. 41-53, ISSN 1802-5420

APPENDIX A: CONSOLIDATED FILE WITH ALL DATA TYPES

Table A1: Sample of file with all data collected

Hole ID	From	To	Rock Type	RDX	UNIT	XRF	gamma original	gamma factored	Final_ u3o8	Easting	Northing	RL
1_930_019BH24	0	1	MDST	MD	RS	167	56	79	79	576298.6	8896159.2	928.9
1_930_019BH24	1	2	MDST	MD	RS	1425	836	1179	1179	576298.6	8896159.2	927.9
1_930_019BH24	2	3	Arkose	AR	S	5867	3429	4115	4115	576298.6	8896159.2	926.9
1_930_019BH24	3	4	Arkose	AR	S	1662	1917	2301	2301	576298.6	8896159.2	925.9
1_930_019BH24	4	5	Arkose	AR	S	786	910	1092	1092	576298.6	8896159.2	924.9
1_930_019BH24	5	6	Arkose	AR	S	1100	1769	2123	2123	576298.6	8896159.2	923.9
1_930_019BH24	6	7	Arkose	AR	S	1303	1636	1963	1963	576298.6	8896159.2	922.9
1_930_019BH25	0	1	MDST	MD	RS	224	6	8	8	576296.4	8896163.0	929.5
1_930_019BH25	1	2	MDST	MD	RS	100	239	337	337	576296.4	8896163.0	928.5
1_930_019BH25	2	3	Arkose	AR	S	1780	3558	4270	4270	576296.4	8896163.0	927.5
1_930_019BH25	3	4	Arkose	AR	S	1058	3507	4209	4209	576296.4	8896163.0	926.5
1_930_019BH25	4	5	Arkose	AR	S	437	2102	2523	2523	576296.4	8896163.0	925.5
1_930_019BH25	5	6	Arkose	AR	S	646	1752	2103	2103	576296.4	8896163.0	924.5
1_930_019BH25	6	7	Arkose	AR	S	1631	1983	2379	2379	576296.4	8896163.0	923.5
1_930_019BH26	0	1	MDST	MD	RS	379	1	1	1	576294.2	8896166.8	929.5
1_930_019BH26	1	2	Arkose	AR	S	339	143	172	172	576294.2	8896166.8	928.5
1_930_019BH26	2	3	Arkose	AR	S	324	990	1188	1188	576294.2	8896166.8	927.5
1_930_019BH26	3	4	Arkose	AR	S	252	701	842	842	576294.2	8896166.8	926.5
1_930_019BH26	4	5	Arkose	AR	S	258	363	436	436	576294.2	8896166.8	925.5
1_930_019BH26	5	6	Arkose	AR	S	243	452	542	542	576294.2	8896166.8	924.5
1_930_019BH26	6	7	Arkose	AR	S	231	548	658	658	576294.2	8896166.8	923.5
1_930_019BH26	7	8	Arkose	AR	S	2225	1406	1688	1688	576294.2	8896166.8	922.5
1_930_019BH27	0	1	MDST	MD	RS	284	26	37	37	576291.9	8896170.6	929.6
1_930_019BH27	1	2	Arkose	AR	S	2877	1620	1944	1944	576291.9	8896170.6	928.6
1_930_019BH27	2	3	Arkose	AR	S	3385	4816	5779	5779	576291.9	8896170.6	927.6
1_930_019BH27	3	4	Arkose	AR	S	3010	4404	5285	5285	576291.9	8896170.6	926.6
1_930_019BH27	4	5	Arkose	AR	S	5859	6251	7501	7501	576291.9	8896170.6	925.6
1_930_019BH27	5	6	Arkose	AR	S	3603	2408	2890	2890	576291.9	8896170.6	924.6
1_930_019BH27	6	7	Arkose	AR	S	2241	1002	1203	1203	576291.9	8896170.6	923.6
1_930_019BH27	7	8	Arkose	AR	S	1464	NS	1464	1464	576291.9	8896170.6	922.6
1_930_019BH28	0	1	MDST	MD	RS	248	49	69	69	576289.7	8896174.4	929.7
1_930_019BH28	1	2	Arkose	AR	S	578	1989	2387	2387	576289.7	8896174.4	928.7
1_930_019BH28	2	3	Arkose	AR	S	4324	4534	5441	5441	576289.7	8896174.4	927.7
1_930_019BH28	3	4	Arkose	AR	S	1219	1407	1689	1689	576289.7	8896174.4	926.7
1_930_019BH28	4	5	Arkose	AR	S	893	851	1021	1021	576289.7	8896174.4	925.7
1_930_019BH28	5	6	Arkose	AR	S	710	701	841	841	576289.7	8896174.4	924.7
1_930_019BH28	6	7	Arkose	AR	S	450	624	749	749	576289.7	8896174.4	923.7
1_930_019BH28	7	8	Arkose	AR	S	382	NS	382	382	576289.7	8896174.4	922.7

Table A1: Sample of file with all data collected-continued

Hole ID	From	To	Rock Type	RDX	UNIT	XRF	gamma original	gamma factored	Final_ u3o8	Easting	Northing	RL
1_930_019BH29	0	1	MDST	MD	RS	253	269	379	379	576287.5	8896178.2	929.6
1_930_019BH29	1	2	MDST	MD	RS	343	3478	4904	4904	576287.5	8896178.2	928.6
1_930_019BH29	2	3	Arkose	AR	S	2717	4336	5203	5203	576287.5	8896178.2	927.6
1_930_019BH29	3	4	Arkose	AR	S	3216	5392	6471	6471	576287.5	8896178.2	926.6
1_930_019BH29	4	5	Arkose	AR	S	2927	6320	7584	7584	576287.5	8896178.2	925.6
1_930_019BH29	5	6	Arkose	AR	S	2040	5013	6016	6016	576287.5	8896178.2	924.6
1_930_019BH29	6	7	Arkose	AR	S	1141	3204	3845	3845	576287.5	8896178.2	923.6
1_930_019BH29	7	8	Arkose	AR	S	671	3119	3743	3743	576287.5	8896178.2	922.6
1_930_019BH30	0	1	Arkose	AR	S	1109	126	152	152	576285.2	8896181.9	929.5
1_930_019BH30	1	2	Arkose	AR	S	2676	2934	3521	3521	576285.2	8896181.9	928.5
1_930_019BH30	2	3	Arkose	AR	S	3516	4540	5448	5448	576285.2	8896181.9	927.5
1_930_019BH30	3	4	Arkose	AR	S	2991	4295	5154	5154	576285.2	8896181.9	926.5
1_930_019BH30	4	5	Arkose	AR	S	4134	4955	5946	5946	576285.2	8896181.9	925.5
1_930_019BH30	5	6	Arkose	AR	S	2522	2394	2873	2873	576285.2	8896181.9	924.5
1_930_019BH30	6	7	Arkose	AR	S	1499	1405	1686	1686	576285.2	8896181.9	923.5
1_930_019BH31	0	1	MDST	MD	RS	553	1041	1468	1468	576283.0	8896185.7	929.4
1_930_019BH31	1	2	Arkose	AR	S	3020	2873	3448	3448	576283.0	8896185.7	928.4
1_930_019BH31	2	3	Arkose	AR	S	2729	2040	2448	2448	576283.0	8896185.7	927.4
1_930_019BH31	3	4	Arkose	AR	S	2893	2946	3535	3535	576283.0	8896185.7	926.4
1_930_019BH31	4	5	Arkose	AR	S	1734	1990	2388	2388	576283.0	8896185.7	925.4
1_930_019BH31	5	6	Arkose	AR	S	1082	1131	1357	1357	576283.0	8896185.7	924.4
1_930_019BH31	6	7	Arkose	AR	S	1058	1266	1519	1519	576283.0	8896185.7	923.4
1_930_019BH36	0	1	MDST	MD	RS	278	105	147	147	576294.5	8896159.3	929.3
1_930_019BH36	1	2	MDST	MD	RS	1151	1374	1937	1937	576294.5	8896159.3	928.3
1_930_019BH36	2	3	Arkose	AR	S	2248	4362	5234	5234	576294.5	8896159.3	927.3
1_930_019BH36	3	4	Arkose	AR	S	2245	2997	3596	3596	576294.5	8896159.3	926.3
1_930_019BH36	4	5	Arkose	AR	S	1414	3111	3733	3733	576294.5	8896159.3	925.3
1_930_019BH36	5	6	Arkose	AR	S	1698	4051	4861	4861	576294.5	8896159.3	924.3
1_930_019BH36	6	7	Arkose	AR	S	1673	4283	5140	5140	576294.5	8896159.3	923.3
1_930_019BH37	0	1	MDST	MD	RS	322	68	96	96	576292.3	8896163.1	929.5
1_930_019BH37	1	2	MDST	MD	RS	1697	2554	3602	3602	576292.3	8896163.1	928.5
1_930_019BH37	2	3	Arkose	AR	S	4789	6942	8330	8330	576292.3	8896163.1	927.5
1_930_019BH37	3	4	Arkose	AR	S	2918	4675	5610	5610	576292.3	8896163.1	926.5
1_930_019BH37	4	5	Arkose	AR	S	1073	3662	4394	4394	576292.3	8896163.1	925.5
1_930_019BH37	5	6	Arkose	AR	S	1629	3766	4520	4520	576292.3	8896163.1	924.5
1_930_019BH37	6	7	Arkose	AR	S	1597	3732	4479	4479	576292.3	8896163.1	923.5
1_930_019BH38	0	1	MDST	MD	RS	340	9	13	13	576290.0	8896166.9	929.5
1_930_019BH38	1	2	Arkose	AR	S	1058	1115	1338	1338	576290.0	8896166.9	928.5
1_930_019BH38	2	3	Arkose	AR	S	3060	4289	5146	5146	576290.0	8896166.9	927.5
1_930_019BH38	3	4	Arkose	AR	S	2952	3396	4075	4075	576290.0	8896166.9	926.5
1_930_019BH38	4	5	Arkose	AR	S	3456	4042	4850	4850	576290.0	8896166.9	925.5

APPENDIX B: GRADE TONNAGE CURVE CALCULATIONS

Table B1: Comparison of Tonnage and Grades at different Grade Cut Offs for Blast hole Data, OK and SGS estimates for Area A

AREA A									
Cut off	**Blast hole**			**Ordinary Kriging**			**Sequential Gaussian Simulation**		
Grade (ppm)	**Grade (ppm)**	**Cum Tons**	**Metal**	**Grade (ppm)**	**Cum Tons**	**Metal**	**Grade (ppm)**	**Cum Tons**	**Metal**
0	1,663	158,693	264	1,630	145,960	238	1,783	140,753	251
100	2,072	127,003	263	1,803	131,722	237	1,797	139,573	251
200	2,197	119,233	262	1,866	126,922	237	1,863	134,244	250
300	2,296	113,538	261	1,920	122,772	236	1,931	128,793	249
400	2,388	108,372	259	1,961	119,681	235	1,987	124,399	247
500	2,470	103,978	257	2,002	116,508	233	2,033	120,779	246
600	2,541	100,276	255	2,044	113,212	231	2,077	117,321	244
700	2,630	95,761	252	2,094	109,307	229	2,105	115,124	242
800	2,712	91,774	249	2,144	105,402	226	2,137	112,399	240
900	2,786	88,276	246	2,219	99,666	221	2,171	109,511	238
1,000	2,845	85,509	243	2,287	94,540	216	2,199	107,070	235
1,100	2,924	81,889	239	2,376	88,194	210	2,240	103,368	232
1,200	3,006	78,309	235	2,474	81,726	202	2,293	98,568	226
1,300	3,112	73,834	230	2,547	77,129	196	2,349	93,564	220
1,400	3,219	69,603	224	2,636	71,760	189	2,423	87,137	211
1,500	3,317	65,983	219	2,727	66,675	182	2,507	80,221	201
1,600	3,389	63,379	215	2,830	61,305	173	2,588	73,916	191
1,700	3,480	60,247	210	2,919	56,993	166	2,674	67,773	181
1,800	3,568	57,318	204	3,018	52,559	159	2,771	61,305	170
1900	3,682	53,738	198	3,088	49,548	153	2,871	55,325	159

Table B2: Comparison of Tonnage and Grades at different Grade Cut Offs for Blast hole Data, OK and SGS estimates for Area B

AREA B									
Cut off	**Blast hole**			**Ordinary Kriging**			**Sequential Gaussian Simulation**		
Grade (ppm)	**Grade (ppm)**	**Cum Tons**	**Metal**	**Grade (ppm)**	**Cum Tons**	**Metal**	**Grade (ppm)**	**Cum Tons**	**Metal**
0	627	304 682	191	616	304 841	188	625	304 801	191
100	816	228 809	187	687	270 310	186	641	296 287	190
200	1 100	160 855	177	831	213 206	177	699	264 686	185
300	1 330	126 760	169	972	171 824	167	768	229 442	176
400	1 513	106 801	162	1 097	143 075	157	861	187 585	162
500	1 669	93 179	156	1 213	121 414	147	976	146 520	143
600	1 812	82 645	150	1 327	103 475	137	1 096	114 682	126
700	1 928	75 161	145	1 429	89 971	129	1 201	92 822	111
800	2 062	67 478	139	1 523	79 081	120	1 312	74 567	98
900	2 180	61 499	134	1 620	69 142	112	1 412	61 301	87
1,000	2 301	55 994	129	1 721	60 113	103	1 513	50 371	76
1,100	2 425	50 926	123	1 814	52 787	96	1 601	42 253	68
1,200	2 535	46 886	119	1 905	46 411	88	1 701	34 571	59
1,300	2 620	43 996	115	1 998	40 709	81	1 801	28 314	51
1,400	2 715	40 946	111	2 091	35 600	74	1 887	23 760	45
1,500	2 827	37 620	106	2 163	31 997	69	1 982	19 562	39
1,600	2 929	34 848	102	2 256	27 799	63	2 100	15 404	32
1,700	3 009	32 789	99	2 351	24 037	57	2 191	12 830	28
1,800	3 134	29 819	93	2 444	20 790	51	2 289	10 534	24
1900	3 260	27 166	89	2 556	17 503	45	2 389	8 593	21

APPENDIX C: PROFIT/LOSS CALCULATED FOR ALL CUT-OFFS

Table C1: Calculated profits/losses at all cut offs for Area A and Area B

Area A profits/loss ($ 000's)				Area B profits/loss ($ 000's)			
Cut off	**SGS**	**OK**	**Actual Data**	**Cut off**	**SGS**	**OK**	**Actual Data**
0	19,665	19,737	22,558	0	-1,247	-1,606	-997
100	19,992	20,364	22,366	100	485	321	667
200	20,065	20,513	22,190	200	2,347	2,475	2,504
300	20,093	20,591	21,956	300	2,730	2,848	2,851
400	20,103	20,616	21,499	400	2,862	2,952	3,023
500	20,096	20,604	21,207	500	2,825	2,921	2,999
600	20,059	20,555	21,094	600	2,707	2,827	2,957
700	19,964	20,451	20,869	700	2,574	2,666	3,009
800	19,824	20,307	20,746	800	2,414	2,486	2,896
900	19,675	20,031	20,539	900	2,231	2,292	2,821
1000	19,464	19,724	20,845	1000	1,997	2,079	2,801
1100	19,129	19,274	20,717	1100	1,786	1,868	2,744
1200	18,728	18,743	20,471	1200	1,504	1,675	2,677
1300	18,282	18,314	20,063	1300	1,359	1,496	2,701
1400	17,734	17,751	19,540	1400	1,163	1,343	2,713
1500	17,247	17,162	19,266	1500	1,027	1,192	2,683
1600	16,633	16,478	19,162	1600	920	1,063	2,673
1700	16,013	15,880	18,783	1700	768	956	2,657
1800	15,335	15,217	18,316	1800	665	858	2,552
1900	14,630	14,731	17,825	1900	560	787	2,390